FETAL AND EARLY NEONATAL CARDIAC VENTRICULAR GEOMETRY AND FUNCTION

FETAL AND EARLY NEONATAL CARDIAC VENTRICULAR GEOMETRY AND FUNCTION

AN ECHOGRAPHIC STUDY

PROEFSCHRIFT

DOOR

ROBERTUS PETRUS LEONARDUS VOSTERS

GEBOREN TE MUNSTERGELEEN

To my Parents

'If a man will begin with
certainties, he shall end in
doubts; but if he will be
content to begin with doubts,
he shall end in certainties'

Sir Francis Bacon

FOREWORD

The study, described in this thesis, was carried out in the
Dept. Obstetrics and Gynaecology (Head: Prof.Dr. A.C.
Drogendijk), of the Academic Hospital Dijkzigt, Rotterdam,
Holland, under the guidance of Prof.Dr. J.W. Wladimiroff.
Till the very last moment he has provided unfailing
enthusiasm enabling the fruition of this thesis. For this
I am very grateful.
The critical remarks and advice from Prof.Dr. A. Versprille,
the second Promotor, were extremely valuable to me.
I owe a great debt of gratitude to Prof.Dr.Ir. N. Bom and
Prof.Jhr. V.H. de Villeneuve for their willingness to act as
Referees.
In the first phase of the practical part of the study, I was
helped a great deal by Wim Vletter of the Dept. Echocardio-
logy. Later Leo Vrij and John Wondergem performed many of
the recordings during their elective period and as student-
assistants. I would like to acknowledge their help.
The contacts with the Dept. Experimental Echocardiography
were very useful. Mr. G. van Zwieten wrote the computer
programmes for the calculation of the collected data.
Mr. C. Ligtvoet advised me about the description of the
technical aspects of the ultrasound investigation.
Mr. H.J.A. Schouten of the Dept. Biostatistics gave useful
statistical advice concerning the results of the study.
Patricia Stewart spent a lot of time correcting the English
text of this thesis.
I would like to thank Alize Bijl for the efficient way in
which she typed this manuscript.
Finally a word of thanks to all who were in any way
connected with this study.
This thesis is dedicated to my parents, who have provided
life long love, support and encouragement.

CONTENTS

Chapter 6

NORMAL VENTRICULAR DYNAMICS DURING THE
LAST TRIMESTER OF PREGNANCY AND EARLY
NEONATAL PERIOD   64

Chapter 1

INTRODUCTORY REMARKS AND DEFINITION OF OBJECTIVES OF THE
PRESENT STUDY

The first documentation pertaining to the fetal cardiovas-
cular system is attributed to Galenus, who in the Second
Century A.D. described what was later to become known as the
foramen ovale and its valve, as well as the ductus arteriosus
and gave some account of their postnatal closure. It was not
until 1564 that a posthumous publication, originating from
Vesalius, contained the first account of the ductus venosus.
In 1626, also in a posthumous publication from Spigelius, it
was pointed out that no direct communication exists between
the umbilical vessels of the fetus and the uterine vessels
of the mother. He also observed that in the fetus the left
and right ventricular walls are of about equal thickness,
whereas in the adult the left ventricular wall predominates.
Two years later, in 1628, William Harvey introduced his con-
cept of the circulation of blood which included the first
account of the fetal circulation. This publication marked
the beginning of the use of a dynamic concept of the cardio-
vascular system. It was not until the present century that
methods of experimental research were applied to the problems
related to the fetal circulation. In 1907, Pohlman pointed
out the need for the use of experimental methods in live
animals in this particular field. His experiments consisted
of the injection of corn starch granules into the circulation
of fetal pigs. Huggett (1927) found, in the exteriorized fetal
goat, a higher oxygen content in carotid arterial blood than
in blood from the descending aorta. In this study, he was
able to refute the longstanding concept (Sabatier, 1778) that
although well-oxygenated blood was directed preferentially to
the ascending aorta to supply the heart and brain, the rest
was returned to the placenta. Further impetus to research in
fetal and neonatal cardiovascular physiology was given by

Barclay, Franklin and Prichard (1944) and by Sir Joseph
Barcroft (1946). The first group introduced cineroentgen
techniques into the study of the circulation in the fetal and
neonatal lamb. To a great extent, Lind, Stern and Wegelius
(1964) have also used angiographic techniques to study human
fetal and neonatal circulation. Recently, several different
techniques have been applied to the study of the heart and
circulation of the fetus and newborn, i.e. observations of
early embryonic hearts and individual embryonic myocardial
cells in tissue culture (Zak, 1973), study of the responses
of isolated papillary muscles in tissue baths (Boerth, 1972;
Friedman, 1973). Most of our present knowledge of fetal and
neonatal cardiovascular anatomy and function, however, was
derived from lamb experiments; in particular by Dawes and
co-workers in Oxford (Dawes, 1968) and Rudolph and co-workers
in San Francisco (Rudolph and Heymann, 1974). Data were
originally collected from the exteriorized preparation,
although it became increasingly evident that the exteriorized
fetus underwent major physiological circulatory changes.
Acute observations of the fetus in utero resulted in more
meaningful data, but once more it was evident that many
physiological functions were affected by the surgical and
anaesthetic procedures introduced. This led to studies of the
fetus in utero after recovery from the effects of surgery in
chronic preparation. Rudolph and Heymann (1974) pointed out
that these chronic preparations may still not be indicative
of the normal physiological state, if only for the high
incidence of spontaneous parturitions up to a week following
surgical intervention.

The non-invasive nature of diagnostic ultrasound examinations
allowed observations of the human fetal and neonatal heart
with no interference to the normal physiological state.
Examinations of the fetal heart by means of pulsed ultra-
sound dates back to 1954 when Edler and Hertz were the first
to obtain motion patterns of fetal cardiac structures. Later,
Robinson (1968) reported on the identification of the intra-

14

ventricular septum. Fetal heart volume measurements were made
by Garrett and Robinson (1970) and Suzuki et al (1974) and
more detailed analysis of fetal cardiac anatomy became
possible as a result of the introduction of grey-scale
techniques (Lee et al, 1977). It was not until the introduction
of real-time scanners that information on cardiac anatomy in
relation to the various stages of the cardiac cycle could be
obtained. The introduction of dynamically focussing linear
array real-time systems, resulting in high resolution images,
has opened-up the possibility of obtaining information on
cardiac geometry and function from a two-dimensional display
(Wladimiroff and McGhie, 1981a). Combined use of two-
dimensional real-time ultrasound and single beam transducers
opened the possibility of studying the fetal and neonatal
heart from time-motion (M-mode) recordings (Hobbins et al,
1978; Wladimiroff et al, 1979).

The objective of the present study was to obtain an answer to
the following questions:
- Does an ultrasound time-motion recording of the fetal and
  neonatal heart allow accurate and reproducible measurements
  of ventricular size and intraventricular septum thickness
  during the various stages of the cardiac cycle.
- If so, do these time-motion recordings contribute in a
  meaningful way to our present knowledge of human fetal and
  neonatal cardiac ventricular geometry and function, both
  under physiological and pathophysiological circumstances.
- When the ventricles are functionally alike, the systolic
  pressure rise on both sides of the septum will be about
  the same. Is it possible to use ultrasound, and in
  particular study of septal motion and thickening in the
  fetus to support the hypothesis that the fetal septum does
  not play a role during ventricular contraction.

Chapter 2

SOME BASIC PRINCIPLES OF DIAGNOSTIC ULTRASOUND PARTICULARLY
WITH RESPECT TO THE M-MODE RECORDING

For medical diagnostic applications, sound waves (longitudinal
pressure waves) at frequencies in the 1 to 10 MHz range must
be employed to obtain the required resolution. These high-
frequency sound waves travel through a medium at a velocity
characteristic of that medium. On reaching an interface with
another medium of different acoustic properties, the ultra-
sound beam may be reflected. The acoustic impedance of a
medium is the product of the velocity of sound in that medium
and the density of that medium. At an interface between media
of different acoustic impedances, a component of the sound
wave energy will be reflected (echo) while another component
of the energy will be transmitted into the second medium etc.
The amplitude of the echoes is determined by:
- the difference in acoustic impedance between two media. The
  echo amplitude from an interface between blood and muscle
  tissue is smaller than that originating from an interface
  between bone and water;
- the emitted sound energy;
- the angle of the sound wave to the reflecting interface.
  Since the reflection of energy is such that the angle of
  incidence equals the angle of reflection, optimal echo
  information will be obtained when the angle between the
  sound beam and reflecting interface is perpendicular;
- the attenuation during passage of sound waves through a
  medium. This attenuation is exponential and therefore is
  expressed in the logarithmic dB notation. Thus an ultrasound
  wave is rapidly attenuated by passage through tissue so that
  the incident intensity on a deeply situated interface will
  be very small as compared with the incident intensity on a
  superficially situated interface.

2.1 Basic principles of an echosystem

Fig. 2.1 shows the block diagram of an echosystem. The timer generates a starting signal for the complete system. After receiving this signal, the pulse transmitter provides electrical energy for the transducer at the desired ultra-sound frequency (probe). This electrical energy is converted into acoustic energy by piezo-electric material in the transducer. In this way a sound wave is generated, which travels into the patient. Simultaneously the horizontal deflection of an oscilloscope is triggered, which starts a line on the oscilloscope screen. After the transmission of the sound wave into the patient, the system is switched into reception. The reflected sound wave (echo) is received by the transducer and converted into an electrical signal by the same piezo-electric
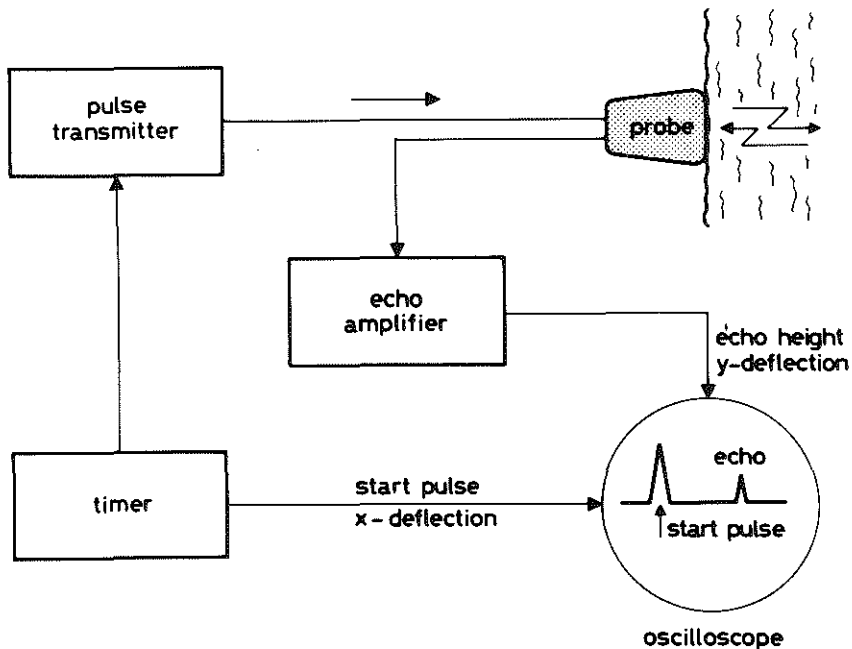
Fig. 2.1 Block diagram of an echosystem. Explanation in text.

material. This signal is amplified (echo-amplifier) and
displayed on the oscilloscope as a spike. The distance between
the starting point and the spike on the screen is proportional
to the distance of the transducer and the structure which
generates the echo. The amplification section of the echo-
system is capable of amplifying weak signals, generated deep
inside the body, more than the strong echoes, generated by
structures near the transducer. This mechanism is called time
gain amplification. The amplitude of the echoes can be
recorded in terms of the amplitude of the Y-deflection of the
oscilloscope. This type is known as the A-mode, i.e. amplitude
mode. An echo can also be displayed in the Brightness-mode
the so-called B-mode. In this type of display, the larger
the echo, the brighter the spot on the oscilloscope screen.
The M-mode records the movement of reflecting structures
along a single sound beam as a function of time, i.e. Motion-
mode.

2.2 M-mode information

It is particularly the M-mode information, which will be more
extensively discussed, since all data presented in this thesis
were obtained from M-mode recordings. The M-mode technique
yields information with a high sampling rate along a single
sound beam. The recorded variable is the distance between the
reflecting surfaces and the transducer as a function of time.
The M-mode will only display movements which occur in the path
of the ultrasound beam (Paragraph 2.3). The line of ultrasonic
data on the oscilloscope screen is brightness modulated. Due
to the high repetition rate echoes will show as moving dots
on this line. The movement of these dots can be recorded on
paper or on the oscilloscope screen itself by
a. movement of light sensitive paper in front of the bright
   line
b. electronic displacement of the subsequent echo lines on
   the oscilloscope screen, such that the adjacent lines

18

produce the well-known M-mode.
The great advantage of the M-mode technique is that changes
in distance between two anatomical structures can be studied.
The quality of the M-mode recording is subject to a number of
factors. In the first place there are certain limiting factors
with respect to the physical properties of ultrasound.
Secondly, M-mode recordings only allow analysis of ultrasound
information originating from one direction. Thirdly,
considerable expertise is required to obtain and interpret
M-mode recordings.

2.3 Limitations of the M-mode technique

2.3.1 Reverberations

Strongly reflecting interfaces may produce echoes, which will
travel backward and forward several times, i.e. reverberations,
before ultimately reaching the transducer. Under these
circumstances, there will be a lengthening of the time inter-
val between emission of the ultrasound wave and subsequent
reception of the echo resulting in so-called 'mirror images'
(Fig. 2.2).

2.3.2 Resolution problems

There are two types of resolution: axial and lateral resolution.
The axial resolution is the ability of a system to differentiate
in the axial direction between two reflectors which are situated
in the beam of the transducer. The axial resolution depends on
the brevity of the ultrasound pulse. With high ultrasound
frequencies short ultrasound pulses may become possible.
However, at high frequencies stronger attenuation exists. It is
therefore necessary to find a compromise between axial
resolution and penetration depth.
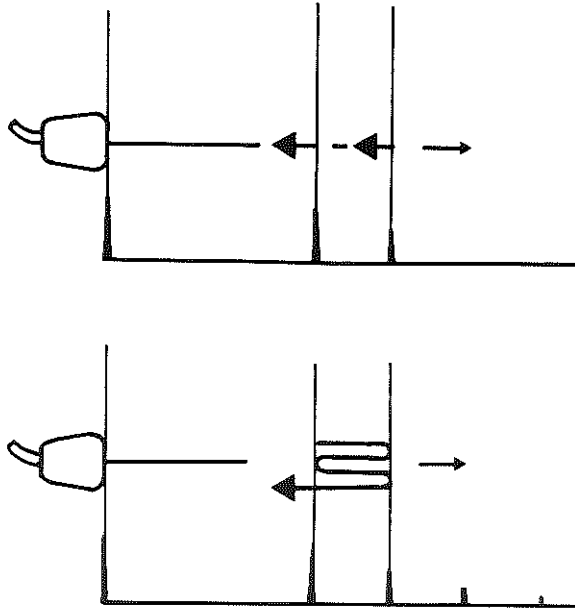
Fig. 2.2 This figure illustrates the mechanism of reverberations between
two strongly reflecting boundaries. Additional echoes appear on
the display behind the echoes whose position represents the
correct boundaries.

The lateral resolution is the ability of a system to
differentiate between two reflectors which are situated in a
plane at right angles to the sound beam. The display of these
reflectors is very much dependent on the profile of the ultra-
sound beam. The area which is covered by the ultrasound beam
can be divided into a 'near field' and a 'far field'. In the
'near field' the beam width is virtually equal to the trans-
ducer width, whereas in the 'far field' the beam will diverge.
All echoes from structures which are situated within the
ultrasound beam, will be received by the transducer.

20

Focussing techniques may improve the shape of the ultrasound beam and thus, the lateral resolution. Focussing systems are now incorporated in all present ultrasound scanners.

2.3.3 Amplification problems

Echoes from deeply situated structures will be small as compared with echoes from near structures. However, as already mentioned, selective amplification can be added to compensate for ultrasound attenuation (time gain compensation). Since attenuation varies from patient to patient, it means that the time gain compensation has to be optimally adjusted by hand in every patient, in order to achieve a display from which echoes of various amplitudes are well represented. Reverberation might occur when the amplification is too large, and essential structures may be missed when it is too small. Both may lead to erroneous interpretations.

2.3.4 Directional problems

The M-mode technique will only allow recording of echo information from one dimension. Information from more than one dimension, i.e. from adjacent structures can be obtained by slowly moving the M-mode transducer during the examination. However, it should be realized that when using M-mode, movement of the adjacent structures can never be visualized simultaneously. In other words, the M-mode technique, in contrast to two-dimensional real-time systems does not allow us to study structural movements in relation to their anatomy. Detailed knowledge of the anatomy of the structure is essential, when carrying out M-mode studies. At present, M-mode systems are nearly always employed in combination with two-dimensional real-time scanners.

2.4 The actual M-mode recording

In the present study a single element technique (2.25 MHz) and line selection from a dynamically focussed linear array (3.1 MHz) real-time system (Organon Teknika) were used.

A single element transducer (Fig. 2.3) is built up with one disc shaped piece of piezo-electric material.
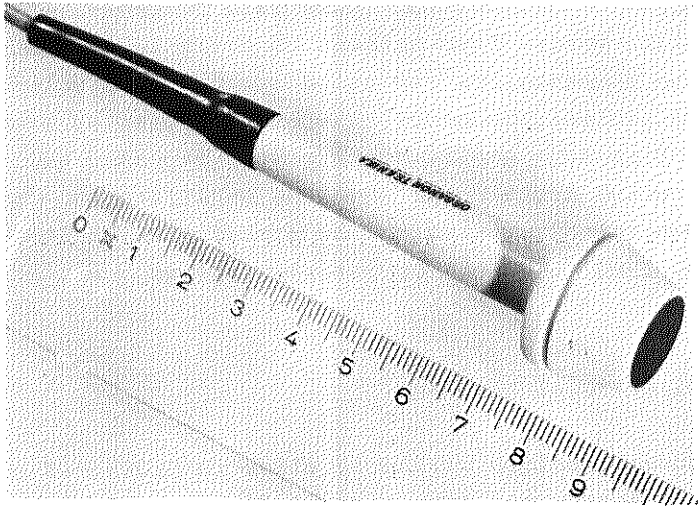
Fig. 2.3 Single element transducer.

In contrast, the transducer of a linear array system contains many rectangular shaped small piezo-electric elements in a row. A combination of n adjacent elements is selected to produce a scan. The next scan is made with n-1 elements of the previous scan and one new adjacent element. In this way a large number of scans is produced by selecting different combinations of adjacent elements. Each scan is displayed in B-mode on an oscilloscope screen, relative to its position. Consequently a two-dimensional image is displayed, built up from a larger

22

number of scans. Fast switching provides 50 images a second,
which means that moving structures can be studied within their
anatomical relationship. One scan in this image can be
selected for M-mode registration. The advantage of selecting
an M-mode line from a two-dimensional image is the possibility
of aiming the M-mode scan at the desired structures.

2.5 Analysis of the M-mode tracing

As has been said before, the M-mode contains information about
the depth of the echo producing structure relative to the
transducer and about the movement patterns of that particular
structure. During the M-mode recording, calibration dots are
introduced, allowing measurements of the velocity with which
the structure moves. Fig. 2.4 depicts the calibration dots in
an M-mode tracing of the fetal heart. On the vertical axis
(depth), the distance between two dots is 1 cm, whereas on the
horizontal axis (time), the distance is 0.5 sec. Measurements
can be carried-out using compasses. It is clear, however, that
this would be a very laborious procedure particularly when a
large amount of information has to be collected. In the present
study, therefore, M-mode echocardiograms were analysed using a
computer system with a digitizing tablet and light pen (Bit
Pad one: resolution 0.1 mm, accuracy $\pm$ 0.081). Fig. 2.5 is a
drawing to show the composition of this equipment with data
analysing facilities. After tracing of the essential features
of an M-mode recording, the computing system can determine
variables during one or more cardiac cycles. The analysis
starts with a command for calibration. This is possible by
indicating three points on the recording with the pen in the
rectangular co-ordinate system of the digitizing tablet: an
origin (free choice), a corresponding point 1 second later
and a point 5 cm above the origin. After calibration the right
and left ventricular endocardial wall echoes, and the intra-
ventricular septum echoes are traced for ten cardiac cycles.
The digitized data are translocated, rotated and scaled

according to the calibration points. The data are filtered by a low-pass filter to remove hand tracing errors and are stored in a fixed element array in memory. The sampling points in this array are equally spaced in time.

The cardiac structures, which were measured as described above, will be discussed in Paragraph 3.2.
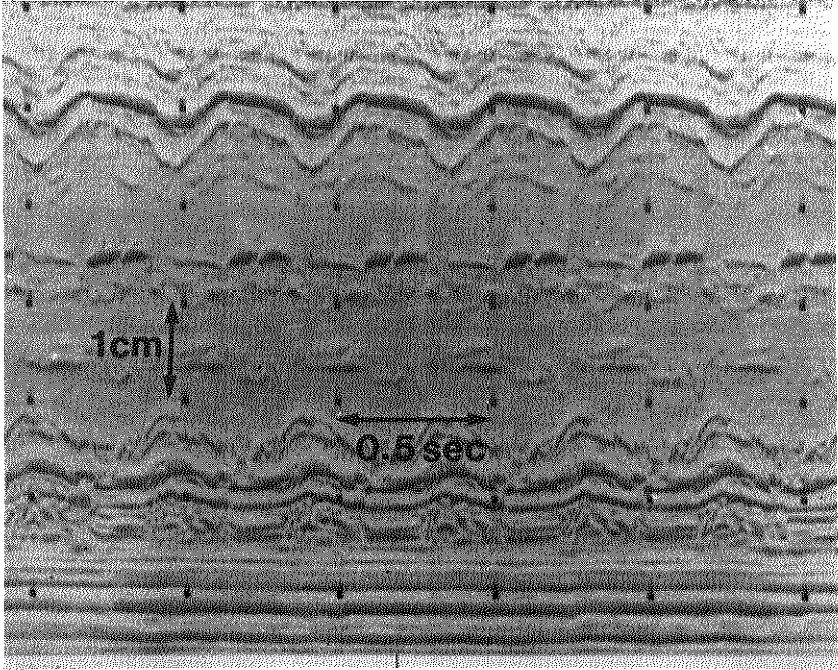
Fig. 2.4 M-mode of a fetal heart, displaying the calibration dots as described in paragraph 2.5.
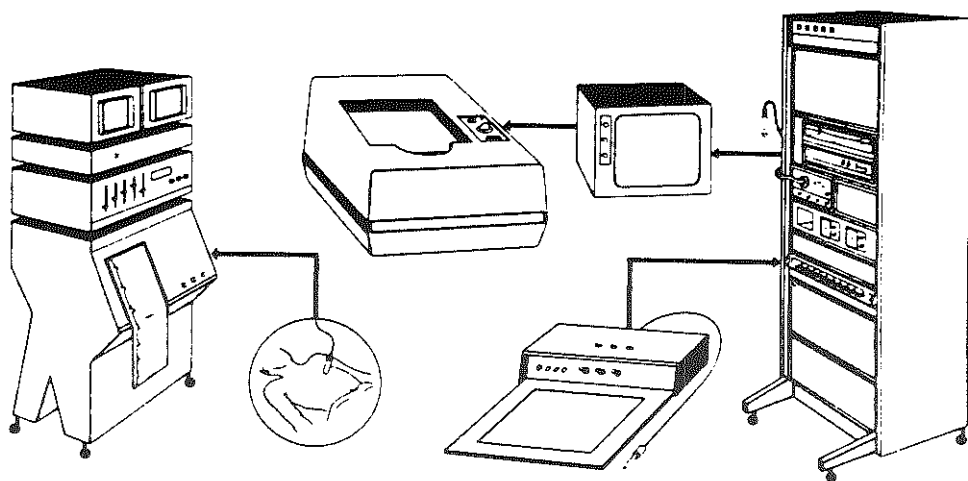
Fig. 2.5 A schematic drawing of the echocardiographic data equipment.
The ultrasound system is shown to the left. The digitizing
tablet and video hard copy device are shown in the middle and
the computer configuration to the right.

Chapter 3

M-MODE RECORDING OF THE FETAL AND NEONATAL CARDIAC VENTRICLES.
TECHNIQUE, ANALYSIS AND REPRODUCIBILITY OF THE MEASUREMENTS

In this chapter the technique of obtaining an M-mode recording
of the fetal and neonatal ventricles will be described first.

3.1 M-mode recording techniques

M-mode recordings were made both during fetal and early
neonatal life. They will be described separately.

3.1.1 The antenatal period

The examination procedure begins with a search for the two-
dimensional image of the largest longitudinal cross-section
through the left and right fetal ventricle by means of a
dynamically focussing linear array real-time scanner
(Organon Teknika)(Wladimiroff et al, 1979). The first step
consists of determining in a cross-section the position of
the fetal spine and chest in the maternal abdomen. In the
next step the transducer is placed at the level of the fetal
heart, in a plane at an angle of 45° to the antero-posterior
axis of the fetal chest and at an angle of 50° to the fetal
spine (Fig. 3.1). This plane will run through the right and
left ventricle at right angles to the intraventricular septum.
The third step represents the identification of the largest
cross-section through the right and left ventricle by making
scans parallel to the scanning plane described until the
following five landmarks are visible on the two-dimensional
image (Fig. 3.2): the left ventricular posterior wall (PW),
the intraventricular septum (IVS), the right ventricular
anterior wall (AW), the mitral valve leaflets (MV) and aortic

26

root (Ao). The continuous visualization of these five land-
marks allows the plane of investigation to remain virtually
unchanged both during the systolic and diastolic phase of the
cardiac cycle.
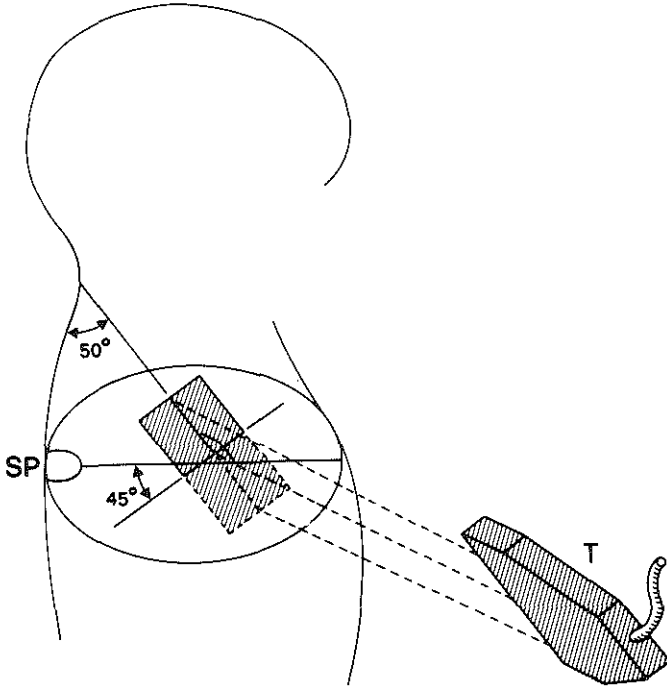
Fig. 3.1 Schematic representation of the transducer position at right
angles to the plane through the intraventricular septum (hatched
area) of the fetal heart. Explanation in text. (Courtesy of the
Brit.J.Obstet.Gynaec.)
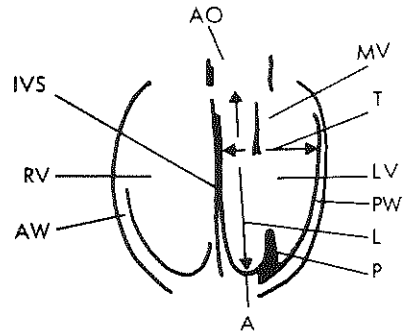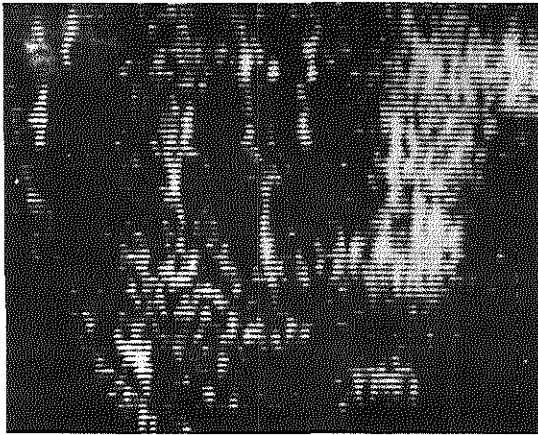
Fig. 3.2 Real-time two-dimensional scan and schematic picture of a
         longitudinal cross-section through the left ventricle (LV) and
         right ventricle (RV) depicting the right ventricular anterior
         wall (AW), the intraventricular septum (IVS), the left
         ventricular posterior wall (PW), the mitral valve leaflets (MV),
         the aortic root (Ao), and the posteromedial papillary muscle
         (P). T and L represent the largest transverse and longitudinal
         diameter of the left ventricle (LV) (Courtesy of the Brit.J.
         Obstet.Gynaec.)

For further clarification, Fig. 3.3 depicts a similar scanning
plane on a post mortem specimen of a fetal heart at 39 weeks
of gestation. This specimen does not show the aortic root.
It should be realized that when the fetus is situated with the
spine in the right lateral position, the ultrasonic beam will
first traverse the left ventricle; when the fetal spine is
situated in the left lateral position, the right ventricle
will be approached first (Fig. 3.4). In the last step of the
procedure a line is selected in the two-dimensional real-time
image as described in Chapter 2, which runs through the left

and right ventricle at right angles to the intraventricular
septum and is situated at the level of the mitral valve
leaflets (Fig. 3.2). An M-mode recording of the cardiac
structures along this line is subsequently made (Fig. 3.5)
depicting the left and right ventricle (LV and RV), the
intraventricular septum (IVS), the left ventricular posterior
wall (LVPW), the right ventricular anterior wall (RVAW) and
the mitral valve leaflets (MV). Particular attention was paid
to optimal visualization of the ventricular endocardium by
means of correct time gain setting.
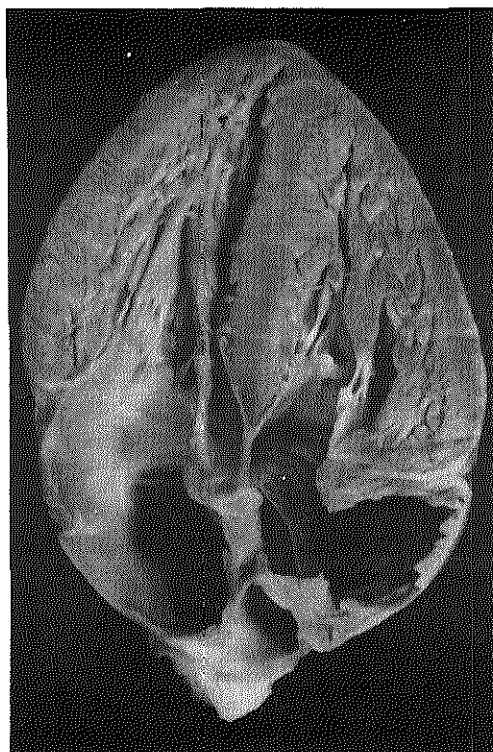
Fig. 3.3 Longitudinal cross-section through a post mortem fetal heart at
        39 weeks of gestation.
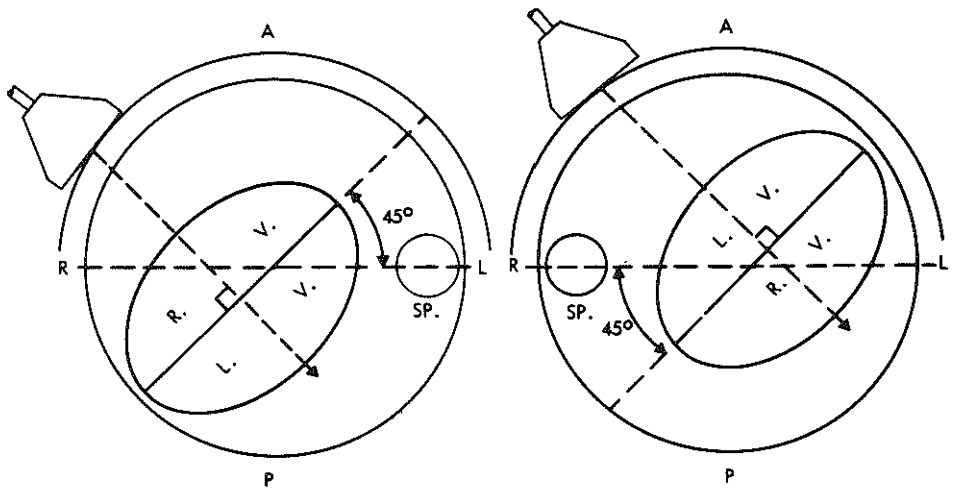
Fig. 3.4 Transducer positioning relative to the fetal chest and heart.
A = anterior, P = posterior, R = right, L = left, SP = spine,
LV and RV = left and right ventricle. When the spine is
situated on the right (right), the ultrasonic beam will first
traverse the left ventricle. When the spine is situated on the
left (left), the ultrasonic beam will first traverse the right
ventricle.
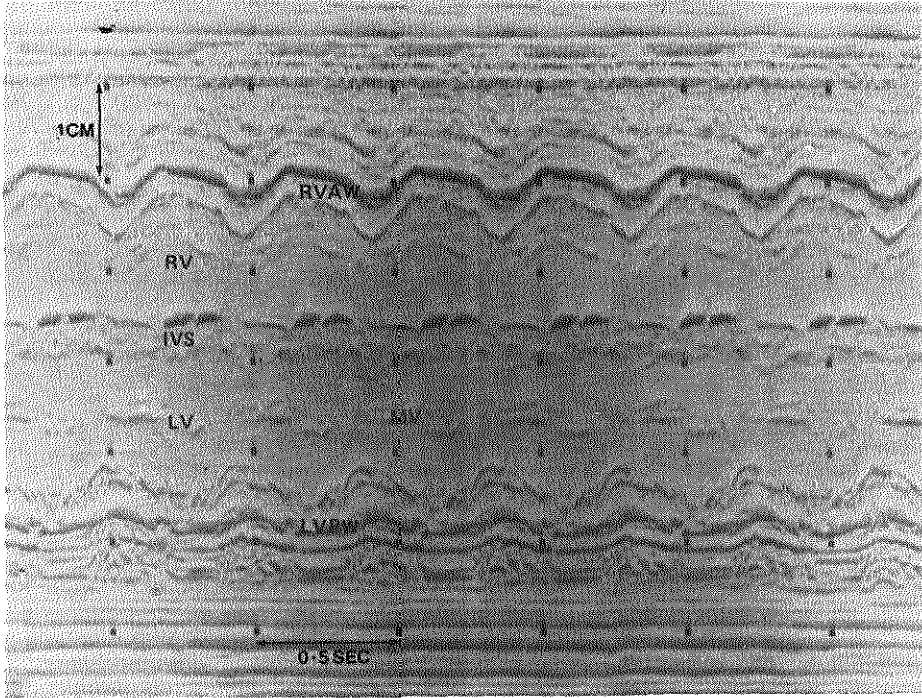
Fig. 3.5 Example of an antenatal M-mode recording. LV = left ventricle,
        RV = right ventricle, IVS = intraventricular septum, LVPW =
        left ventricular posterior wall, RVAW = right ventricular
        anterior wall, MV = mitral valve leaflets.

3.1.2 The early neonatal period

During the neonatal period a single element transducer as
described in Chapter 2 was used. In contrast to the fetal
study, real-time ultrasound orientation of the position of
the heart is not necessary in the neonate. The infant is
slightly turned to the left-lateral position to avoid possible
interference of sound absorbing lung tissue between heart and

transducer. The single element transducer is first positioned
in the left parasternal region of the chest at the level of
the 2nd intercostal space. The mitral valve is used as a land-
mark. The sequential directions of the sound beam in the
sagittal plane of the left ventricle through the long axis
from the aorta to the apex are schematically shown in Fig. 3.6.
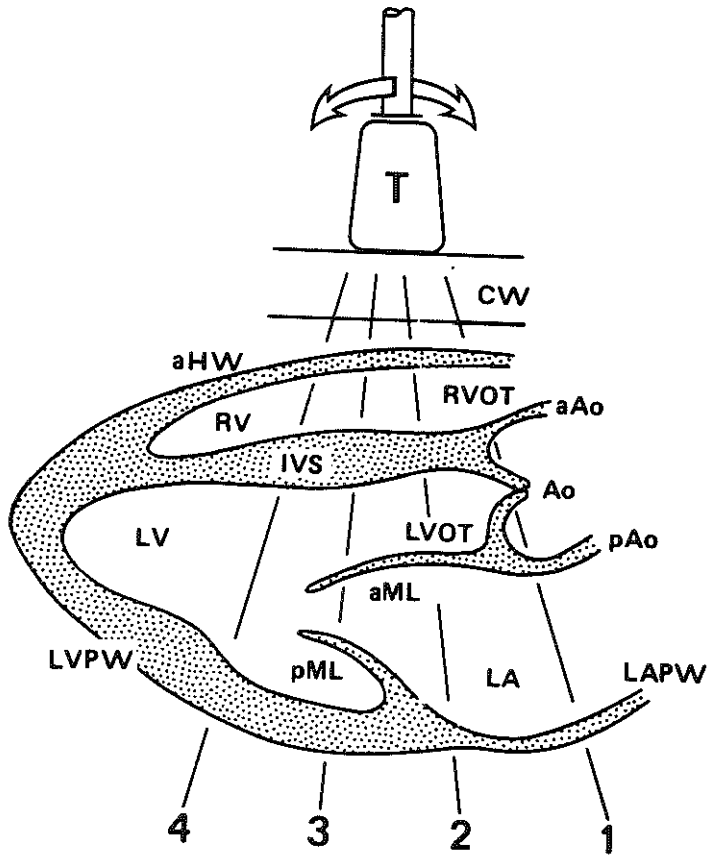
Fig. 3.6 Schematic longitudinal cross-section of the neonatal heart.
A scan is performed when the transducer is swept from the aorta
(direction 1) towards the apex (direction 4). Explanation in
text.

The resulting M-mode scan is represented in Fig. 3.7.
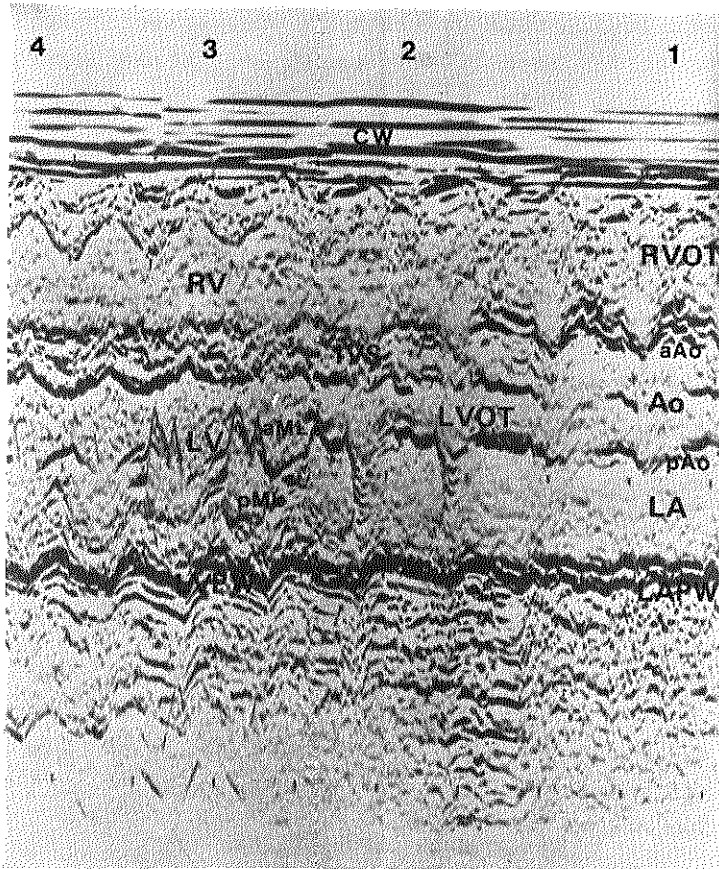
Fig. 3.7 M-mode scan of the neonatal heart following the sagittal plane
through the long axis of the left ventricle. The directions of
the sound beam labelled 1 to 4 on the diagram of Fig. 3.6
correspond to the areas labelled 1 to 4 on this record.

Four anatomic areas with specific cardiac structures and
motion patterns corresponding to basic transducer directions,
must be distinguished (Roelandt, 1977).

33

Area 1.

This area is recorded when the sound beam is aimed from the
mitral valve position in a superior and medial direction to-
wards the base of the heart. It traverses the chest wall (CW),
right ventricular outflow tract (RVOT), anterior aortic wall
(aAo), posterior aortic wall (pAo), left atrial cavity (LA)
and left atrial posterior wall (LAPW).

Area 2.

This area is recorded by directing the transducer slightly
inferiorly and laterally from area 1. This sound beam
traverses the intraventricular septum (IVS), left ventricular
outflow tract (LVOT) and anterior mitral valve leaflets (aML).
Particular attention should be paid to the septal-aortic
continuity.

Area 3.

This area is visualized by further tilting the transducer from
direction 2 to direction 3, causing a sound beam to traverse
the right and left ventricular cavity (RV and LV), posterior
mitral leaflet (pML) and left ventricular posterior wall
(LVPW).

Area 4.

This area is obtained by angling the transducer still further
inferiorly and laterally towards the apex. The sound beam now
passes the right and left ventricular cavity (RV and LV),
intraventricular septum (IVS) and left ventricular posterior
wall (LVPW).

This M-mode scan is of importance both with respect to
anatomical information and transducer position during the
recording. In the present study, M-mode recordings of area 3
were made for measurement of the transverse diameter of the
left and right ventricle (LV and RV) and thickness of the
intraventricular septum (IVS) both during the end-diastolic
and end-systolic phase of the cardiac cycle.

34

3.1.3 Comparison of the antenatal and neonatal recording technique

Comparison of antenatal and neonatal recording data is only permitted if M-mode recordings have been made through the same cross-section of the heart. Care has been taken that the beam orientation through the heart was approximately equal. In the antenatal period a scan was made along a plane through the longitudinal axis of the heart as described in Paragraph 3.1.1, allowing visualization of five landmarks: left ventricular posterior wall (LVPW), intraventricular septum (IVS), right ventricular anterior wall (RVAW), mitral valve (MV) and aortic root (Ao). The same procedure was carried out during the neonatal period. An M-mode scan was made along a plane running through the longitudinal axis of the heart as described in Paragraph 3.1.2, resulting in the same landmarks as observed in the antenatal scan, justifying comparison of both scans.

3.2 Analysis of fetal and neonatal M-mode recordings.

In both fetal and neonatal M-mode recordings a number of variables were measured with the objective of gathering information on cardiac geometry and function during the antenatal and neonatal period. The results of this study will be presented in Chapters 5 and 6. The following variables were measured, using an X-Y digitizer (Paragraph 2.5):
- The transverse axis in mm of the left (D_{lv}) and right (D_{rv}) ventricle in the end-diastolic (ED) and end-systolic (ES) phase of the cardiac cycle. The transverse axis of the left ventricle (LV) runs from the endocardial surface of the left ventricular posterior wall (LVPW) to the endocardial surface of the intraventricular septum (IVS). The transverse axis of the right ventricle (RV) runs from the endocardial surface of the right ventricular anterior wall (RVAW) to the endocardial surface of the intraventricular septum (IVS).

The end-diastolic phase (ED) of the cardiac cycle was
determined by the beginning, and the end-systolic phase
(ES) by the maximum of the inward movement of the endo-
cardial surface of the ventricular walls.
- The thickness in mm of the intraventricular septum (T_{vs})
  in the end-diastolic and end-systolic phase of the cardiac
  cycle.
- The beat-to-beat interval in msec. as expressed by the time
  interval between the end-systolic phase of two consecutive
  cycles. It was realized that measurement of beat-to-beat
  interval without an abdominal ECG was subject to some
  inaccuracy. Initial attempts to obtain simultaneous fetal
  M-mode and ECG recordings were unsuccessful for one or more
  of the following reasons:
  . frequent manipulations of the large-size linear array
    real-time transducer on the maternal abdomen, thereby
    touching the ECG-electrodes;
  . fetal movements.
  It was therefore decided for calculation of the beat-to-
  beat interval, to measure the distance between the end-
  systolic phase of the consecutive cardiac cycles to the
  nearest 0.5 mm corresponding with a time interval of 25
  msec. (10 mm = 500 msec, see Paragraph 2.5). As will be
  shown in Paragraph 3.3 this resulted in an acceptable
  reproducibility of this particular measurement.

3.3 Accuracy and reproducibility of M-mode measurement

In general terms the errors which are inherent in a measure-
ment may be divided into two groups, systematic and random.
Systematic errors give a measure of the difference between
the measurements and the corresponding real values. Random
errors give a measure of the reproducibility of the technique.

3.3.1 Systematic errors

The systematic error can be divided into the error of the
instrumentation and the error caused by the finite beam width
of the ultrasound wave. The error of the instrumentation can
be considered as very small. The markers on the M-mode
recording are generated by a highly stable oscillator, with
an accuracy well below 0.1%. The sawtooth generator, which
gives the vertical deflection on the M-mode recorder, has a
linearity better than 1%. Moreover this generator writes the
echo information with the markers, which means that the
resulting error is even less. The system is calibrated at an
ultrasound velocity of 1540 m sec^{-1} to generate the 1 cm
intervals on the M-mode tracing. This coincides with the
velocity through blood (Wells, 1977). Since a differential
measurement is taken (i.e. between two points of the fetal
heart), no errors will be introduced by the other structures
positioned between the transducer and the fetal heart, which
may show a different ultrasound velocity. In conclusion it is
reasonable to assume that the errors due to instrumentation
are well below 1%.

As outlined in Chapter 2, the ultrasound beam is not needle-
shaped but shows a well-defined pattern. In particular, the
finite beam width of the transducer may give ambiguous results
for the exact position of a reflector. Fig. 3.8 shows
schematically a cavity with the beam profile from a transducer.
As can be observed, the measured diameter is always shorter
than the real diameter. This has been confirmed in the
literature (Kececioglu-Draelos et al, 1982; Barrett et al,
1982). To assess the error caused by the finite beam width
one must be aware of the beam profile of the transducer used
during the examination. Moreover the exact definition of the
beam width must be established, since the strength of the
ultrasound field diminishes gradually in a plane perpendicular
to the transducer.
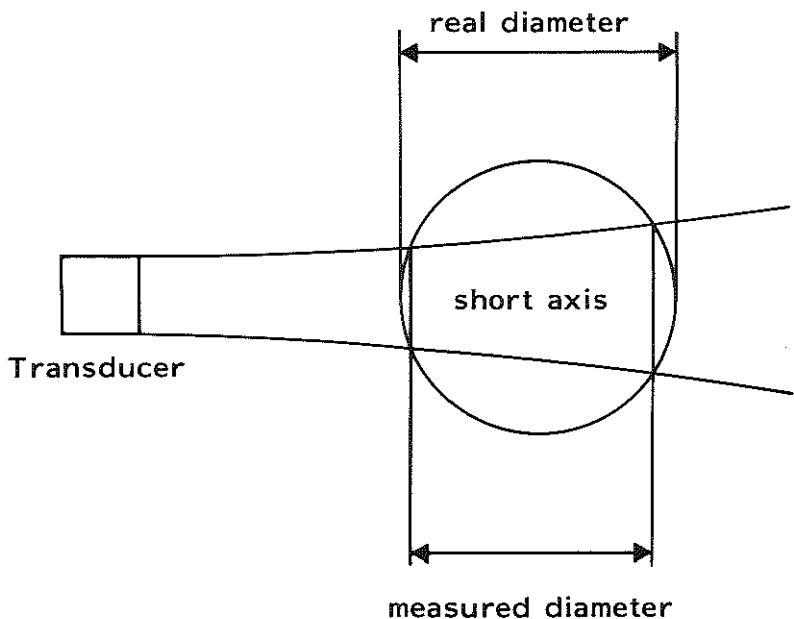
Fig. 3.8 Schematic representation of a cavity with the beam profile from
a transducer.

Fig. 3.9 shows a computer simulation of an ultrasound field
from a particular transducer. White represents the highest
intensity of the ultrasound field, black is zero intensity.
From this simulation it can be observed that maximum intensity
is present on the main axis. This is called the main lobe.
From the main axis the field diminishes and becomes zero.
Further away from the main axis other maxima can be observed,
the so-called side lobes of the ultrasound field. In practice
it must be realized that by applying more amplification, the
weaker off-axis echoes may also be registered. Care was taken
during the investigation to minimize time gain amplification.

38
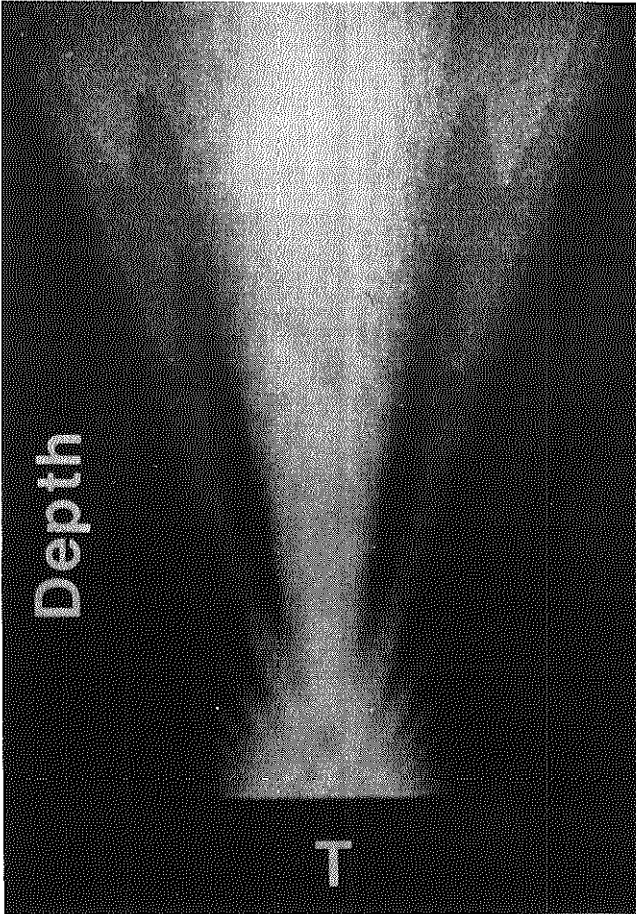
Fig. 3.9 A computer simulation of an ultrasound field. White is maximum
intensity, black is zero intensity. Calculated sound intensity
showing beam pattern of a focussed (at 6 cm) disc-shaped 3.12
MHz transducer. Total depth is 16 cm.

A well-accepted definition for the beam width of the trans-
ducer is the distance between two points in a plane
perpendicular to the transducer, symmetrically positioned to
the main axis, where the ultrasound power is half of its
maximum. This figure, which of course may be depth dependent,
is specified by all manufacturers of ultrasound equipment.
However, it is questionable if these figures can be used to
estimate the errors as is indicated by Figure 3.8. For example:
using a beam width of a dynamically focussed system of 3 mm,
the error still caused an underestimation of all measurements.
This error was 4.6% at 10 mm diameter, 3% at 15 mm diameter
and 2.3% at 20 mm diameter; and 13.2%, 8.7% and 6.7%
respectively in volume measurements. The echoes generated at
the edges of the ultrasound field may not be registered.
Furthermore these echoes are reflected not perpendicular, but
in a direction away from the transducer. An approach to
establish the error caused by the finite beam width would be
to use measurements from a fetal heart in a watertank. The
latter should be done using a fresh fetal heart, not older than
four hours post mortem (S. Goldberg, personal communication).
This, however, is impractical. In addition an unrealistic time
gain compensation would have to be introduced in these
experiments, which would make the results disputable. As
mentioned before, as described in the literature (Kececioglu-
Draelos et al, 1982; Barrett et al, 1982), the measured
diameter is always shorter than the real diameter. In these
studies contours were obtained from apical views. This means
that the entire contour measurements are influenced by
curvature as well as by lateral resolution. This method was
shown to yield an error between 10% and 20%. As a model the
calculations of volume and surface derived from a single
(M-mode) dimension may be less accurate compared to a contour
derivation. However, the ultrasound volume estimation based
on single measurements is, as far as ultrasound errors are
concerned probably more accurate.

40

3.3.2 Random errors

Random errors may arise from:
- positioning of the transducer. The correct position of the
  transducer is solely determined by the definition of certain
  structures within the measuring object, i.e. the specific
  image characteristics as described in Paragraph 3.1. There
  will, however, always be a difference between the adopted
  and ideal transducer position. The resulting error can be
  assessed by repeating the measurement several times.
- movement of structures. Real-time systems allow
  visualization of moving structures. The potential error
  arising from transducer positioning may therefore become
  even larger, since movement of the measured object may be
  translated into a re-positioning of the transducer.
- the investigator. The reproducibility of the measurement
  is also determined by the care and patience of the
  investigator when carrying out the measurement.

3.3.3 Reproducibility of the antenatal measurements

a. Interobserver variation
   Two different investigators, independently, measured the
   following parameters in ten consecutive fetal cardiac cycles
   from patients chosen at random between 28 and 41 weeks of
   gestation: the transverse diameter of the right and left
   ventricle (D_{rv} and D_{lv}), thickness of the intraventricular
   septum (T_{vs}) in the end-diastolic (ED) and end-systolic (ES)
   phase of the cardiac cycle in mm, and beat-to-beat interval
   in msec. First the mean of each of the parameters derived
   from 10 cardiac cycles was calculated for each patient.
   From these mean values the root of the pooled variance was
   subsequently calculated for all 10 patients together, using
   the formula
   $$\sqrt{\frac{1}{n} \sum_k s_k^2}$$, n = number of patients, S_k = standard

deviation for patient no. k, calculated from the two
measurements (one from each investigator) for this
particular patient. The results are presented in Table 3.1.
b. Intraobserver variation

In 10 consecutive fetal cardiac cycles from 10 patients
chosen at random between 28 and 41 weeks of gestation, the
same parameters as mentioned in Paragraph 3.3.3a were
measured twice at an interval of several days by one
investigator. The results of the root of the pooled
variance of the parameters are presented in Table 3.1.
c. Intrapatient variation

With an interval of 20 minutes two periods of 10 consecutive
fetal cardiac cycles from 10 patients randomly chosen were
measured by one investigator (Table 3.1).
d. Interpatient variation

Ten patients randomly chosen with a similar pregnancy
duration (33 weeks) were included. In each patient 10
consecutive fetal cardiac cycles were studied and a mean
of the parameters presented in Paragraph 3.3.3a was
calculated. From these values the mean and standard
deviation for all 10 patients together was established.
This standard deviation, which is a measure of the inter-
patient variation, is presented in Table 3.1.

3.3.4 Reproducibility of the neonatal measurements

The method of calculating the intra- and interobserver
variation, as well as the intra- and interpatient variation
in the neonatal period was similar to that described in
Paragraph 3.3.3. The intra- and interobserver variation as
well as the intrapatient variation were calculated for the
same parameters as defined in Paragraph 3.3.3a in 10 infants
chosen at random, from 10 min before delivery till 48 hours
following delivery. The interpatient variation was determined
in 10 infants on the 2nd day post partum. The results are
given in Table 3.2.

	LV ED	LV ES	RV ED	RV ES	IVS ED	IVS ES	beat-to-beat interval
interobserver variation	0.39	0.35	0.60	0.49	0.13	0.09	0.07
intraobserver variation	0.02	0.06	0.04	0.04	0.03	0.06	0.06
intrapatient variation	0.05	0.03	0.05	0.04	0.05	0.05	0.06
interpatient variation	1.44	1.10	1.39	1.12	0.28	0.29	0.35

Tabel 3.1 Reproducibility of the measurements during the antenatal period.
This table presents the root of the pooled variance as a measure for the inter-observer variation, intraobserver variation and intrapatient variation calculated for the LV and RV diameters in the ED and ES phase, the thickness of the IVS in the ED and ES phase, and beat-to-beat interval. The standard deviation is a measure for the interpatient variation expressed as twice the mean values of the above-mentioned parameters.

| | LV | | RV | | IVS | | beat-to-beat |
	ED	ES	ED	ES	ED	ES	interval
interobserver variation	0.14	0.19	0.10	0.14	0.09	0.07	0.08
intraobserver variation	0.06	0.05	0.04	0.03	0.05	0.07	0.07
intrapatient variation	0.11	0.07	0.08	0.09	0.13	0.05	0.11
interpatient variation	0.55	0.54	0.37	0.31	0.59	0.72	0.32

Table 3.2 Reproducibility of the measurements in the neonatal period.

This table presents the root of the pooled variance as a measure for the inter-observer variation, intraobserver variation and intrapatient variation calculated for the LV and RV diameters in the ED and ES phase, the thickness of the IVS in the ED and ES phase, and beat-to-beat interval. The standard deviation is a measure for the interpatient variation expressed as twice the mean values of the above-mentioned parameters.

Both in the antenatal and neonatal period the root of the
pooled variance calculated for the interobserver variation,
intraobserver variation and intrapatient variation is
considerably smaller than the standard deviation established
for the interpatient variation. Since the systemic error is
of minor importance only, it can be concluded from these data
that the M-mode measurements as described in this Chapter are
sufficiently accurate and reproducible to characterize each
patient.

3.4 Discussion

In the child and the adult, M-mode echocardiography has
rapidly achieved popularity as a non-invasive technique for
obtaining quantitated dimensional measurements of cardiac
chamber size, wall thickness, wall motion velocities, great
vessel dimensions and valve motion (Pombo et al, 1970;
Feigenbaum, 1972; Epstein et al, 1975; Sahn et al, 1978).
Edler and Hertz (1954) were the first to establish motion
patterns of fetal cardiac structures. Murata et al (1971)
pointed out that information such as the shape of cardiac
motion curves, the depth of a moving structure from the
surface, relative velocity of motion, the heart rate and
phase relationship could be collected from M-mode recordings.
He also used other parameters, such as the fetal'electro-
cardiogram (ECG), phonocardiogram and Doppler signals. More
detailed descriptions of motility patterns of fetal intra-
cardiac structures became available through the work by
Egeblad et al (1975). They primarily scanned the heart by
B-mode and subsequently obtained motility patterns of the
cardiac structures and diameters by means of M-mode recording.
Movements of the aortic and pulmonary root as well as atrio-
ventricular valves were recorded relative to the systolic and
diastolic phase of the cardiac cycle. During the last 5 years
marked improvement in two-dimensional real-time imaging has
resulted in even more detailed and accurate M-mode data on

fetal and neonatal cardiac structures. Ianniruberto et al
(1977) analysed mitral valve opening and closure times.
It was Hobbins et al (1978) and later both our own laboratory
(Wladimiroff et al, 1979; Vosters et al, 1979; Wladimiroff et
al, 1980; Wladimiroff and McGhie, 1981b) and Allan et al
(1982) in London, which established M-mode data on left and
right ventricular chamber size in the term fetus. Lately,
M-mode echocardiography has shown to be useful in the prenatal
diagnosis of congenital heart disease and cardiac dysrhythmias.
Baars et al (1977) published a case of fetal paroxysmal tachy-
cardia at term. Kleinman et al (1978) diagnosed a complete
atrioventricular block on the basis of an abnormality of
mitral valve and left ventricular posterior wall motion at
28 weeks of gestation and in a second fetus an atrial flutter
at 38 weeks of gestation.

In this chapter we presented the technique of obtaining a
satisfactory M-mode recording during both the fetal and
neonatal period. We opted for the long-axis view of the cardiac
ventricles as a standard plane for M-mode echocardiography.
Sahn et al (1980) obtained fetal and newborn cardiac measure-
ments from two-dimensional views showing the four cardiac
chambers. Their preference for this particular view was based
on work by Bommer et al (1979), who suggested that measurement
of the right ventricle on four chamber apical views at the
level just below the tricuspid valve correlates closely with
the maximum right ventricular short axis dimensions measured
from anatomical casts. It is, however, not possible to obtain
an M-mode recording of both cardiac ventricles at right angles
to the intraventricular septum from this particular cross-
section. With regard to the level of the ventricles at which
to measure the transverse dimensions on a long-axis view, we
recorded at the level of the mitral valve leaflets. This
position was recommended for ventricular measurements in
examinations of small hearts by the Committee on M-mode
standardization of the American Society of Echocardiography
(Sahn et al, 1978).

Up until now only Sahn et al (1980) in their two-dimensional study and Wladimiroff et al (1980) in their M-mode cardiac study have examined the reproducibility of their measurements. As previously mentioned one of the factors which affects the accuracy of echocardiographic measurements, is the clarity of the interface delineation. This applies in particular to the visualization of the endocardial echo on either side of the intraventricular septum and endocardial echo of the right. ventricular anterior wall and left ventricular posterior wall. The endocardial echo is less intense than the epicardial-pericardial complex and lies very close to a cluster of intraventricular echoes which probably arise from the posterior chordae (Popp and Harrison, 1970).

This problem of identifying boundaries of a structure because of poor quality, either secondary to instrumentation or to mid-anterior position of the fetal spine, excessive movements or maternal obesity was the main reason for rejecting a number of M-mode recordings, as will be discussed in Chapter 4.

In our own study we did not follow the classic method of millimeter ruler and callipers, but used a light-pen X-Y digitizer, as described in Paragraph 2.5, for the various cardiac measurements. This system has an accuracy of $\pm$ 0.08%. Nonetheless, the greatest measurement problem is not in the actual determination of the distance between two points, but in the process of determining between which points the distance should be measured. Despite the fact we were not in possession of a simultaneous fetal ECG-recording for a more accurate estimation of the end-diastolic and end-systolic phase of the cardiac cycle, the figures on intra- and inter-observer variation of the left and right ventricular transverse dimension, septal thickness and beat-to-beat interval showed an acceptable reproducibility of these measurements both in the antenatal and early neonatal period.

Chapter 4

PATIENT SELECTION AND STATISTICAL TESTS IN THE PRESENT STUDY

The cardiac M-mode recordings in the present study were
obtained in the Department of Obstetrics and Gynaecology of
the Academic Hospital Rotterdam - Dijkzigt between June 1978
and January 1981.

4.1 Uncomplicated pregnancy

Data were derived from 246 randomly selected subjects with an
uncomplicated pregnancy between 28 and 41 weeks of gestation.
All women were of caucasian origin and all gave consent to
participate in the study.

4.1.1 Selection procedure.

Pregnancy was considered uncomplicated if the following
conditions were met:
a. maternal age between 20 and 30 years;
b. a regular menstrual cycle; known date of last menstrual
   period; confirmation of calculated gestational age from
   either a single fetal crown-rump length measurement between
   7 and 12 weeks or a single measurement of the fetal
   biparietal diameter (BPD) between 13 and 22 weeks of
   gestation;
c. presence of a single fetus;
d. uneventful antenatal period and delivery:
            - normal fetal growth, as established by clinical
              and ultrasound examination;
            - spontaneous delivery after a pregnancy duration
              of at least 37 weeks;
            - birth weight between 10th and 90th percentile for

weight of gestation according to the Tables of
Kloosterman (1970), corrections being made for
maternal parity and fetal sex;
- Apgar score at 1 minute 8 or more;
- no congenital abnormalities.

The study of cardiac geometry and function consisted of two
parts:
- a cross-sectional antenatal study between 28 and 41 weeks
  of gestation in 193 out of 246 normal subjects, i.e. a
  rejection rate of 22%. The various reasons for failing to
  obtain an acceptable cardiac M-mode recording have been
  discussed in Chapter 3.
- a longitudinal antenatal-early neonatal study in 15 out of
  18 normal subjects (rejection rate 17%). In this group of 15
  women it was possible to obtain an M-mode recording of the
  fetal heart within 12 hours of delivery, since labour was
  induced for elective reasons immediately following the ultra-
  sound scan. Induction of labour was carried out by means of
  amniotomy and intravenous Oxytocin drip and was always
  followed by a spontaneous delivery 2 to 8 hours later. If
  necessary analgesics were administered to a maximum of two
  doses of 50 to 75 mg of Pethidin i.m. A second cardiac
  M-mode recording was carried out within 10 minutes following
  delivery and a further 3 recordings at 4 hours, 24 hours and
  48 hours respectively. These serial measurements allowed
  comparison of antenatal cardiac findings with those obtained
  during the first 48 hours following delivery.

4.1.2 Statistical tests

All cross-sectional antenatal data were related to gestational
age. If a linear change in a particular cardiac parameter was
observed, its significance was examined by means of the Pearson
product-moment correlation test. In cases with significant
change, the expected mean value based on the linear regression

line was presented for each week of gestation. In cases with
no significant change, all antenatal values of that particular
cardiac parameter were lumped together and the mean $\pm$ 1 SD
calculated. If a curvilinear change was noted, the mean value
for each week of gestation was given. Statistical significance
was subsequently assessed by means of the Wilcoxon non-paired
rank test.

All data from the longitudinal antenatal-neonatal study were
related to the five periods described in section 4.1.1 and
the mean value for each period was calculated. The significance
of any chance between these periods was examined by means of
the Wilcoxon matched-pair signed rank test.

4.2 Complicated pregnancy

A total of 25 pregnant women with fetal growth retardation
were studied. The selection procedure for these patients was
similar to that described in paragraphs 4.1.1a, b and c.
A technically acceptable M-mode recording was collected in 19
out of 25 subjects (rejection rate 24%). Results will be
presented in Chapter 7.

Fetal growth retardation was suspected when there was a
negative discrepancy of 2 weeks or more between the uterine
fundal height and gestational age during two successive
antenatal check-ups. Subsequent confirmation of a retardation
of fetal growth was obtained from ultrasonic measurements of
fetal head and chest size. Fetal head size was established
by means of measurement of the fetal biparietal diameter
(BPD) and fetal chest size as expressed by the transverse
chest area (Wladimiroff et al, 1978). Both fetal BPD and
chest area were situated on or below the lower limit (5th
percentile) of the normal curves according to Wladimiroff
et al (1978). Birth weights were classified in 3 categories:
between the 5th and 10th percentile, between 2.3rd and 5th

percentile, and below the 2.3rd percentile according to the
Tables of Kloosterman (1970), corrections being made for
maternal parity and fetal sex.

Chapter 5

NORMAL VENTRICULAR GEOMETRY DURING THE LAST TRIMESTER OF
PREGNANCY AND EARLY NEONATAL PERIOD

In this chapter the results from our own study on fetal and
neonatal ventricular geometry will be presented.

5.1 Left and right ventricular transverse diameter
    (D_{lv} and D_{rv})

Figs. 5.1 and 5.2 demonstrate the data distribution of the
transverse diameter of the left ventricle in the end-diastolic
(ED) and end-systolic (ES) phase of the cardiac cycle against
gestational age, and the linear regression line. There is a
linear increase in the transverse diameter of the left
ventricle both in the end-diastolic (ED)($p < 0.001$) and end-
systolic (ES) phase ($p < 0.001$) of the cardiac cycle. The
slope of the regression line is 0.49 mm wk^{-1} in the end-
diastolic (ED) and 0.44 mm wk^{-1} in the end-systolic (ES)
phase.

Figs. 5.3 and 5.4 show the transverse diameter of the right
ventricle in the end-diastolic (ED) and end-systolic (ES)
phase of the cardiac cycle. Here also, a linear increase in
the transverse diameter can be observed (ED: $p < 0.001$;
ES: $p < 0.001$). The slope of the regression line is 0.49
mm wk^{-1} in the end-diastolic (ED) and 0.44 mm wk^{-1} in the
end-systolic (ES) phase. The ratio between the right and left
ventricular transverse diameter ($\frac{D_{rv}}{D_{lv}}$) at corresponding
moments in the cardiac cycle was related to age.
No significant change in ratio was observed between 28 and 41
weeks of gestation (Figs. 5.5 and 5.6). For the entire
antenatal study period the mean right-to-left ventricular
ratio was 1.00 ± 0.04 during end-diastole (ED) and

1.00 ± 0.04 during end-systole (ES).

Figs. 5.7 and 5.8 represent the data distribution and mean
values of the transverse diameter of the left ventricle
during end-diastole (ED) and end-systole (ES) within 12 hours
before and 10 minutes, 4 hours, 24 and 48 hours following
delivery. A significant increase ($p < 0.01$) in transverse
diameter during end-diastole (ED) from 17.7 to 19.2 mm could
be observed within 10 minutes following delivery; this was
followed by a fairly constant pattern during the remainder
of the study period. The increase in transverse diameter
immediately following delivery, was also significant during
end-systole (ES)($p=0.02$), i.e. from 14.1 to 15.0 mm. However,
from this moment no further changes occurred. The transverse
diameter of the right ventricle (Figs. 5.9 and 5.10)
demonstrated a highly significant reduction in size
immediately following delivery from 17.7 to 10.5 mm during
end-diastole (ED)($p < 0.01$) and from 14.3 to 8.8 mm during
end-systole (ES)($p < 0.01$). During the remainder of the study
period the transverse diameter stayed virtually unaltered.
The right-to-left ventricular ratio (Figs. 5.11 and 5.12)
underwent a significant reduction within 10 minutes following
delivery from 1.00 to 0.55 during end-diastole (ED)($p < 0.01$)
and from 1.00 to 0.59 during end-systole (ES)($p < 0.01$).
This reduction continued till 4 hours following delivery.

5.1.1 Discussion

Up until 10 years ago, published data on fetal heart size
were restricted to measurements obtained from autopsies.
Garrett and Robinson (1970) were the first to measure heart
size in live fetuses using a compound-B scanner. They showed
the greatest transverse diameter of the heart to be about 50%
of the corresponding diameter of the chest. There was no
difference in growth between the fetal heart and chest in the
last 8 weeks of pregnancy. The heart occupies 21% of the

cross-sectional area of the chest. Later, Suzuki et al (1974), using a compound-B scanner, established fetal total cardiac volume during the last trimester of pregnancy, whereby it was assumed that the configuration of the heart approaches a prolate ellipse. Values from 20 to 60 ml were found. Only a limited number of reports is available on cardiac ventricular geometry in the human fetus and early neonate. The published data were either obtained from a compound-B scanner, a two-dimensional real-time system or from T-M recordings. Comparison of the results derived from these three different methods is difficult, particularly since the first scanning technique must be considered less accurate with regard to the delineation of the endocardial lining of both ventricles and the definition of the end-diastolic and end-systolic phase of the cardiac cycle. The low success rate in the studies by Garrett and Robinson (1970) and Winsberg (1972) is understandable in the light of the less-developed equipment available at that time (Table 5.1). However, even in a more sophisticated set-up as has been employed in our own study, an antenatal success rate of only 67% (Wladimiroff et al, 1979) and 78% (present study) had to be accepted. The success rate of 72% in Sahn's study (1980) is partly based on the fact that when the fetal lie was unsatisfactory, the mother was often asked to return at a later time, at which time the examination was successfully completed. When looking at the actual figures for the left ventricular transverse diameter as produced by the various investigators, again problems arise. Whereas Winsberg (1972), Allan et al (1982) and ourselves (Wladimiroff et al, 1979; present study) have carried out measurements from long-axis views of the fetal heart at the level of the mitral valve leaflets, Sahn et al (1980), as well as Garrett and Robinson (1970), studied left and right ventricular geometry from 4-chamber views. In neither study a difference between the end-diastolic and end-systolic phase of the cardiac cycle was made, although Sahn had carried out all his measurements on a real-time scanner. It is not surprising that with differences in equipment, scanning planes and periods of

54

pregnancy during which the measurements were made the results
have been variable.

Both transverse and longitudinal axis measurements on the
fetal left and right ventricle have also been performed in
the fetal lamb. Kirkpatrick et al (1973) using ultrasound in
a chronically instrumented lamb at term measured a left
ventricular transverse diameter of 12.5 $\pm$ 0.3 mm (1 SEM) in
end-diastole (ED) and 9.5 $\pm$ 0.4 mm (1 SEM) in end-systole (ES).
These values are much smaller than those found by ourselves
in the human fetus. This is probably largely due to the fact
that in the lamb experiment the ultrasonic crystals were not
placed perpendicular to the longitudinal axis of the left
ventricle but in the sulcus just posterior to the papillary
muscle, across a chord rather than at the true maximum
internal diameter. There are also a number of anatomical
studies on the fetal left-to-right ventricular relationship
available. Spigelius (1626) and Harvey (1628) in the 17th
chapter of the Motis Cordis recognized that in the human fetus
and newborn the left and right ventricular wall are
of approximately equal thickness. During the last century,
however, some doubts have arisen as to their exact equality.
These doubts could be mainly ascribed to the work by Müller
(1883), although later it appeared that there were serious
flaws in the selection of material and methods used in this
particular study. From more recent work it seems that the
two ventricles are of equal thickness in mid-gestation, but
that there is a slight right ventricular preponderance at
term (Hort, 1955, 1966; Emery and MacDonald, 1960; Recavarren
and Arias-Stella, 1964). Emery and Mithal (1961) reported a
mean weight of the left ventricle at birth of 5.7 $\pm$ 1.1 gr
(1 SD) and of the right ventricle 6.3 $\pm$ 1.4 gr (1 SD). Keen
(1955) and Hort (1966) used only the free walls of the
ventricles. Keen concluded that both ventricles were of
approximate equality at term, whereas Hort found the left
ventricle to be smaller. The difference was ascribed to a
difference in the plane of sections. Hort also concluded

that at birth the external surface of the right ventricular
wall was larger than the left.

Ventricular weights were also studied in the lamb and pig.
The advantage here is that in contrast to the human fetus
which had usually died from progressive asphyxia, freshly
killed animal fetuses could be studied. Both in the fetal
lamb (Dawes, Mott and Widdicombe, 1954; Romero, Covell and
Friedman, 1972) and in the pig (Yuan, Heymann and Rudolph,
1966) no significant difference in left and right ventricular
weight could be established. Dawes (1969) suggested that
either there is a species difference or the ventricular
inequality in man at birth is determined by the mode of death
or the method used to weigh the ventricles.

From Table 5.2 it can be seen that during the early neonatal
period only limited data on cardiac geometry are available.
The success rate in obtaining a particular cardiac plane for
geometric measurements was low, not only by using a compound-B
scanner (Winsberg, 1972) but also by using a real-time method
(Sahn et al, 1980). The recording failures in the study by
Wladimiroff et al (1980) and in the present work were always
due to problems in the antenatal measurement. Since these
were longitudinal studies, failure to obtain a satisfactory
antenatal recording resulted in dropping the patient from
the neonatal follow-up altogether. For reasons similar to
those pointed-out in the discussion on the antenatal data in
Table 5.1, comparison of results from different investigators
is difficult. Although reasonable agreement exists on left
ventricular transverse diameter during the end-diastolic (ED)
phase of the cardiac cycle as reported by Winsberg (1972),
Wladimiroff et al (1980) and ourselves, left ventricular
transverse diameter during the end-systolic (ES) phase in the
present study is significantly larger than that observed by
Winsberg. There is also a substantial difference in right-to-
left ventricular ratio as obtained by Sahn et al (1980) and
ourselves. The marked reduction in neonatal right ventricular

56

transverse diameter (69% in end-diastole (ED) and 63% in end-
systole (ES)) and therefore in right-to-left ventricular ratio
is in agreement with findings in the neonatal pig in which the
right ventricle adopts a more shell-shaped size, whereas the
left ventricle retains its original balloon-like shape
(Harinck, 1974; Versprille et al, 1977). These animal
experimental data suggested that the observed reduction in
right ventricular transverse diameter is caused by functional
geometric changes induced by loading one side of the heart
following clamping of the cord and subsequent lung expansion.
In contrast to the pronounced change in right ventricular
transverse diameter, the left ventricular transverse diameter
soon after birth exhibits only a slight increase of 9% in
end-diastole (ED) and 8% in end-systole (ES) as a result of
the rise in aortic pressure. Serial sonocardiometric measure-
ments in the lamb from late term through birth demonstrated
an initial increase of ± 8% in left ventricular transverse
diameter as the chest was delivered and a further increase
of ± 5% with the onset of pulmonary ventilation
(Kirkpatrick et al, 1973). These figures are close to the
8-9% calculated in our own study. The constancy of the left
and right ventricular transverse diameter values during the
remainder of the neonatal study period underlines the very
short period following delivery during which the changes in
left and right ventricular size take place.

Anatomical studies on human neonatal hearts have shown that
after birth the left ventricular wall grows rapidly while the
right does not. The free wall of the right ventricle has even
been found to be reduced in weight by 20% over the first
month after birth (Keen, 1955; Hort, 1955). Emery and Mithal
(1961), however, pointed out that the left ventricular weight
preponderance which they established by the end of the 4th
week of life is not due to atrophy of the right ventricle,
but is the product of difference in growth. Left ventricular
preponderance was established at an even earlier stage in
the neonatal lamb (Romero et al, 1972): at 7-14 days following

delivery the free wall of the right ventricle was reported to be about 25% heavier than that of the fetal right ventricle, whereas the free wall of the left ventricle had almost doubled in weight.

5.2 Left ventricular volume (Q_{lv})

Wladimiroff and McGhie (1981a) developed a method for estimating left ventricular volume from two-dimensional real-time ultrasonic images. The scanning plane through the long-axis of the fetal heart was identical to that used for the M-mode studies (Paragraph 3.1.1). The dynamics of the largest longitudinal cross-section through the left ventricle was recorded on video tape during 10 to 15 cardiac cycles. Based on a fetal heart rate between 120 and 150 beats per minute which corresponds with a beat-to-beat interval between 400 and 500 milliseconds and an image repetition frequency of the video-display of 20 milliseconds, 25 consecutive still frames within one cardiac cycle were studied for establishing the end-diastolic (ED) and end-systolic (ES) phase of the left ventricle. In the final step the transverse and the longitudinal axis of the left ventricle were measured by means of a computer-linked light pen system. The transverse axis was measured at the level of the mitral valve leaflets and ran from the endocardial surface of the intraventricular septum to the endocardial surface of the left ventricular posterior wall. The longitudinal axis ran from the base of the aortic root to the endocardial surface of the left ventricular apex. The end-diastolic (ED) phase of the cardiac cycle was determined by the largest, the end-systolic (ES) phase by the smallest measurement of this particular axis. The longitudinal axis of the right ventricle could not be obtained since the pulmonary trunk does not show in this particular scanning plane. In each subject, three consecutive cardiac cycles of acceptable technical quality were studied this way and the mean value for the transverse and

longitudinal axis of the left ventricle in the end-diastolic
(ED) and end-systolic (ES) position calculated. The measuring
error in 95% of the recordings studied was, in the transverse
axis 4.9% or less in the end-diastolic (ED), and 4.7% or less
in the end-systolic (ES) position. For the longitudinal axis
it was 4.0% or less in the end-diastolic (ED) and 4.1% or less
in the end-systolic (ES) position.

Based on the assumption that the antero-posterior axis of the
left ventricle, which cannot be measured, is equal to the
transverse axis and the shape of the left ventricle is
approaching a prolate ellipsoid, an estimation of left
ventricular volume (Q_{lv}) can be made, using the following
formula (Ten Cate et al, 1974):

$$Q_{lv} \ (ml) \ = \ \frac{\Pi}{6} \text{ x transverse axis}^2 \text{ x longitudinal axis}$$

The results showed that in the 3rd trimester of pregnancy
the longitudinal-to-transverse axis ratio of the left
ventricle is 1.75 $\pm$ 0.1 (1 SD) during the end-diastolic (ED)
phase and 1.90 $\pm$ 0.1 (1 SD) during the end-systolic (ES) phase
of the cardiac cycle. A separate study carried out on 10
infants during the first two days after birth showed an
unaltered relationship between the two diameters. This is in
agreement with the finding that the shape of the left
ventricle does not change significantly during this period
of early neonatal life. From the above-mentioned it was
decided to multiply the transverse diameter of the fetal and
neonatal left ventricle measured from M-mode recordings by
1.75 during end-diastole (ED) and by 1.90 during end-systole
(ES) in order to obtain an estimate of the longitudinal axis
of the left ventricle.

Antenatally there is a curvilinear increase in left
ventricular volume (Q_{lv}) both during the end-diastolic (Q_{lved})
(Fig. 5.13) and end-systolic (Q_{lves}) phase (Fig. 5.14) of
the cardiac cycle. Due to this curvilinear increase in volume,

the mean values for Q_{lved} and Q_{lves} were calculated for each week of gestation. Q_{lved} rose from 1.5 ml and Q_{lves} from 0.7 ml at 28 weeks to 5.6 ml and 2.8 ml respectively at 40 weeks of gestation ($p < 0.001$). During the first 10 minutes following delivery a further rise in Q_{lved} from 5.5 ml to 6.6 ml; $p < 0.01$ (Fig. 5.15) and Q_{lves} from 2.7 to 3.2 ml; p 0.05 (Fig. 5.16) was noted. During the remainder of the neonatal period no significant change in Q_{lv} occurred.

5.2.1 Discussion

Assessment of volume was restricted to the left ventricle, since no information could be obtained on the longitudinal axis of the right ventricle on the same long-axis plane. For the calculation of left ventricular volume during the end-diastolic and end-systolic phase of the cardiac cycle, assumptions were made for the shape of the left ventricle as well as for the relationship between the transverse and antero-posterior diameter of the ventricle. The theoretical basis for the prolate ellipsoid shape of the left ventricle was originally derived from angiographic studies in the adult (Dodge et al, 1960; Davila and Sanmarco, 1966; Hermann and Bartle, 1968). Later studies of our own based on human fetal autopsy specimens support this approach. It is clear that, based on the previous assumption that the antero-posterior axis of the left ventricle is equal to the transverse axis and the shape is approaching a prolate ellipse, the values for left ventricular volume presented in the cross-sectional and longitudinal study should only be considered to be an approximation rather than a true representation of that ventricular volume. Verification of our data was not possible due to the absence of comparative studies in the literature.

5.3 Thickness of the intraventricular septum (T_{vs})

Antenatally, the change in the intraventricular septal
thickness depicted a linear increase, both in the end-
diastolic (ED)(p < 0.001, Fig. 5.17) and end-systolic (ES)
phase (p < 0.001, Fig. 5.18) of the cardiac cycle. During
the first 4 hours following delivery, a further rise in
thickness could be observed during end-systole (ES)(Fig.
5.19), i.e. within 10 minutes: from 2.6 to 3.8 mm (p < 0.01);
at 4 hours: from 3.8 to 4.4 mm (p < 0.01). During end-diastole
(ED) no significant changes occurred (Fig. 5.20).

5.3.1 Discussion

From our data on intraventricular septal thickness it appears
that during the antenatal period there is no significant
difference in septal thickness between end-diastolic and
end-systolic phase of the cardiac cycle. The increase in
septal thickness from 28 weeks to 40 weeks of gestation was
33% (end-diastole, ED) and 32% (end-systole, ES) respectively.
Comparable data on septal thickness are only available from
two other studies. In one study carried-out in the human
fetus (Allan et al, 1982) slightly higher septal thickness
values were found. The number of observations between 28 and
40 weeks was, however, much smaller (n=42) than that in our
own study. In another study in fetal dogs (Williams et al,
1978) near term values of 2.08 $\pm$ 0.27 mm (1 SD) at aortic
valve level and 2.83 $\pm$ 0.40 mm (1 SD) at mid-ventricular
wall level were found. This implies that septal thickness
varies considerably with respect to the level at which the
measurement is carried out. Our septal thickness values at
term of 2.6 mm in the end-diastolic phase and 2.5 mm in the
end-systolic phase of the cardiac cycle are in reasonable
agreement with those observed in dogs, since in our study
the level of measurement is nearer to the mid-ventricular
than the aortic valve level. Antenatal information on septal

development was also obtained from weight studies in the
human fetus, in which the septum was either kept separate
(Keen, 1955) or allotted between the left and right ventricle
in proportion to their respective weight (Müller, 1883; Lewis,
1914; Herrmann and Wilson, 1922). Anatomical studies (Fulton
et al, 1952; Keen, 1955) have shown that the septum in its
increase follows the free wall of the left ventricle closely
and is not influenced by the behaviour of the right
ventricular free wall. Hislop and Reid (1972) also found that
the septum grew with the left ventricle rather than with the
right, supporting the two previous investigators. However,
this does not mean that the septum, by its contraction, does
not assist the right and left ventricle. From these studies
it also appeared that the increase in intraventricular septal
weight during the 3rd trimester of pregnancy is approximately
200-250%. At term the weight of the septum averaged about 18%
of the total ventricular weight. In the neonatal period the
intraventricular septal thickness showed a pronounced increase
of 46% during the end-systolic phase, whereas no significant
changes occurred during the end-diastolic phase of the cardiac
cycle. The significance of these changes with respect to
ventricular function will be discussed in Chapter 6.

5.4 Summary

A. Combined use of two-dimensional real-time and M-mode
   technique as described in Chapter 3 provides an acceptable
   M-mode recording of 3rd-trimester fetal and early neonatal
   ventricular transverse diameter and septal thickness in
   over three quarters of the subjects studied.
B. During the 3rd trimester of pregnancy left and right
   ventricular transverse diameter were equal in size both
   during the end-diastolic and end-systolic phase of the
   cardiac cycle. They followed a linear growth pattern.
   Left ventricular volume followed a curvilinear growth
   profile resulting in an increase, which is approximately

4-fold; left ventricular volume during the end-diastolic phase of the cardiac cycle was about twice that during the end-systolic phase. The intraventricular septal thickness showed a linear increase of 33%. There was no difference in septal thickness between the end-diastolic and end-systolic phase of the cardiac cycle.

C. Immediately following delivery left ventricular transverse diameter and volume were characterized by a slight further increase, whereas the right ventricular diameter underwent a marked reduction, caused by functional geometric changes induced by loading one side of the heart. During the remaining 48 hours no significant changes in ventricular size could be observed. The intraventricular septum showed a further pronounced dimensional increase of 46% during the end-systolic phase without any significant change during the end-diastolic phase of the cardiac cycle.

Chapter 6

NORMAL VENTRICULAR DYNAMICS DURING THE LAST TRIMESTER OF
PREGNANCY AND EARLY NEONATAL PERIOD

As already has been explained in Chapter 3, in each patient
the beat-to-beat interval was measured to the nearest 5 msec
and a mean value over 10 consecutive cardiac cycles was
subsequently calculated. Since the observed neonatal changes
in right ventricular size, discussed in Chapter 5, are most
likely geometrically determined, the neonatal cardiac
functions, studied, were only derived from left ventricular
data.

6.1 Beat-to-beat interval

Fig. 6.1 represents the beat-to-beat interval for 193 normal
pregnancies between 28 and 41 weeks of gestation. There was
a wide distribution of the individual data and no relationship
between this dynamic variable and gestational age. Postnatally
there was a rise in beat-to-beat interval (Fig. 6.2) which
became significant 4 hours following delivery ($p < 0.05$).
The remainder of the neonatal study period was characterized
by a stable interval.

6.1.1 Discussion

Beat-to-beat interval is influenced by conditions such as age,
circadian rhythm, stress, hypoxia, drugs and a number of
pregnancy-related diseases (i.e. diabetes mellitus, hyper-
tension etc.). In our study a normal pregnant population was
investigated. In the fetal study, mothers were always placed
in supine position, during the afternoon between 2.00 and
5.00 hours, and no drugs were administered.

64

As already stated in Paragraph 4.1.1 birth weight was always
between 10th and 90th percentile for weight of gestation
according to the Tables of Kloosterman (1970) and the Apgar
score at 1 minute was 8 or more. Visser et al (1981) observed
a reduction in fetal heart rate between 24 and 40 weeks with
a tendency to rise thereafter. We did not observe any
significant change in beat-to-beat interval relative to
gestational age. The variation in heart rate was always
within the range of 3-15 beats min^{-1}, which means that no
M-mode recordings were collected during an acceleration
(>15 beats min^{-1}) or deceleration (>15 beats min^{-1}) of the
fetal heart rate. During the first 10 minutes following
delivery, a slight increase in beat-to-beat interval was
noted. These findings disagree with those reported by Cordero
(1972) and de Jong et al (1974), who observed an elevation of
heart rate immediately following delivery. This difference
may be explained by the fact that the recordings in our study
were nearly always produced near the 10 minute time mark
rather than the first few minutes following delivery. This
would mean that we missed the increase in heart rate which
apparently occurs in the first few minutes following birth.
Mean beat-to-beat interval demonstrated a further rise to a
maximum of 490 msec at 4 hours.

6.2 Left and right ventricular shortening (ΔD_{lv} and ΔD_{rv})

The shortening (ΔD) of the transverse diameter (D) of the
left and right ventricle during systole is expressed by the
following formula:

$$\Delta D \ (mm) \ = \ D_{ed} - D_{es}$$

Antenatally (Figs. 6.3 and 6.4) there was a linear increase
in ΔD from 3.3 to 3.9 mm for the left ventricle (p < 0.001)
and from 3.3   4.0 mm for the right ventricle (p < 0.001).
The first 10 minute period following delivery is characterized

by a rise in left ventricular shortening (ΔD_{lv}, Fig. 6.5) from 3.8 to 4.3 mm (p = 0.02). As stated in the introduction of this chapter no functional data from the neonatal right ventricle were obtained.

6.2.1 Discussion

The antenatal rise in left and right ventricular shortening (ΔD_{lv} and ΔD_{rv}, Figs. 5.1-5.4) may reflect increasing circulatory demands associated with fetal growth. The data also indicate functional equality of both ventricles. The presence of an intrinsic relationship between resting (end-diastolic) fibre length and cardiac performance has been pointed out in several studies utilizing isolated cardiac muscle (Friedman, 1972), chick embryo (Faber et al, 1974) and acute intact fetal lamb models (Brinkman et al, 1965) or neonatal lamb models (Downing et al, 1965). In the adult animal and man, changes in extent of ventricular shortening and stroke volume as a result of changes in end-diastolic fibre length, i.e. the Frank-Starling mechanism (Frank, 1895; Starling, 1918) is well-established. In the fetus, however, some controversy existed as to the presence and importance of the Frank-Starling mechanism in the intact fetal heart. Rudolph and Heymann (1974) in chronically instrumented fetal lamb suggested that the Frank-Starling mechanism was of minor importance compared with the role of changing heart rate. Kirkpatrick et al (1976), however, pointed out that the fetuses in this particular study were operating close to the apex of their respective ventricular function curves since their end-diastolic pressures at rest were above the upper limit of the normal range (2.5-8 mmHg). Another criticism was the non-physiological way of changing fetal heart rate: bradycardia by vagal stimulation, tachycardia by atrial pacing. Kirkpatrick et al (1976) noted in their chronically instrumented fetal lambs during both spontaneous changes of heart rate and variations due to respiratory

66

efforts, changes in left ventricular end-diastolic diameter,
which resulted in alterations of stroke volume that maintained
a stable cardiac output. These data demonstrate that the
Frank-Starling mechanism is effective in the fetal lamb.
In our own antenatal study, the cross-sectional design did
not allow us to examine the effect of fetal heart rate on
left ventricular end-diastolic diameter. Moreover, all
recordings were obtained during fetal apnoea. The increase
in left ventricular ED-diameter following delivery was not
accompanied by a change in beat-to-beat interval (Fig. 6.2).
The increase in left ventricular ED-diameter and therefore
of shortening, is rather, determined by circulatory
alterations which following birth, impose on the left
ventricle both an added volume and pressure load. With the
onset of breathing pulmonary vascular resistance is markedly
reduced (Dawes et al, 1953). Closure of the low-resistance
placental circuit causes an increase in aortic pressure
(Dawes et al, 1953) and closure of the ductus arteriosus is
associated with a further rise in aortic pressure (Dawes et
al, 1955). This would result in a reduction of stroke volume
for a given left ventricular ED-diameter and pressure. Since
blood flow to the left side of the heart will increase, this
will result in a larger end-diastolic fibrelength.

6.3 Left ventricular stroke volume (Q_{lvs}), output (Q'_{lv})
   and ejection fraction ($\frac{Q_{lvs}}{Q_{lved}}$)

6.3.1 Left ventricular stroke volume (Q_{lvs})

The difference between left ventricular volume in the end-
diastolic (Q_{lved}) and end-systolic (Q_{lves}) phase of the
cardiac cycle represents left ventricular stroke volume
(Q_{lvs}). Likewise left ventricular volume (Q_{lv}), Q_{lvs}
demonstrated a curvilinear increase during the last
trimester of pregnancy (Fig. 6.6). The mean Q_{lvs} value for
each week of pregnancy was therefore presented. Mean Q_{lvs}

rose from 0.9 ml at 28 weeks to 2.8 ml at 40 weeks of
gestation (p < 0.001). From the antenatal-neonatal study
there appeared to be a further increase in Q_{lvs} during the
first 24 hours following delivery (Fig. 6.7), i.e. from 2.7
ml before, to 3.4 ml within 10 minutes after delivery
(p < 0.01), and up to 3.5 and 3.6 ml 4 hours, 24 hours and
48 hours later.

6.3.2 Left ventricular output (Q'_{lv})

Left ventriucular output (Q'_{lv}) was calculated from the
product of stroke volume and heart rate. Mean Q'_{lv} increased
in a curvilinear fashion from 125 ml min^{-1} at 28 weeks to
391 ml min^{-1} at 40 weeks of gestation (p < 0.001, Fig. 6.8).
A further marked increase in Q'_{lv} occurred within 10 minutes
following delivery from 379 to 467 ml min^{-1} (p < 0.001, Fig.
6.9). In 19 patients fetal Q'_{lv} measurements were carried
out within 7 days of delivery allowing calculation of fetal
Q'_{lv} per kg body weight (Table 6.1). A mean volume of 126 $\pm$
11 ml $kg^{-1}min^{-1}$ was found. In 15 out of 19 patients there
were also neonatal Q'_{lv} values available within 10 minutes
following delivery. A mean volume of 151 $\pm$ 12 ml $kg^{-1}min^{-1}$
was calculated (Table 6.1).

6.3.3 Left ventricular ejection fraction ($\frac{Q_{lvs}}{Q_{lved}}$)

Left ventricular ejection fraction ($\frac{Q_{lvs}}{Q_{lved}}$) was obtained from
the following formula:

$$\frac{Q_{lvs}}{Q_{lved}} \% = \frac{Q_{lved} - Q_{lves}}{Q_{lved}} \times 100$$

Antenatally (Fig. 6.10) there was a significant linear
reduction in $\frac{Q_{lvs}}{Q_{lved}}$ from 60% at 28 weeks to 50% at 40 weeks
(p < 0.001).

68

During the neonatal period no marked changes in $\frac{Q_{lvs}}{Q_{lved}}$ were observed (Fig. 6.11).

6.3.4 Discussion

Since the changes at birth have a profound influence on the circulation, data on fetal and neonatal left ventricular stroke volume, output and ejection fraction will be discussed separately.

6.3.4.1 Fetal left ventricular function

For a better understanding of fetal ventricular function, a short review of the fetal circulation will be presented.

6.3.4.1a Fetal circulation

Most of our current knowledge of the fetal circulation was obtained from experimental work in the fetal lamb. The principle characteristics of the fetal circulation are the following:
- both parts of the heart work in parallel to drive blood from the great veins to the aorta via two shunts: the foramen ovale at atrial level and the ductus arteriosus at arterial level;
- both shunts have a low flow resistance;
- the systemic circulation has a low flow resistance as a result of a low parallel resistance in the placental circuit;
- umbilical venous return reaches the inferior vena cava partly via the ductus venosus (40-60%) and partly via the portal circulation.
With respect to the distribution of blood to the various parts of the fetal body, most data are presented as a fraction of the combined output of both ventricles, which seems

reasonable on the basis of the parallel function of the fetal
ventricles. Venous return via the inferior vena cava provides
about 70% of combined ventricular output and the venous return
via the superior vena cava about 20%. Only very small amounts
of return from the superior vena cava crosses the foramen
ovale, whereas about 40% of the venous return via the inferior
vena cava representing 30% of combined ventricular output
crosses the foramen ovale into the left atrium. About 80%
of the right ventricular output passes across the ductus
arteriosus to the descending aorta (data derived from Rudolph
and Heymann, 1974). Only about 20% of the right ventricular
output goes to the lungs because of a relative high
pulmonary resistance. This high resistance is mainly the
result of low lung tissue PO_2 (Dawes et al, 1953; Reynolds,
1956; Lauer et al, 1965). The placenta receives 40-50% of
the combined ventricular output.

6.3.4.1b Left ventricular stroke volume (Q_{lvs}), output (Q'_{lv})
        and ejection fraction $(\frac{Q_{lvs}}{Q_{lved}})$

In our own study both fetal Q_{lvs} and Q'_{lv} showed a 3-fold
increase during the third trimester of pregnancy. In Fig.
6.12 both mean Q'_{lv} values and 50 percentile fetal weight
values for male infants of primigravida (Tables of Klooster-
man, 1970) have been plotted against gestational age. From
this figure it can be seen that Q'_{lv} parallels fetal weight
with advancing gestation. Similar observations were made in
the fetal lamb between 60 and 147 days of gestation (Rudolph
and Heymann, 1970). Considerable data are available on the
actual ventricular output per kg fetal body weight. Table
6.2 demonstrates that the vast majority of ventricular output
estimations were derived from the fetal lamb. Initially,
measurements were carried out under acute circumstances in
fetal lambs exteriorized from the uterus with umbilical-
placental blood flow maintained (Dawes et al, 1954; Assali
et al, 1965; Mahon et al, 1966; Rudolph et al, 1967). With

70

the employment of this set-up, combined ventricular output
has been measured by either the Fick method (Dawes et al,
1954), indicator dilution curves (Mahon et al, 1966) or
electromagnetic flow transducers (Assali et al, 1965). It
has been demonstrated that exteriorization of the fetus from
its intrauterine environment results in a progressive fall
in umbilical blood flow both in the lamb (Heymann and Rudolph,
1967) and previable human fetus (Rudolph et al, 1971).
Chronically instrumented fetal lambs which were kept in utero
offered data which could be considered nearer the
physiological situation (Rudolp et al, 1974; Faber and Green,
1972; Kirkpatrick et al, 1975; Rudolph and Heymann, 1977;
Anderson et al, 1981). Only two ultrasonic studies on fetal
ventricular output have been reported in the literature
(Winsberg, 1972; Wladimiroff and McGhie, 1981). Obviously
ultrasound, being a non-invasive technique, provides only
indirect information on cardiac function. On the other hand,
because of its non-invasiveness it is the only technique
allowing assessment of cardiac function in the human fetus
under entirely physiological circumstances. The gestational
age at which the ventricular output studies were conducted
varied considerably between the different investigators. It
is probably because of the different techniques of
investigation, the variable physiological circumstances and
the wide range of gestational ages that the estimated
ventricular output figures show such little agreement.

Left ventricular output in the fetal lamb varies between 97
(Assali et al, 1965) and 250 ml $kg^{-1}min^{-1}$ (Kirkpatrick et al,
1973). The ultrasonically determined Q'_{lv} values ranged
between 109 (Winsberg, 1972) and 126 ml kg^{-1} min^{-1} (present
study). Right ventricular output also showed a large variation
from 138 (Assali et al, 1965) to 327 ml $kg^{-1}min^{-1}$ (Rudolph et
al, 1974). This high value reported by Rudolph may be the
result of a decreased right to left shunt due to a rise in
left atrial pressure. This may be determined by the geometric
influence of the flow probes on the left side of the heart.

In a number of fetal lamb studies only combined ventricular output values were presented. Combined ventricular output was calculated as being as low as 235 ml $kg^{-1}min^{-1}$ (Assali et al, 1965) and as high as 1080 ml $kg^{-1}min^{-1}$ (Rudolph et al, 1967). Another striking detail in these fetal ventricular output studies is the difference of opinion on the contribution of each ventricle to the total output. Right-to-left ventricular output relationship varied from equal (50%-50%, Mahon et al, 1966) to left ventricular preponderance (45%-55%, Dawes et al, 1954) or right ventricular preponderance (59%-41% by Assali et al, 1965, 60%-40% by Anderson et al, 1981 and 67%-33% by Rudolph et al, 1974). Based on these relationships and a mean Q'_{lv} value of 126 ml $kg^{-1}min^{-1}$ in our study, an approximation of total ventricular output in the human fetus could be made. From Table 6.3 it can be seen that total ventricular output may be as low as 229 ml $kg^{-1}min^{-1}$ and as high as 382 ml $kg^{-1}min^{-1}$.

If we accept that the proportion of total cardiac output distributed to the different parts of the fetal body and to the placenta is not essentially different between the human fetus and the fetal lamb, a total cardiac output of about 250 ml $kg^{-1}min^{-1}$, i.e. a 50%-50% right-to-left ventricular relationship, seems to be likely for the following reasons:
- in the fetal lamb, about 70% of the total cardiac output is directed to the descending aorta (Shinebourne, 1974) and 40-50% to the placenta (Rudolph and Heymann, 1975).
- based on a 50%-50% right-to-left ventricular relationship a similar flow distribution pattern was observed in the human fetus: blood flow in the descending aorta based on mean velocity profiles was estimated at 170-185 ml $kg^{-1}min^{-1}$ (Wladimiroff and McGhie, 1981) and in the umbilical vein at 110-120 ml $kg^{-1}min^{-1}$ (Gill and Kossoff, 1979; Eik-Nes et al, 1980).
The magnitude of the fetal cardiac output is impressive when compared with that in the adult at rest. Together with low resistance shunts like the ductus arteriosus and placenta,

the high fetal cardiac output may represent a compensatory
mechanism of the circulation against the low oxygen levels
of the fetal blood in order to meet the high metabolic
demands of the fetal tissues.

6.3.4.2 Neonatal left ventricular function

6.3.4.2a Neonatal circulation

The haemodynamic changes following birth are primarily a
result of changes in flow resistance in two vascular areas:
the pulmonary artery and the placenta. With lung expansion
and ventilation, there is a fall in pulmonary vascular
resistance (Dawes, 1968; Rudolph et al, 1977). It was shown
that physical expansion of the lungs with gas without oxygen
produced a small drop in vascular resistance. The main effect
was related to the increased PO_2 (Assali et al, 1968; Heymann
et al, 1967). Whether oxygen has a direct dilatory effect on
the pulmonary vascular smooth muscle, or whether it stimulates
the release of a chemical mediator, is not known. There is
a possibility that kinins may be involved in the decrease in
pulmonary vascular resistance after birth because bradykinin
is a potent pulmonary vessel dilator in the fetal lamb
(Campbell et al, 1968). Recent studies (Heymann et al, 1979)
indicated that also PGE_1 may be involved in the fall in
pulmonary resistance. Severing the umbilical circulation
implies abolition of the placental circulation which results
in a rise in systemic vascular resistance. The changes just
described will have pronounced effects on the circulatory
pattern. Aortic pressure rises, pulmonary artery pressure
drops, the flow direction in the ductus arteriosus reverses
from left to right. Also the closure of the foramen ovale
is effected by the reversal of the fetal right-to-left atrial
pressure difference.

6.3.4.2b Left ventricular stroke volume (Q_{lvs}), output (Q'_{lv})
       and ejection fraction ($\frac{Q_{lvs}}{Q_{lved}}$)

An increase in ventricular output has been described which
was initially more pronounced for the right ventricle.
However, due to the left-to-right shunt of well-oxygenated
blood the ductus arteriosus closes and right ventricular
output soon becomes virtually equal. Actual figures of
ventricular output reported in the literature and obtained
from the present study are given in Table 6.4. As in the
fetus, ventricular output values measured in the early
neonate varied considerably. An initial discrepancy in left
and right ventricular output was found by Burnard (1966) in
the human neonate. In our own study a significant increase
in mean Q_{lvs} (2.7$\rightarrow$3.4 ml) and in mean Q'_{lv} (379$\rightarrow$467 ml min^{-1}
or 126$\rightarrow$151 ml kg^{-1}min^{-1}) was noted. This increase may reflect
not only the closure of the low-resistance placental circuit,
but also the need for increased blood flow to the brown
adipose tissue, which is responsible for the metabolic
response (heat production) to the relatively cold extrauterine
environment, in which the newborn finds itself immediately
after birth (Dawes, 1968). If the aortic pressure rises from
about 45$\rightarrow$65 mmHg and the systemic flow from 126$\rightarrow$151 ml kg^{-1}
min^{-1} and given that the venous pressure remaines unchanged,
the systemic resistance will increase by a factor 65/45 x
126/151 = about 1.2. This is less than the factor 2 which one
would expect on the basis of abolition of the placental
circuit which is perfused by about half the combined cardiac
output. This smaller than expected rise in peripheral
resistance indicates vasodilation elsewhere in the neonatal
circulation such as intestinal tract, kidneys, liver and the
brown adipose tissue. Whereas Q_{lvs} stayed nearly constant
during the remainder of the study period, Q'_{lv} demonstrated
a slight fall which may be determined by the reduction of
neonatal heart rate during this period. Left ventricular
ejection fraction did not significantly change as a result
of a fairly constant end-diastolic to end-systolic ventricular

74

volume relationship.

6.4 Dynamics of the intraventricular septum

The dynamics of the intraventricular septum (IVS) are
characterized by:
- the change in thickness during systole (ΔTvs) which is
  expressed by the following formula:

$$\Delta Tvs \ (mm) \quad = \quad T_{vsed} - T_{vses}$$

- direction of IVS motion relative to the left ventricular
  posterior wall during systole, measured at the level of
  the mitral valve leaflets.

6.4.1 The change in IVS thickness during systole (ΔTvs)

Antenatally there was virtually no change in septal thickness
(Fig. 6.13; mean value 0.06 ± 0.2 mm), whereas neonatally
an increase in septal thickness occurred during systole
(Fig. 6.14) from 0.02 mm before delivery to 0.9 mm within
10 minutes ($p < 0.01$) and 1.4 mm 4 hours following delivery
($p < 0.01$).

6.4.2 Direction of IVS motion relative to the left ventricular
      posterior wall during systole

The septal motion in healthy adults and neonates clearly
suggests the contribution of septal contraction to left
ventricular pump function. Study of septal motion may
therefore indicate this function for the fetus as well.
During the antenatal period (Table 6.5), in over half the
cases (56%) no measurable septal motion during systole was
observed. Septal motion towards the left ventricular

posterior wall (non-paradox) was noted in 34% and motion away
from the left posterior wall during systole (paradox) was only
observed in 11% of the cases. There was a fairly constant
distribution of the three septal motion patterns with respect
to gestational age. Only at 40 weeks there appeared to be a
predominantly non-paradoxic septal motion pattern. Within 10
minutes following delivery (Table 6.6) septal motion was
non-paradoxic in all neonates. At 48 hours only one neonate
exhibited paradoxic septal motion.

6.4.3 Discussion

No data on the change in intraventricular septal thickness
during systole could be found in the literature. The lack of
any change in intraventricular septal thickness during the
antenatal study period suggests non-involvement of the intra-
ventricular septum in the process of ventricular contraction
and indicates functional uniformity of both ventricles.

A number of reports are available on the direction of intra-
ventricular septal motion relative to the left ventricular
posterior wall during systole as shown in Table 6.7. Although
all results were collected from M-mode recordings, they
substantially differ between the various investigators.
Winsberg (1972) and Egeblad et al (1975) noted close to or
even 100% non-paradoxic septal motion, whereas Kleinmann et
al (1978) and we observed this type of motion in only 44 and
34% of the cases studied. Of interest is the close resemblance
in percentage of paradoxic septal motion (14 and 11%) in the
studies conducted by Kleinmann et al (1978) and ourselves.
In the same studies absence of any septal motion was
established in 42 and 55% of the fetuses. The occurrence of
three different septal motion patterns under otherwise
entirely normal physiological circumstances does not
contribute to the supposition that non-paradoxic and paradoxic
septal movement reflect left and right ventricular overload.
Looking at the data for each week of gestation (Table 6.5),

76

there was no significant difference in the distribution of
the three intraventricular septal motion patterns between 28
and 39 weeks. From 39 to 40 weeks there was, however, a shift
from absent to non-paradoxic septal motion. This is more
likely to be a coincidental finding rather than some sort of
a mechanism being responsible.

The significant thickening of the intraventricular septum
during systole which was observed soon after birth implies
active involvement in left ventricular contraction. The
direction of intraventricular septal motion relative to the
left ventricular posterior wall during systole was always
non-paradoxic during the first 24 hours following delivery.
No structural or functional cardiac abnormalities were
observed in the newborn which exhibited paradoxic septal
movement 48 hours after birth. No further cardiac follow-up
was carried out, and the infant subsequently developed well.

6.5 Summary

A. During the last trimester of pregnancy no significant
   changes in beat-to-beat interval (mean: 426 msec) were
   observed. There was a significant linear increase in left
   and right ventricular shortening indicating increasing
   circulatory demands associated with fetal growth as well
   as functional equality of both ventricles. Left
   ventricular stroke volume and cardiac output demonstrated
   a 3-fold rise, resulting at term in a mean value of 2.8 ml
   and 391 ml min^{-1} (126 ml kg^{-1}min^{-1}) respectively. Total
   cardiac output in the term fetus would be about 255
   ml kg^{-1}min^{-1} in case of a 50%-50% right-to-left
   ventricular output relationship. There is a reduction in
   left ventricular ejection fraction as a result of an
   increase in left ventricular volume which is larger in
   end-diastole than in end-systole. There is virtually no
   change in septal thickness during systole suggesting

non-involvement in the process of ventricular contraction.
In more than 50% of the fetuses no measurable septal
motion during systole was observed. Paradoxic septal
movement only occurred in about 10% of the cases studied.

B. Postnatally, there was a significant rise in beat-to-beat
   interval during the first 4 hours following birth. Left
   ventricular shortening demonstrated a further rise during
   the first 10 minutes after delivery, probably to maintain
   or even increase stroke volume as a result of a larger
   blood supply. There was a further marked elevation of left
   ventricular stroke volume and cardiac output up to mean
   values of 3.4 ml and 467 ml min^{-1} (151 ml $kg^{-1}min^{-1}$)
   within 10 minutes following delivery. This increase may
   reflect both closure of the low-resistance placental
   circuit and the necessary increase in blood flow to the
   brown adipose tissue in order to compensate for the heat
   loss in the newborn immediately after birth. Left
   ventricular ejection fraction did not change significantly.
   There is a pronounced thickening of the intraventricular
   septum during systole indicating active involvement of
   the septum in ventricular contractility. The septal motion
   is predominantly non-paradoxic.

Chapter 7

VENTRICULAR GEOMETRY AND DYNAMICS IN THE GROWTH-RETARDED
FETUS

This chapter deals with cardiac ventricular geometry and
dynamics in the growth-retarded fetus during the last
trimester of pregnancy. As described for normal pregnancies
ten consecutive cardiac cycles were evaluated. As has been
mentioned in Paragraph 4.1, a technically acceptable M-mode
was collected in 19 out of 25 subjects. A maximum time inter-
val of 28 days between M-mode cardiac examination and
delivery was chosen in order to allow cardiac data to be
related to birth weight and fetal outcome in a reasonable
number of patients. The introduction of this time interval
resulted in 15 out of 19 patients available for further
analysis. In 13 patients no obvious cause for the fetal
growth retardation could be found. The remaining two patients
were hypertensive, i.e. blood pressure readings of 145/95 or
more were obtained on different occasions. There was no
oedema or proteinuria. Other relevant data are presented in
Table 7.1. Mean pregnancy duration was 34 weeks (range 28-38
weeks), the mean time interval between M-mode evaluation and
delivery was 1.4 weeks (range 0-4 weeks). Mean maternal
parity was 1.4 (range 0-5). Birth weight was below the 10th
percentile in all 15 and below the 5th percentile in 10 of
the newborns according to the Tables of Kloosterman (1970).
In two newborns (nos. 10 and 14; Table 7.1) birth weight was
situated below the 2.3rd percentile. Confirmation of growth
retardation was obtained from ultrasonic measurement of fetal
head and chest size in 14 out of 15 patients. In one patient
only fetal biparietal diameter measurements (BPD) were
carried out. Gruenwald (1963, 1966) and Naeye (1966) were the
first to point out that the head-to-trunk relationship in
small-for-dates is often essentially different from that
observed in the normal-size infant. This changed relationship

is characterized by a limited reduction of brain weight as compared with a marked weight reduction of liver, lungs and thymus. These morphological observations resulted in measurements of trunk size (chest size, upper-abdominal size) in normal and complicated pregnancy (Hansmann et al, 1973; Campbell and Wilkin, 1975; Campbell and Thoms, 1977).

Table 7.2 presents the biparietal diameter (BPD), chest area and head-to-chest ratio data classified according to the percentile limits of the normal curves produced by Bloemsma (1978). From this Table it can be seen that the majority of the BPD values and all chest values were situated below the 5th percentile of the normal curve. The head-to-chest ratio was above the 95th percentile of the normal curve in 8 out of 15 patients. At the time of the M-mode cardiac examinations, normal fetal heart rate patterns were observed reflecting satisfactory fetal condition. The majority of the infants (13) were born in good health, i.e. an Apgar score at 1 minute of 7 or more. Two infants, nos. 14 and 15, were slightly depressed at birth: the Apgar score at 1 minute was 4 and 5, at 5 minutes 8. None of the newborns exhibited any congenital abnormalities.

7.1 Fetal cardiac geometry

Table 7.3 presents the end-diastolic and end-systolic values of the transverse diameter of the left and right ventricle, the right-to-left ratio of these ventricular diameters, the left and right ventricular volumes and the intraventricular septal thickness in all individuals.

In Figs. 7.1-7.10 these geometrical data are plotted in the respective diagrams, as presented in Chapter 5. In the majority of patients, the transverse diameter of both the fetal left (D_{lv}) and right ventricle (D_{rv}) during end-diastole and end-systole was slightly reduced, i.e. nearly all values

were situated below the linear regression line (Figs. 7.1-7.4). The right-to-left ventricular ratio ($\frac{D_{rv}}{D_{lv}}$) of end-diastolic and end-systolic diameter was normal in all cases (Figs. 7.5 and 7.6). Left ventricular end-diastolic volume (Q_{lved}) was nearly always and end-systolic volume (Q_{lves}) always below the normal mean for gestational age (Figs. 7.7 and 7.8). The volumes were always reduced particularly after 33 weeks. The values for the intraventricular septal thickness (Figs. 7.9 and 7.10) showed a distribution pattern, which was rather similar to that observed for the left and right ventricular transverse diameter. The majority of the data was situated below the linear regression line, only a few clearly reflected reduced septal thickness both during end-diastole and end-systole.

7.2 Fetal cardiac dynamics

Individual data on fetal cardiac dynamics are presented in Tables 7.4 and 7.5. In Figs. 7.11-7.16 these functional data are plotted in the diagrams presented in Chapter 5. Beat-to-beat interval was not essentially different between small-for-dates and normal-size infants (Fig. 7.11). The same accounts for the left (ΔD_{lv}) and right ventricular shortening (ΔD_{rv}) values (Figs. 7.12 and 7.13) which fell well within the normal distribution pattern. All data on left ventricular stroke volume (Q_{lvs}, Fig. 7.14) fell below the normal mean values for gestational age. An overall tendency to reduced left ventricular function could also be detected in the left ventricular output (Q'_{lv}) figures (Fig. 7.15). It is of interest to note that in 10 small-for-dates which were studied within 7 days of delivery, left ventricular output per kg body weight was not essentially different from that observed in a normal population (mean 126 $\pm$ 11 (1 SD)). Finally, in 11 out of 15 small-for-dates, left ventricular ejection fraction ($\frac{Q_{lvs}}{Q_{lved}}$) was situated above the linear regression line (Fig. 7.16).

7.3 Discussion

No reports in the literature were found on ventricular
geometry and function in the small-for-date infant. We
assumed that the fetal growth retardation as observed in our
study was most likely determined by decreased uteroplacental
blood flow due to placental malfunction, since none of the
newborns showed signs of congenital infections or defects.
Moreover, serial fetal biparietal diameter (BPD) measurements
which were carried out in 10 out of 15 patients pointed at a
'late-flattening' type of growth retardation. Experiments on
rats (Wigglesworth, 1964; Winick, 1971) and rhesus monkeys
(Hill et al, 1971) as well as pathologic findings in the
human fetus (Gruenwald, 1963) suggest a relationship between
the late-flattening type of fetal growth retardation and
placental vascular insufficiency. In these studies, brain-
to-body ratio was elevated suggesting a brain sparing effect.
Indeed in 11 out of 14 patients who were ultrasonically
monitored, head-to-chest ratio was increased, in 8 cases the
ratio values were situated above the 95th percentile limit
of the normal curve. The brain sparing effect is explained
by the redistribution of blood within the fetus. This is
because of peripheral vasoconstriction and cerebral vascular
dilatation (Cohn et al, 1974) during chronic reduction of
oxygen transfer in order to maintain the circulation through
the brain and heart at the expense of blood supply to those
tissues which, in the short run, are less vital for fetal
survival. The results on cardiac geometry in the growth-
retarded fetus suggest only a moderate reduction in fetal
left and right ventricular size and intraventricular septal
thickness, particularly when taking into account the birth
weights below the 5th percentile. Only in a few cases could
a marked reduction of septal thickness be established. If
oxygen deprivation persists, the anaerobic metabolism of the
fetus becomes gradually exhausted. This will lead to myocardial
depression, decrease in ventricular force and output, hypo-
tension and eventually fetal death. In our study, fetal heart

82

rate patterns at the time of the M-mode recordings were
entirely normal, indicating a satisfactory fetal condition.
This is supported by normal right-to-left ventricular ratio
values, normal beat-to-beat intervals and normal shortening
of the left and right ventricular transverse diameter on
M-mode recordings. Although left ventricular stroke volume
and output were to some extent reduced, particularly during
the latter weeks of pregnancy, values per kg fetal body
weight were normal. This demonstrates once more the close
relationship between left ventricular output and fetal weight.
Of interest is that preliminary data on blood flow in the
descending aorta measured by a combined two-dimensional
real-time and pulsed Doppler system as introduced by Eik-Nes
et al (1980) showed fairly constant blood flow values per
kg fetal body weight (Eik-Nes et al; Wladimiroff et al, 1981).

The significance of the rise in left ventricular ejection
fraction ($\frac{Q_{lvs}}{Q_{lved}}$) is difficult to interpret for two reasons:
- there is a wide distribution of the individual normal data;
- there is a lack of any relationship between the magnitude
  of the ejection fraction and the severity of the growth
  retardation: three out of five clearly elevated ejection
  fraction values originated from 'border line' small-for-
  dates, i.e. between the 5th and 10th percentile for weight
  related to gestation (pat.no. 1, 2, 3, 9 and 10; Table
  7.4).

Finally, structural cardiac abnormalities occur more often
in the small-for-date infants, particularly in the so-called
'low profile' type of growth retardation with symmetrical
reduction of fetal head and body size. Cardiac examination
of the small-for-dates should therefore not only be restricted
to M-mode recording of the cardiac ventricles, but also
encompass an extensive search for possible structural cardiac
defects. A more detailed insight into the structural
composition of the fetal heart has been obtained by Allan et
al (1980) who related ultrasonic images of the fetal heart

to post mortem specimens. At present, a full analysis of the
structural composition and functional capacity of the fetal
heart should include the use of two-dimensional real-time
equipment together with M-mode and pulsed Doppler facilities.

7.4 Summary

- In the majority of small-for-dates, intrauterine growth
  retardation was of the 'late-flattening type'; the head-to-
  chest ratio was increased, indicating a brain sparing
  effect.
- Left and right ventricular transverse diameter and intra-
  ventricular septal thickness were generally slightly
  reduced.
- All small-for-dates demonstrated normal heart rate patterns
  at the time of cardiac M-mode recordings, indicating normal
  values for right-to-left ventricular ratio and shortening
  of the transverse diameter of both ventricles during systole.
- The slight reduction in left ventricular stroke volume and
  left ventricular output reflects reduced fetal weight rather
  than diminished ventricular function, since both stroke
  volume and output expressed per kg fetal body weight showed
  considerable agreement with the values observed in normal
  size infants.

SUMMARY

Chapter 1

Most of our present knowledge of fetal and neonatal cardio-
vascular anatomy and function is derived from chronic and
acute lamb experiments. The disadvantage of these experiments
is that many physiologic functions were influenced by the
surgery and anaesthesia.
By using ultrasound techniques it is possible to study the
human fetal and neonatal heart under physiologic conditions.
In the study, described in this thesis, the possibility of
using M-mode registration to accurately and reproducibly
measure ventricular size and intraventricular septal thick-
ness in fetal and neonatal hearts during various periods of
the cardiac cycle was investigated.
If this is so, these M-mode registrations will lead to a
greater insight into fetal and neonatal cardiac ventricular
geometry and funtion under physiologic and pathophysiologic
circumstances.

Chapter 2

In this chapter some basic principles of ultrasound
investigation, with particular reference to M-mode technique
are described. The limitations of the M-mode technique are
discussed in short. In this study a combination of single
element and a line selection from a dynamic focussed linear
array real-time system (Organon Teknika) was used.
The analysis of the M-mode registration using a computer
system with a digital tableau and light pen (Bid Pad One)
is extensively discussed.

The technique for obtaining an M-mode recording of the cardiac
ventricles in the antenatal and neonatal period is discussed
separately.

Comparison of the results from both periods is only permitted
when the same angle and cross-section through the heart has
been obtained.

The following parameters were measured to gather information
about cardiac geometry and function during the antenatal and
neonatal period:
- the end-systolic and end-diastolic transverse cross-
  section of the right and left ventricle in mm.
- the end-systolic and end-diastolic thickness of the
  intraventricular septum in mm.
- beat-to-beat interval in msec.

The accuracy and reproducibility of the measurements is
discussed. The sources of error in the measurements are
divided into systematic and random errors. The systematic
error is inherent to the intrumentation and the finite beam-
width of an ultrasound wave. The instrumentation error is
calculated at less than 0.1%. Due to the finite ultrasound
beamwidth a constant underestimation is made, resulting in
an error of approximately 10% in the volume calculations in
this study.

The random errors are due to:
- transducer positioning
- structural movement
- experience of the investigator

Reproducibility of the measurements in both periods was
established with the use of intra- and interobserver variation,
and intra- and interpatient variation. It is concluded that
the measurements obtained from the M-mode registrations are
adequately reproducible.

Chapter 4

The selection criteria of the pregnancies are stated.
Uncomplicated pregnancy and fetal growth retardation are
defined. Further, the statistical methods used to test the
results of the cross-sectional study during the antenatal
period, and the longitudinal study during the antenatal-
early neonatal period are described.

Chapter 5

In this chapter the results of normal ventricular geometry
during the last trimester of pregnancy and early neonatal
period are presented. During the third trimester there was
a linear increase in the growth of the right and left
ventricle. The transverse diameter of the ventricles is
equal, both in the end-diastolic and end-systolic phase of
the cardiac cycle.
The findings in the literature are not entirely concordant
with those of this study. Closer examination of these
findings indicate that discrepancies may be due to differences
in investigative procedures.
Left ventricular volume showed an approximately four-fold
curvilinear increase at the end of pregnancy. The volume was
approximately twice as great in end-diastole compared with
end-systole.
The intraventricular septum showed a linear increase in
thickness, revealing no difference in thickness during
end-diastole or end-systole.
Directly after birth there was a further increase in the
transverse diameter and volume of the left ventricle, while
the transverse diameter of the right ventricle showed a
clear reduction, resulting from functional geometric and
volume changes in both ventricles. After birth there was
an increase in intraventricular septal thickness only during
the end-systolic phase of the cardiac cycle.

Chapter 6

This chapter contains the results of normal ventricular
function in the last trimester and the first 48 hours after
birth. The beat-to-beat interval did not change significantly
during the third trimester of pregnancy. The right and left
ventricle showed a linear increase in shortening probably
due to increasing circulatory demands of the growing
fetus.
The left ventricular stroke volume and cardiac output
increased three-fold. Assuming an equal output of the right
and left ventricle, the total cardiac output was 255
ml kg^{-1}min^{-1} in the term fetus.
There was a reduction in left ventricular ejection fraction
caused by the larger increase in volume during end-diastole
compared with end-systole.

Intraventricular septal thickness remained nearly the same
during systole which implied that the septum played no role
during ventricular contraction. In more than 50% of the cases
there was no clear septal motion during systole, while in
10% there was paradoxic motion.
During the first four hours post partum there was a
significant increase in beat-to-beat interval. Within the
first 10 minutes after birth the left ventricular shortening
increased, as a result of higher stroke volume following
larger blood supply. Termination of placental circulation and
increased demands of blood flow to the various organs of the
neonate resulted in a rise in left ventricular output within
10 minutes of birth. No significant change in the ejection
fraction of the left ventricle was noted.

Post partum there was a clear increase in intraventricular
septal thickness during systole, in contrast to the antenatal
period. It may be concluded that the septum plays an active
role in ventricular function after birth.
A review of various authors who have calculated antenatal

and neonatal ventricular function is given. The results of these authors may not be compared with the results of our study in view of the different methods applied.

Chapter 7

This chapter deals with ventricular geometry and function in the growth retarded fetus in the last trimester of pregnancy. There is no information on this subject in the literature. Repeated measurements of fetal biparietal diameter revealed 'late-flattening' type of growth retardation in the majority of cases (10 out of 15 patients). In 11 of 14 patients the head-chest ratio was increased, suggesting a brain sparing effect. In general, the transverse diameter of the right and left ventricle and intraventricular septal thickness in the growth retarded group was less than in the group with normal growth.
All growth retarded fetuses showed normal heart rate in the investigation. This indicated normal fetal cardiovascular function, emphasised by normal values being found for right-left ratio, and shortening of both ventricular transverse diameters during systole. A reduction in left ventricular stroke volume and output points more toward lower fetal weight than decreased ventricular function. The values of left ventricular stroke volume and output per kg fetal body weight were closely related to those of fetuses with normal weight for gestational age.

SAMENVATTING

Hoofdstuk 1

Het merendeel van onze huidige kennis van de foetale en
neonatale cardiovasculaire anatomie en functie is verkregen
uit het chronische en acute lammeren experiment. Het bezwaar
van deze experimenten is dat door de chirurgische en anaes-
thesiologische procedures vele fysiologische functies werden
beïnvloed. Met behulp van ultrageluidsonderzoek is het moge-
lijk om het humane foetale en neonatale hart te bestuderen
onder geheel fysiologische omstandigheden.
In het onderzoek, beschreven in dit proefschrift, werd een
antwoord gezocht op de vraag of door middel van ultrasound
M-mode registratie nauwkeurige en reproduceerbare metingen
van de ventrikel grootte en intraventriculaire septum dikte
van het foetale en neonatale hart kunnen worden verricht
gedurende de verschillende periodes van de hartcyclus. Als
dit zo is, draagt deze M-mode registratietechniek dan bij
tot een groter inzicht in onze kennis van de foetale en
neonatale cardioventriculaire geometrie en functie zowel
onder fysiologische als pathofysiologische omstandigheden.

Hoofdstuk 2

In dit hoofdstuk worden enkele basisprincipes van het ultra-
geluidsonderzoek, voornamelijk met betrekking tot de M-mode
techniek, uiteengezet. In het kort worden de beperkingen van
de M-mode techniek besproken. Voor het eigen onderzoek werd
voor het vervaardigen van een M-mode registratie gebruik ge-
maakt van een combinatie van een single element techniek en
een lijnselectie van een dynamisch gefocusseerd linear-array
real-time systeem (Organon Teknika). Uitvoerig wordt ingegaan
op de wijze waarop een M-mode registratie werd geanalyseerd.

Dit gebeurde met behulp van een computer systeem met een digitaal tableau en lichtpen (Bid Pad One).

Hoofdstuk 3

Hierin wordt de techniek voor het verkrijgen van een M-mode registratie van de cardiale ventrikels in de antenatale en neonatale periode afzonderlijk beschreven. Vergelijking van de resultaten in beide periodes is alleen dan geoorloofd als de registraties zijn gemaakt door dezelfde doorsnede van het hart, ervoor zorg dragend dat de richting van de ultrageluids-bundel door het hart zowel antenataal als neonataal ongeveer gelijk is.

De volgende parameters werden gemeten met het doel om infor-matie te verkrijgen over de cardiale geometrie en functie gedurende de antenatale en neonatale periode:

- de transversale doorsnede in mm van de linker en rechter ventrikel in de eind-diastolische en eind-systolische fase van de hartcyclus.
- de dikte van het intraventriculaire septum in mm eveneens in de eind-diastolische en eind-systolische fase.
- het beat-to-beat interval in msec.

Vervolgens wordt ingegaan op de nauwkeurigheid en reproduceer-baarheid van de metingen. De foutenbronnen, inherent aan de meting, worden onderverdeeld in systematische en toevallige fouten.

De systematische fouten worden veroorzaakt door fouten in de instrumentatie, en fouten in de eindige bundelbreedte van een ultrageluidsgolf.

De fout in de instrumentatie wordt op minder dan 0,1% geschat. Tengevolge van de fout in de eindige bundelbreedte van de ultrageluidsgolf wordt een constante onderschatting in de metingen gemaakt; voor de volumeberekening in dit onderzoek betekent dit een fout, die geschat wordt op ongeveer 10%.

De toevallige fouten kunnen ontstaan door:
- transducerpositionering
- bewegende structuren
- ervaring van de onderzoeker

De reproduceerbaarheid van de metingen zowel in de antenatale als in de neonatale periode werd getoetst met behulp van de intra- en interobserver variatie, alsmede intra- en inter-patient variatie in de eerder genoemde parameters. Uit de resultaten mag worden geconcludeerd dat de metingen verricht aan de M-mode registraties in dit onderzoek voldoende repro-duceerbaar zijn.

Hoofdstuk 4

De criteria voor de selectie van de zwangeren worden bespro-ken. De ongestoorde zwangerschap en de foetale groeivertraging worden gedefinieerd. Tevens wordt besproken op welke wijze de resultaten van het transversale onderzoek in de antenatale periode en van het longitudinale onderzoek in de antenatale-vroeg neonatale periode statistisch zijn getoetst.

Hoofdstuk 5

In dit hoofdstuk worden de resultaten vermeld van de normale ventriculaire geometrie gedurende het laatste trimester van de zwangerschap en de vroeg neonatale periode. Gedurende het derde trimester van de zwangerschap was er een lineare toe-name van de groei van de linker en de rechter ventrikel. De transversale diameter van beide ventrikels was gelijk, zowel in de eind-diastolische als in de eind-systolische fase van de hartcyclus. De bevindingen in de literatuur komen niet geheel overeen met de onze. Doch bij de beschouwing van deze gegevens blijkt dat de verschillende resultaten nauwelijks met elkaar vergeleken kunnen worden tengevolge van de wisselende onderzoekprocedures.

92

Het linker ventrikelvolume toonde een kromlijnige toename
dat ongeveer het 4-voudige bedroeg aan het einde van de
zwangerschap. In de eind-diastolische fase was het volume
ongeveer twee maal zo groot als in de eind-systolische fase.
Het intraventriculaire septum liet eveneens een rechtlijnige
toename in dikte zien, waarbij er geen verschil was tussen
de dikte in de eind-diastolische en eind-systolische fase
van de hartcyclus.
Onmiddellijk na de geboorte was er een verdere toename in
transversale diameter en volume van de linker ventrikel waar
te nemen, terwijl de transversale diameter van de rechter
ventrikel een duidelijke afname liet zien, veroorzaakt door
functioneel geometrische veranderingen door volumeveranderin-
gen in beide hartshelften. De intraventriculaire septumdikte
nam na de geboorte alleen toe in de eind-systolische fase van
de hartcyclus.

Hoofdstuk 6

Dit hoofdstuk bevat de resultaten van de normale ventriculaire
functie gedurende het laatste trimester van de zwangerschap en
de periode tot 48 uur na de geboorte. Het beat-to-beat inter-
val toonde geen significante veranderingen in het 3e trimester
van de zwangerschap.
De linker en rechter ventriculaire verkorting nam rechtlijnig
toe, mogelijk als een gevolg van de verhoogde circulatoire
behoefte bij de groeiende foetus.
Het slagvolume en de output van de linker ventrikel liet een
3-voudige toename zien. De totale cardiac output bedroeg op
basis van eenzelfde output van de rechter en linker ventrikel
ongeveer 255 ml kg^{-1}min^{-1} in de à terme foetus.
Er trad een afname op van de linker ventrikel ejectie fractie
als gevolg van een grotere toename van het volume in de eind-
diastolische fase dan in de eind-systolische fase van de
hartcyclus.
De intraventriculaire septumdikte bleef gedurende de systole

nagenoeg gelijk, hetgeen suggereert dat het septum geen rol
speelt in het proces van de ventriculaire contractie. In meer
dan 50% van de gevallen werd geen duidelijke septumbeweging
gezien tijdens de systole, terwijl er in 10% sprake was van
een paradoxale beweging.

Gedurende de eerste vier uur post partum was er een signifi-
cante toename in het beat-to-beat interval. De verkorting
van de linker ventrikel nam gedurende de eerste tien minuten
na de geboorte verder toe ter vergroting van het slagvolume
als gevolg van een grotere bloedtoevoer. Ook de output van
de linker ventrikel steeg binnen tien minuten post partum,
als gevolg van zowel het uitvallen van de placenta circulatie,
als van een verhoogde behoefte aan bloedflow naar de ver-
schillende organen van de neonaat. De ejectie fractie van de
linker ventrikel veranderde niet significant.

In tegenstelling tot in de antenatale periode was er post
partum een duidelijke toename van de intraventriculaire sep-
tumdikte tijdens de systole waar te nemen, waaruit mag worden
geconcludeerd dat het septum na de geboorte een actieve rol
gaat spelen in de ventriculaire functie.

Een overzicht wordt gegeven van onderzoekers die zowel in de
antenatale als in de neonatale periode ventriculaire functies
hebben berekend. De resultaten van de verschillende auteurs
mogen niet direct met de resultaten uit ons onderzoek worden
vergeleken vanwege de verschillen in toegepaste methodieken.

Hoofdstuk 7

Dit hoofdstuk behandelt de ventriculaire geometrie en functie
in de groei-vertraagde foetus tijdens het laatste trimester
van de zwangerschap. Over dit onderwerp zijn in de literatuur
geen gegevens bekend. Herhaalde metingen van de foetale
distantia biparietalis duiden in het merendeel van de gevallen
(10 van de 15 patiënten) op het 'late flattening' type groei-
vertraging. De hoofd-romp ratio was bij 11 van 14 patiënten
verhoogd, hetgeen een hersen sparend effect suggereert.

In het algemeen waren in de groep van de groeivertraagde
foetus in de transversale diameters van de linker en rechter
ventrikel, en de intraventriculaire septum dikte kleiner in
vergelijking met deze groep van de foetus met een normale
groeisnelheid.
Bij alle groeivertraagde foetus was een normaal hartritme
ten tijde van het onderzoek. Dit indiceert een normale foe-
tale cardiovasculaire functie, temeer daar er normale waarden
werden gevonden voor de rechts-links ratio en verkorting van
de transversale diameters van beide ventrikels gedurende de
systole.
De afname van het linker ventriculaire slagvolume en output
wijst meer in de richting van een lager foetaal gewicht dan
een verminderde ventriculaire functie, daar de waarden van
zowel het slagvolume als van de output van de linker ventrikel
per kg foetaal lichaamsgewicht overeenkwamen met de waarden
zoals die werden gevonden bij de foetus met een normaal ge-
wicht voor de duur van de zwangerschap.

APPENDIX

Tables and Figures from Chapters 5, 6 and 7

authors	ultrasound technique	scanning plane of the heart	gest.ag (wks)
Garrett and Robinson (1970)	compound B-scanner	4-chamber view	32-40
Winsberg (1972)	compound B-scanner and M-mode	long-axis view	20-40
Wladimiroff et al (1979)	2-D real-time scanner and M-mode	long-axis view	34-41
Sahn et al (1980)	2-D real-time scanner	4-chamber view	20-41
Allan et al (1982)	2-D real-time scanner and M-mode	short and long axis view	16-39
Vosters (present work)	2-D real-time scanner and M-mode	long-axis view	28-40

*These figures represent the 50th percentile values at a fetal weight of 3500 grams

Table 5.1 Reported data in literature on fetal left and right ventricular transverse diameter (D_{lv} and D_{rv}) and right-to-left ventricular ratio ($\frac{D_{rv}}{D_{lv}}$) during the end-diastolic (ED) and end-systolic (ES) phase of the cardiac cycle

No. of patients studied	success rate	D_{lv} (mm)		D_{rv} (mm)		$\dfrac{D_{rv}}{D_{lv}}$	
		ED	ES	ED	ES	ED	ES
96	21%	--	--	--	--	0.81	
150	19%	13.1	7.2	--	--	--	--
8	67%	14.1	--	14.5	--	1.0	--
69	72%	14.0*		16.0*		1.18	
254	67%	15.0		15.0		1.0	
246	78%	17.5	13.6	17.4	13.5	1.0	1.0

authors	ultrasound technique	scanning plane of the heart	no. of patients studied
Winsberg (1972)	compound B-scanner and M-mode	long-axis view	50
Sahn et al (1980)	2-D real-time scanner	4-chamber view	69
Wladimiroff et al (1980)	2-D real-time scanner and M-mode	long-axis view	15
Vosters (present work)	2-D real-time scanner and M-mode	long-axis view	18
? not mentioned in publication			

Table 5.2 Reported data in literature on early neonatal left and right ventricular transverse diameter (D_{lv} and D_{rv}) and right-to-left ventricular ratio ($\frac{D_{rv}}{D_{lv}}$) during the end-diastolic (ED) and end-systolic (ES) phase of the cardiac cycle

eonatal age	success rate	D_{lv} (mm)		D_{rv} (mm)		$\dfrac{D_{rv}}{D_{lv}}$	
		ED	ES	ED	ES	ED	ES
1 day	22%	17.5	10.0	– –	– –	– –	– –
6 hours	28%	?		?		0.99	
0 min.	73%	17.0	– –	9.7	– –	0.57	– –
0 min.	83%	19.2	15.0	10.5	8.8	0.55	0.59

pat.no.	Q'_{lv} (ml min^{-1})		birth weight (gr)	Q'_{lv} (ml kg^{-1}min^{-1})	
	antenatally	neonatally		antenatally	neonatally
1	363	412	2900	125	142
2	362	421	2860	127	147
3	430	525	3015	143	174
4	365	425	2925	116	145
5	353	410	2720	130	151
6	410	466	3400	121	137
7	358	438	2780	129	158
8	417	483	3035	138	159
9	355	430	3120	114	138
10	440	560	3110	142	180
11	425	518	3070	139	169
12	392	469	3280	120	143
13	372	440	3130	119	141
14	370	450	3270	113	138
15	402	483	3320	121	145
16	444	–	3210	139	–
17	374	–	3180	118	–
18	405	–	3500	116	–
19	391	–	3110	126	–
	$\bar{X}$ 391	$\bar{X}$ 462	$\bar{X}$ 3102	$\bar{X}$ 126	$\bar{X}$ 151
	SD $\pm$ 20	SD $\pm$ 22	SD $\pm$ 56	SD $\pm$ 11	SD $\pm$ 12

Table 6.1 Mean $\pm$ S.D. of a) antenatal and neonatal Q'_{lv} in ml min^{-1} and ml kg^{-1}min^{-1}

b) birth weight
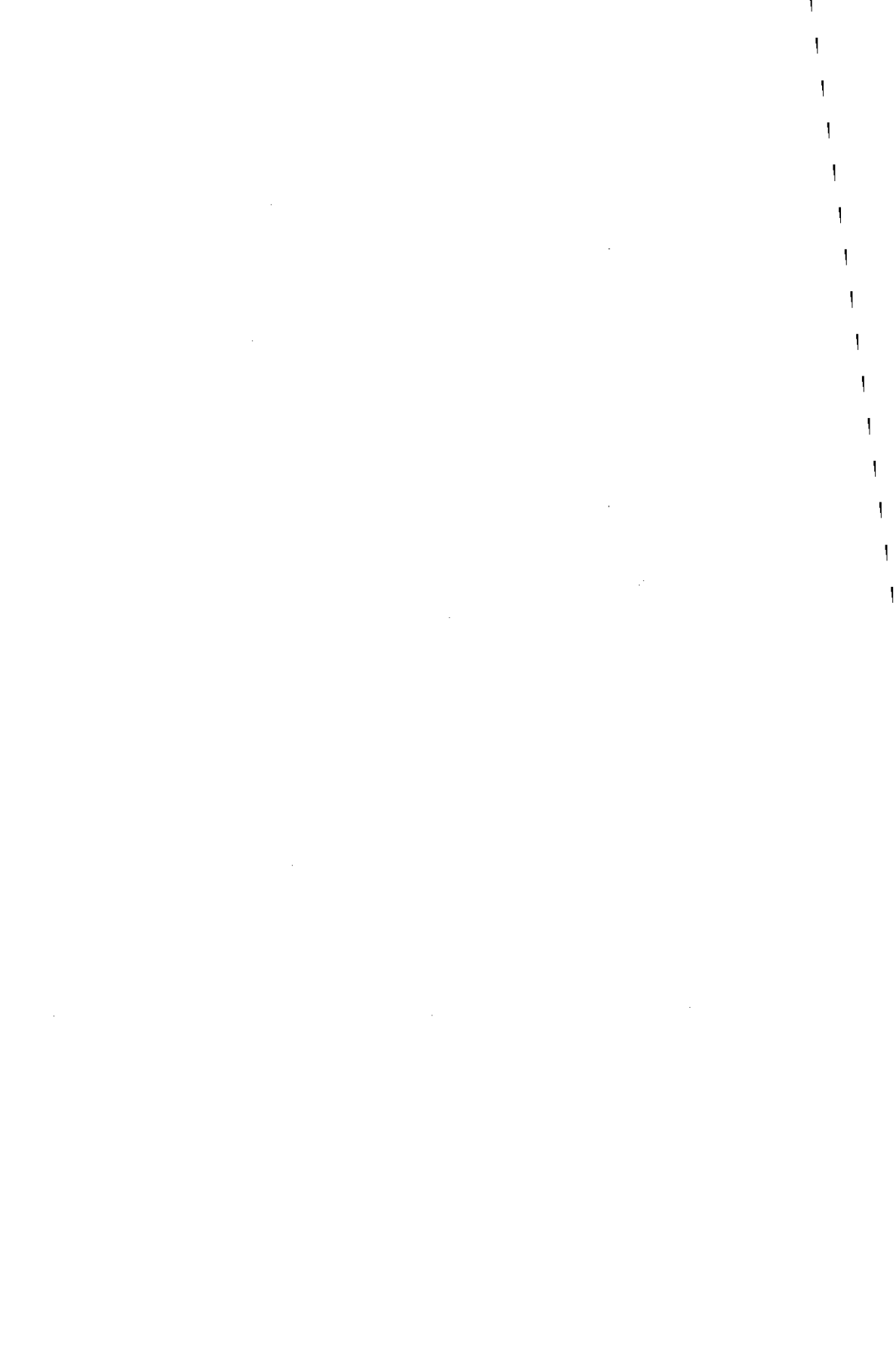
authors	methods applied	gestational age
Dawes et al (1954)	exteriorized fetal lamb; oxygen content measurements; Fick method	132-139 days
Assali et al (1965)	exteriorized fetal lamb; electromagnetic flow transducers	term
Mahon et al (1966)	exteriorized fetal lamb; dye dilution technique	138-147 days
Rudolph et al (1967)	exteriorized fetal lamb; radionuclide labelled microspheres	95-138 days
Heymann and Rudolph (1967)	fetal lamb; radionuclide labelled microspheres	60-150 days
Rudolph et al (1971)	human fetus; hysterectomy radionuclide labelled microspheres	10-20 weeks
Faber and Green (1972)	chronic sheep preparation indwelling arterial and venous catheters	? days (1.5-5.2 kg body weight)
Winsberg (1972)	human fetus; M-mode ultrasound	31-40 weeks
Rudolph et al (1974)	fetal lamb; radionuclide labelled microspheres	115-140 days

104

Q'_{lv} (ml kg^{-1}min^{-1})	Q'_{rv} (ml kg^{-1}min^{-1})	total cardiac output (ml kg^{-1}min^{-1})
174 (55%)	142 (45%)	316
97 (41%) (less coronary)	138 (59%)	235
182 (50%)	180 (50%)	362
-	-	280-1080
-	-	377- 548
-	-	175- 660
-	-	658
109	-	-
163 (33%)	327 (67%)	490

authors	methods applied	gestational age
Kirkpatrick et al (1975)	fetal lamb; chronic sheep preparation; dye dilution technique	118-124 days
Anderson et al (1981)	fetal lamb; microsphere-dilution method for total cardiac output; electromagnetic flow sensor for individual ventricular output	unknown radiographically estimated from fetal size and degree of bone
Wladimiroff and McGhie (1981)	human fetus; 2-D real-time ultrasound	27-40 weeks
Vosters (present study)	human fetus; M-mode ultrasound	28-40 weeks

Table 6.2 Data from literature on fetal cardiac output calculations

Q'_{lv} $(\text{ml kg}^{-1}\text{min}^{-1})$	Q'_{rv} $(\text{ml kg}^{-1}\text{min}^{-1})$	total cardiac output $(\text{ml kg}^{-1}\text{min}^{-1})$
250	–	–
185 (40%)	277 (60%)	462
114-123	–	–
126	–	–

right-to-left ventricular output relationship	estimated total ventricular output in the human fetus based on Q'_{lv} of 126 ml $kg^{-1}min^{-1}$
45%/55% (Dawes et al, 1954)	229 ml $kg^{-1}min^{-1}$
50%/50% (Mahon et al, 1966)	252 ml $kg^{-1}min^{-1}$
59%/41% (Assali et al, 1965)	307 ml $kg^{-1}min^{-1}$
60%/40% (Anderson et al, 1981)	315 ml $kg^{-1}min^{-1}$
67%/33% (Rudolph et al, 1974)	382 ml $kg^{-1}min^{-1}$

Table 6.3 Approximation of total ventricular output in the human fetus based on right-to-left ventricular output relationships by different investigators and a mean Q'_{lv} value of 126 ml $kg^{-1}min^{-1}$ in our own study

authors	methods applied	Q'_{lv} (ml kg^{-1}min^{-1})	Q'_{rv} (ml kg^{-1}min^{-1})	Q'_{lvrv} (ml kg^{-1}min^{-1})
Cross et al (1959)	neonatal lamb; catheterization of the right ventricle; Fick method for right ventricular output	325	–	–
Assali et al (1964)	exteriorized lamb; electromagnetic flow transducers	131	–	–
Downing et al (1964)	neonatal lamb; pump-operated arteriovenous by-pass	300	–	–
Burnard (1966)	human neonate; thermodilution method for left ventricular output; Fick method for right ventricular output	348	233	581
Stahlman et al (1967)	neonatal lamb; catheterization of the left atrium and main pulmonary artery; indicator-dilution technique	–	–	450
Arcilla et al (1967)	human neonate; cardiac catheterization and dye indicator dilution technique	–	–	180–240
Vosters (present study)	human neonate; M-mode ultrasound	151	–	–

Table 6.4 Data from literature on neonatal cardiac output calculations

gestational age (wks)	no of patients studied	A*	O*	B*
28	14	5	9	0
29	16	6	8	2
30	14	4	8	2
31	18	8	8	2
32	16	5	10	1
33	15	4	8	3
34	15	4	9	2
35	16	6	10	0
36	13	4	8	1
37	15	6	9	0
38	14	2	9	3
39	15	3	8	4
40	12	9	3	0
total	193	66	107	20
percentage		34%	56%	11%

*A = septal motion towards left ventricular posterior wall
during systole (non-paradox)

O = no measurable septal motion

B = septal motion away from left ventricular posterior wall
during systole (paradox)

Table 6.5 Direction of intraventricular septal motion relative to the
left ventricular posterior wall during systole measured at the
level of the mitral valve leaflets in the antenatal study

	antepartum	post partum			
		10 min	4 hours	24 hours	48 hours
A[*]	11	15	15	15	14
O[*]	4				
B[*]	0				1

[*]A = septal motion towards left ventricular posterior wall during systole (non-paradox)

 O = no measurable septal motion

 B = septal motion away from left ventricular posterior wall during systole (paradox)

Table 6.6 Direction of intraventricular septal motion relative to the left ventricular posterior wall during systole measured at the level of the mitral valve leaflets in the antenatal-neonatal study

author	no of patients studied	gestational age (wks)	IVS motion relative to left ventricular wall during systole·		
			non-paradox (A)	no motion (O)	paradox (B)
Winsberg (1972)	150	20-41	close to 100%		
Egeblad et al (1975)	20	36-40	100%		
Kleinmann et al (1978)	90	18-41	44%	42%	14%
Vosters (present study)	193	28-40	34%	55.5%	10.5%

Table 6.7 Data from literature on intraventricular septal motion relative to the left ventricular posterior wall during systole

pat.no.	gestational age (wks)		maternal parity	fetal sex	birth weight	
	cardiac ex.	delivery			gr.	perc.
1	28	30	4	♀	1010	10>w⩾5
2	31	34	1	♀	1360	10>w⩾5
3	31	31	1	♂	1170	10>w⩾5
4	33	36	2	♂	1900	5>w⩾2.3
5	33	36	1	♂	1750	5>w⩾2.3
6	33	34	5	♀	1560	10>w⩾5
7	33	34	1	♀	1150	5>w⩾2.3
8	34	38	1	♀	2130	5>w⩾2.3
9	36	37	2	♂	2070	5>w⩾2.3
10	36	37	1	♂	1700	2.3>w
11	37	37	1	♂	1975	5>w⩾2.3
12	38	39	1	♀	2540	10>w⩾5
13	38	39	1	♀	2400	5>w⩾2.3
14	38	38	0	♂	1980	2.3>w
15	38	38	0	♂	2220	5>w⩾2.3

Table 7.1 General data on the 15 small-for-dates: gestational age (wks) at the time of cardiac examination; gestational age (wks) at the time of delivery; maternal parity; fetal sex; birth weight (grams and percentiles)

pat.no.	gest.age (wks)	BPD (perc.)	chest area (perc.)	head-to-chest ratio (perc.)	birth weight (perc.)
1	28	5	<5	N	10>w⩾5.
2	31	N	5	>90⩽95	10>w⩾5
3	31	N	<5	>90⩽95	10>w⩾5
4	33	<5	<5	N	5>w⩾2.3
5	33	N	–	–	5>w⩾2.3
6	33	N	5	N	10>w⩾5
7	33	<5	<5	>95	5>w⩾2.3
8	34	<5	<5	>95	5>w⩾2.3
9	36	<5	<5	>95	5>w⩾2.3
10	36	<5	<5	>95	2.3>w
11	37	<5	<5	>95	5>w⩾2.3
12	38	N	<5	>95	10>w⩾5
13	38	<5	<5	>95	5>w⩾2.3
14	38	<5	<5	>95	2.3>w
15	38	<5	<5	>90⩽95	5>w⩾2.3

Table 7.2 Biometric data on the 15 small-for-dates with respect to the upper and lower
percentiles of the normal BPD, chest area and head-to-chest ratio curves.
N = within normal limits; <5 = below 5th percentile; >90⩽95 = between 90th
and 95th percentile; >95 = above 95th percentile of the normal curves

pat.no.	gest. age (wks)	D_{lv} (mm) ED	ES	D_{rv} (mm) ED	ES	$\dfrac{D_{rv}}{D_{lv}}$ ED	ES	Q_{lv} (ml) ED	ES	IVS (mm) ED	ES	birth weight (perc.)
1	28	10.6	6.8	10.9	7.4	1.02	1.08	1.1	0.3	1.5	1.5	10>w⩾5
2	31	11.1	6.8	11.0	6.8	1.0	1.0	1.3	0.3	1.4	1.4	10>w⩾5
3	31	10.8	6.5	10.7	6.5	1.0	1.0	1.2	0.3	2.5	2.4	10>w⩾5
4	33	13.8	10.6	13.6	10.6	0.98	1.0	2.4	1.2	2.0	1.9	5>w⩾2.3
5	33	13.5	10.3	13.6	10.3	1.0	1.0	2.3	1.1	2.3	2.0	5>w⩾2.3
6	33	14.6	11.6	14.2	11.3	0.97	0.97	2.8	1.3	1.8	1.7	10>w⩾5
7	33	12.5	9.4	12.3	9.1	0.98	0.97	1.8	0.8	1.4	1.5	5>w⩾2.3
8	34	13.2	9.1	13.2	9.6	1.0	1.05	2.1	0.7	1.7	1.7	5>w⩾2.3
9	36	13.2	8.6	12.8	8.8	0.96	1.02	2.1	0.6	2.1	1.8	5>w⩾2.3
10	36	12.2	7.9	11.8	8.1	0.97	1.02	1.8	0.5	1.6	1.5	2.3>w
11	37	14.5	9.8	14.8	9.9	1.02	1.0	2.8	0.9	2.1	2.0	5>w⩾2.3
12	38	15.5	11.0	15.3	11.1	0.98	1.0	3.4	1.4	2.9	2.6	10>w⩾5
13	38	15.5	11.5	14.7	11.3	0.95	0.98	3.4	1.3	2.6	2.6	5>w⩾2.3
14	38	14.9	10.2	14.4	9.7	0.96	0.94	3.1	1.1	1.8	1.8	2.3>w
15	38	15.3	11.0	15.3	11.0	1.00	1.00	3.2	1.4	2.2	2.2	5>w⩾2.3

Table 7.3 Geometrical data on the 15 small-for-dates with respect to birth weight

pat.no.	gest.age (wks)	beat-to-beat int. (msec)	ΔD (mm) LV	ΔD (mm) RV	Ω_{lvs} (ml)	Ω'_{lv} (ml min^{-1})	$\dfrac{\Omega_{lvs}}{\Omega_{lved}}$ (%)	birth weight (perc.)
1	28	374	3.8	3.5	0.8	121	72	10>w⩾5
2	31	407	4.3	4.2	1.0	148	71	10>w⩾5
3	31	400	3.7	3.8	0.9	135	73	10>w⩾5
4	33	493	3.2	3.0	1.2	148	50	5>w⩾2.3
5	33	507	3.2	3.3	1.2	143	52	5>w⩾2.3
6	33	396	3.0	2.9	1.5	230	54	10>w⩾5
7	33	410	3.1	3.2	1.0	147	55	5>w⩾2.3
8	34	429	4.1	3.6	1.4	196	66	5>w⩾2.3
9	36	391	4.6	4.0	1.5	230	71	5>w⩾2.3
10	36	385	4.3	3.7	1.3	203	72	2.3>w
11	37	418	4.7	4.9	1.9	274	67	5>w⩾2.3
12	38	442	4.6	4.2	2.0	280	58	10>w⩾5
13	38	417	4.0	3.4	2.1	302	61	5>w⩾2.3
14	38	442	4.7	4.7	2.0	272	64	2.3>w
15	38	400	4.3	4.2	1.8	275	56	5>w⩾2.3

Table 7.4 Data on cardiac functions in the 15 small-for-dates

pat.no.	gest.age (wks)	Q'_{lv} (ml min^{-1})	birth weight (gr)	Q'_{lv} (ml kg^{-1}min^{-1})
3	31	135	1170	116
6	33	230	1560	147
7	33	147	1150	128
9	36	230	2070	112
10	36	203	1700	119
11	37	274	1975	137
12	38	280	2540	110
13	38	302	2400	126
14	38	191	1980	132
15	38	275	2220	124

Table 7.5 Relationship between left ventricular output (Q'_{lv}) per kg body weight and birth weight in the 15 small-for-dates
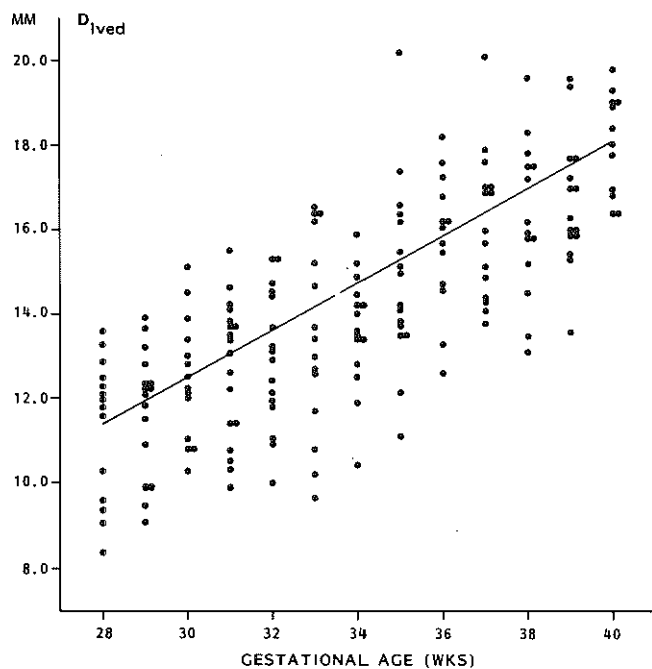
Fig. 5.1 Normal values and linear regression line for the left
ventricular diameter (ED) in the antenatal study (D_{lved})
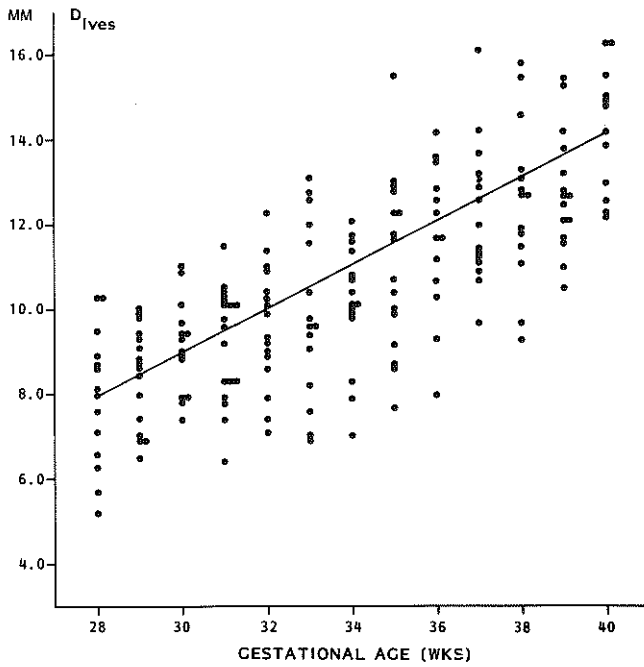
Fig. 5.2 Normal values and linear regression line for the left
ventricular diameter (ES) in the antenatal study (D_{lves})
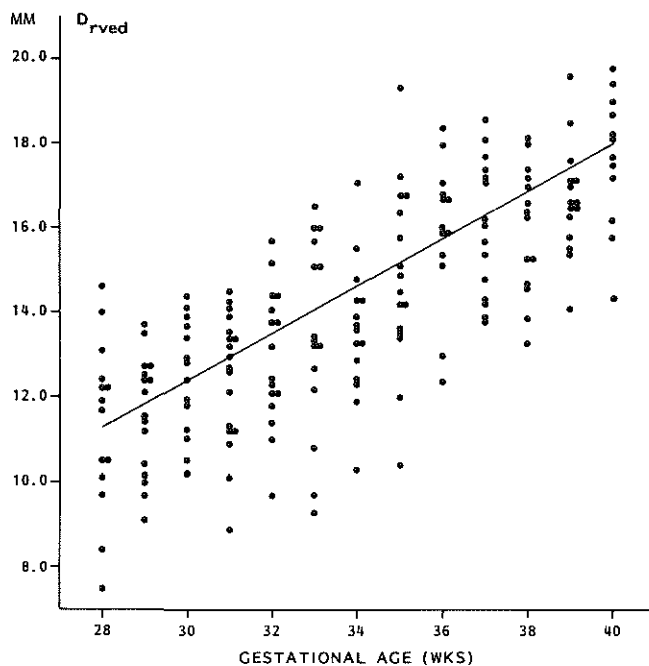
Fig. 5.3 Normal values and linear regression line for the right
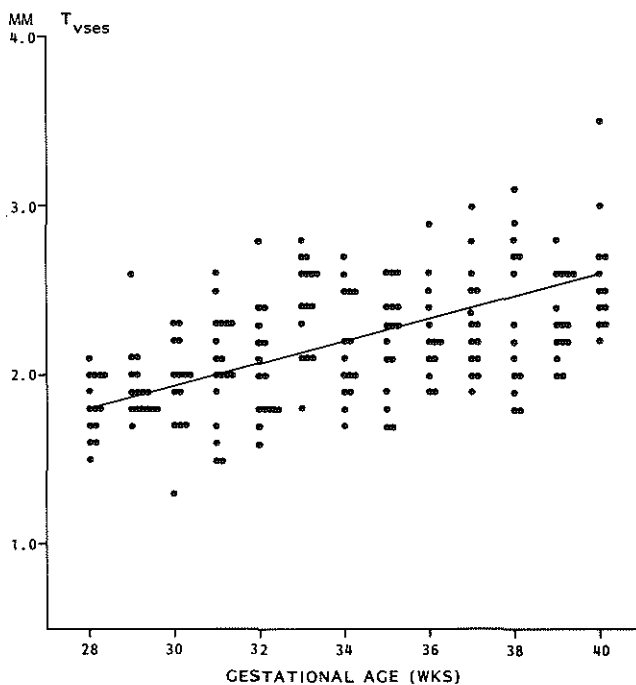ventricular diameter (ED) in the antenatal study (D_{rved})
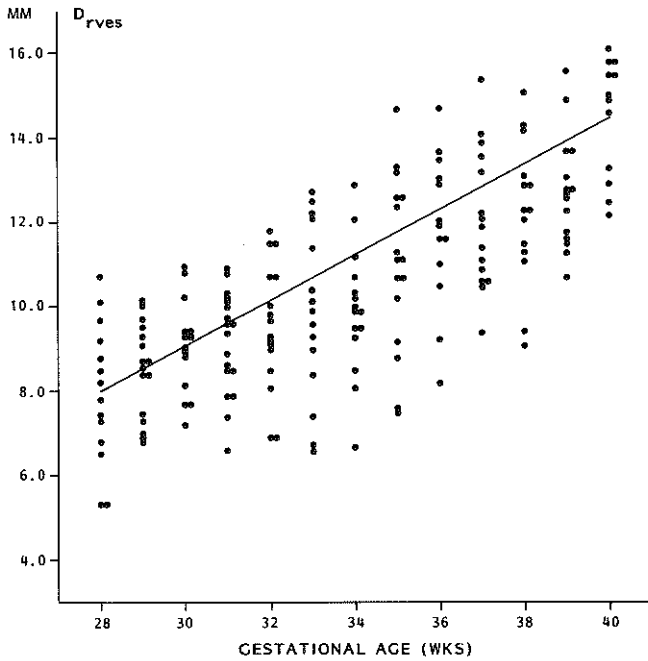
Fig. 5.4 Normal values and linear regression line for the right
ventricular diameter (ES) in the antenatal study (D_{rves})
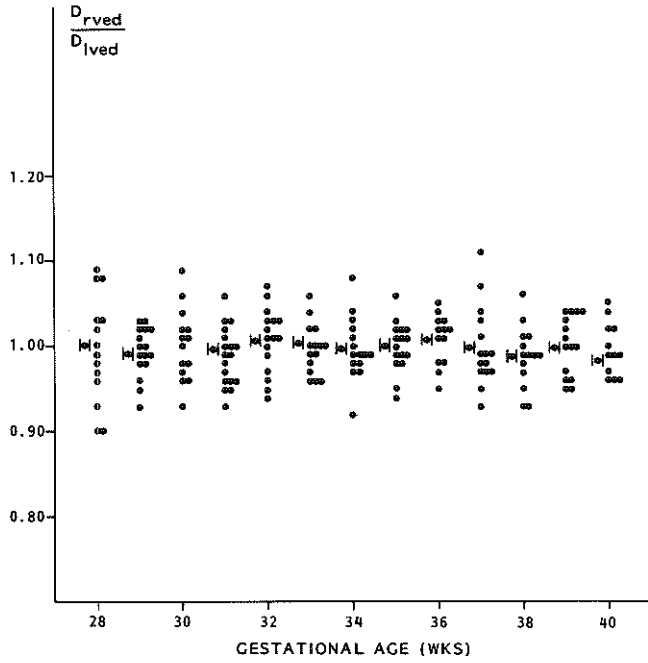
Fig. 5.5 Normal values for the right-to-left ratio of ventricular diameters (ED) in the antenatal study ($\frac{D_{rved}}{D_{lved}}$)

122
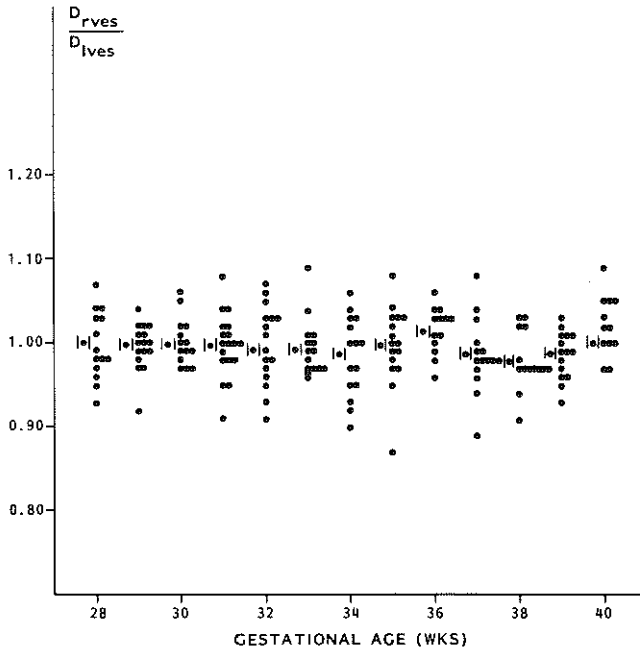
Fig. 5.6 Normal values for the right-to-left ratio of ventricular
diameters (ES) in the antenatal study $(\frac{D_{rves}}{D_{lves}})$
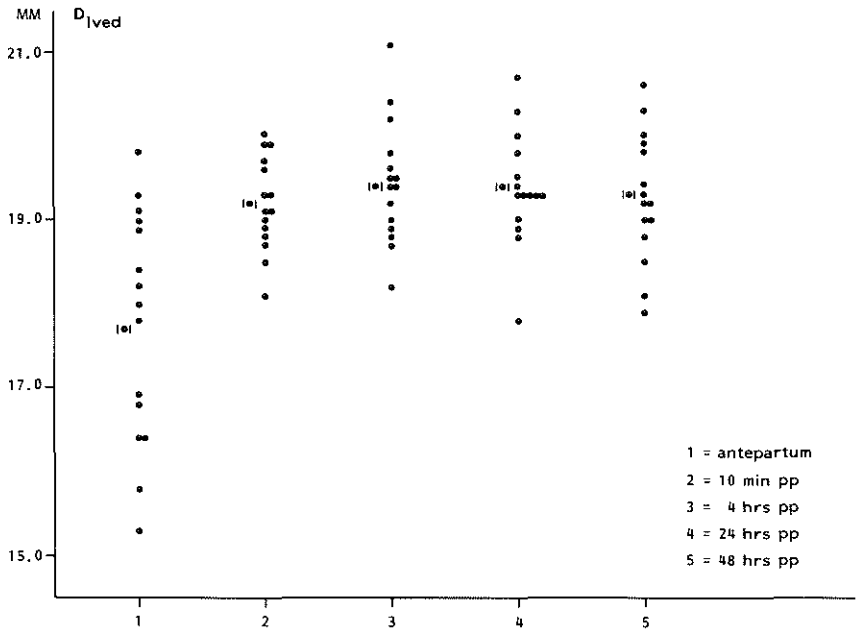
Fig. 5.7 Normal values (⟨·⟩ = mean) for the left ventricular diameter (ED) in the antenatal-neonatal study (D_{lved})

124
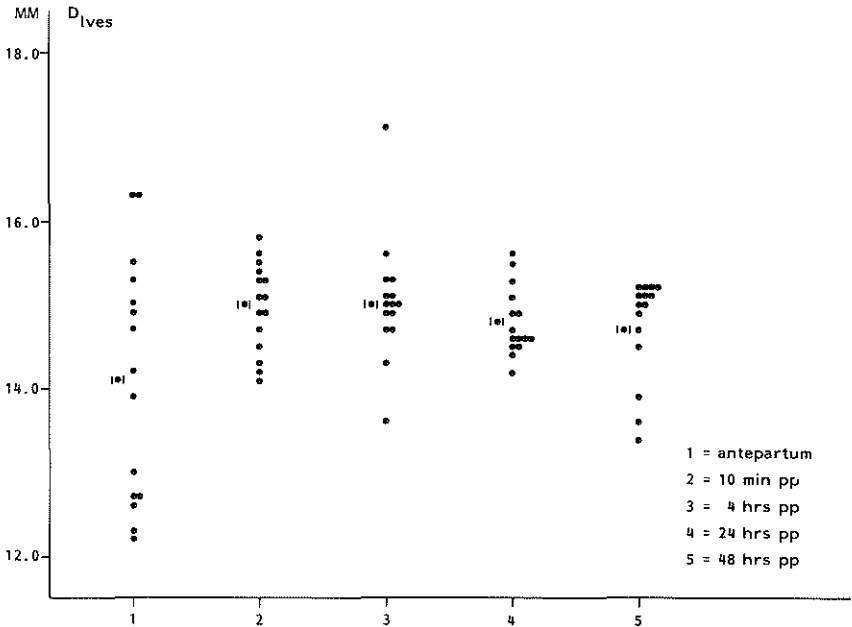
Fig. 5.8 Normal values (|.| = mean) for the left ventricular diameter
(ES) in the antenatal-neonatal study (D_{lves})
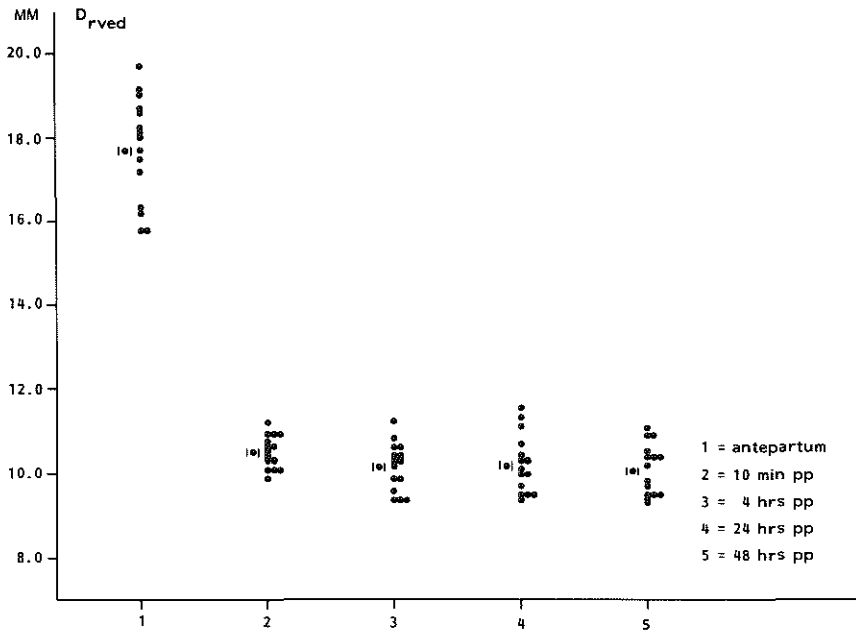
Fig. 5.9 Normal values (|.| = mean) for the right ventricular diameter
(ED) in the antenatal-neonatal study (D_{rved})

126
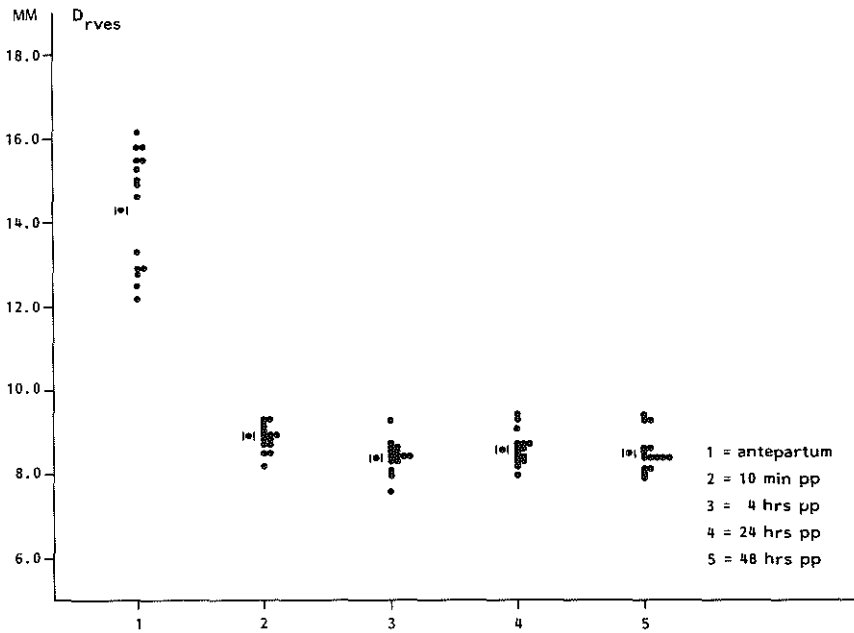
Fig. 5.10 Normal values ($\vdash\!\cdot\!\dashv$ = mean) for the right ventricular diameter
(ES) in the antenatal-neonatal study (D_{rves})
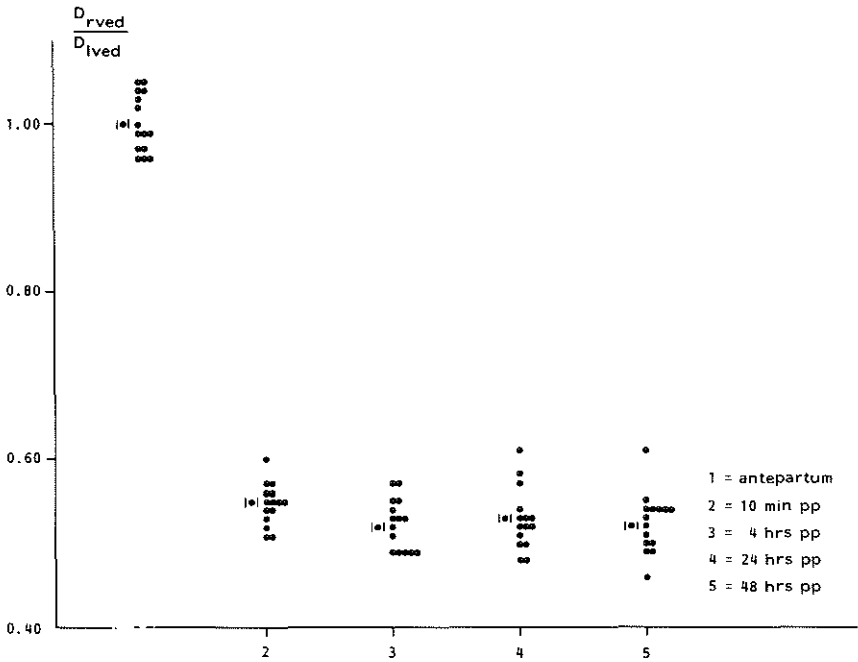
Fig. 5.11 Normal values (ı.ı = mean) for the right-to-left ratio for ventricular diameters (ED) in the antenatal-neonatal study $(\frac{D_{rved}}{D_{lved}})$
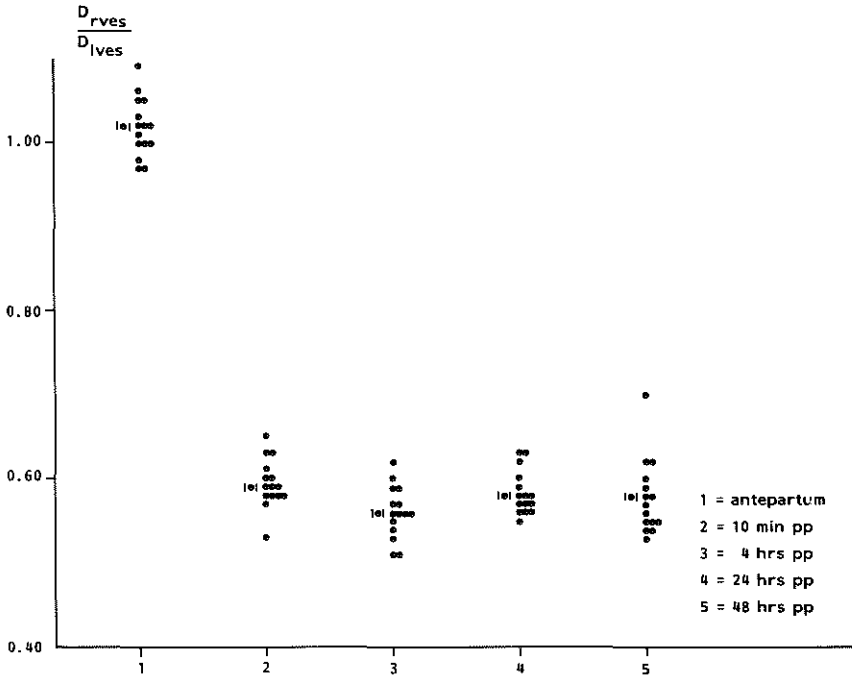
Fig. 5.12 Normal values (¡ . ¡ = mean) for the right-to-left ratio for ventricular diameters (ES) in the antenatal-neonatal study $(\frac{D_{rves}}{D_{lves}})$
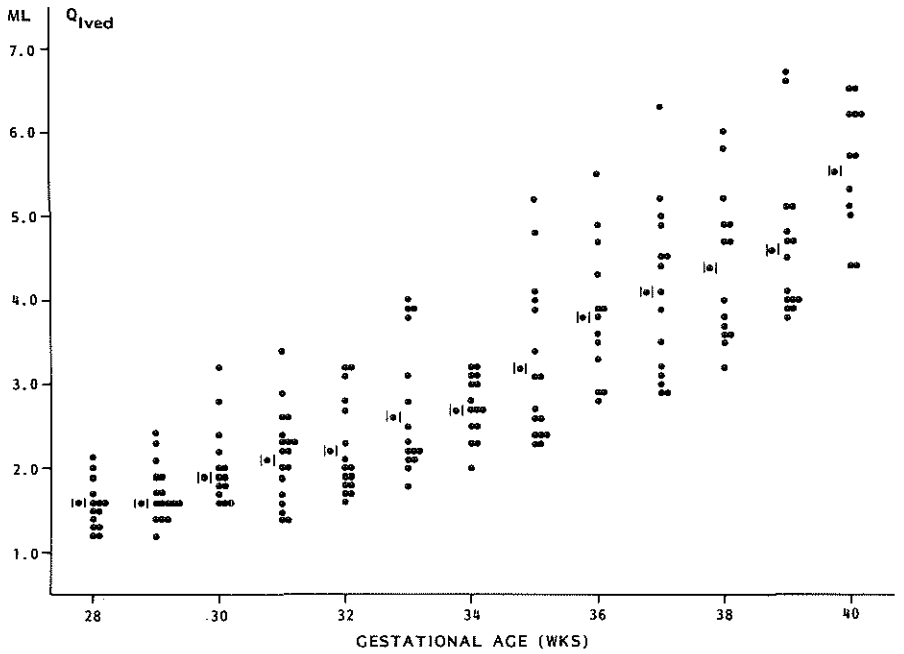
Fig. 5.13 Normal values ($_{|\cdot|}$ = mean) for left ventricular volume (ED) in the antenatal study (Q_{lved})

130
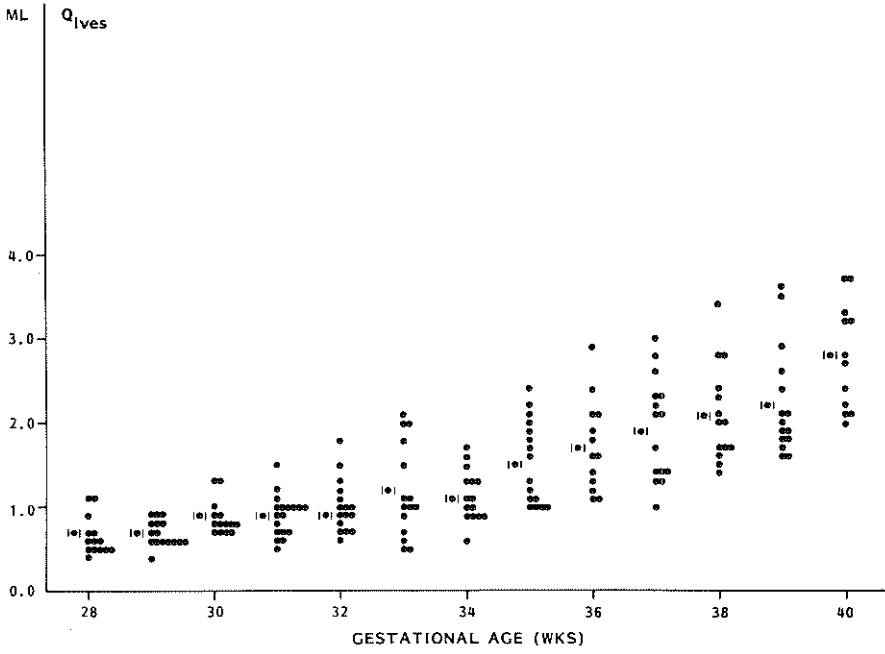
Fig. 5.14 Normal values (⌐.⌐ = mean) for left ventricular volume (ES) in the antenatal study (Q_{lves})
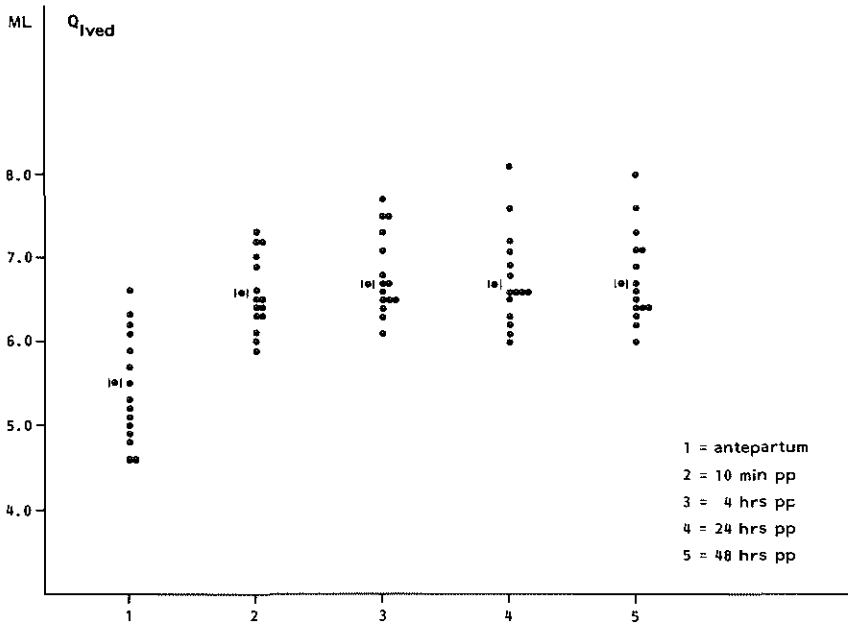
Fig. 5.15 Normal values (|.| = mean) for left ventricular volume (ED)
in the antenatal-neonatal study (Q_{lved})
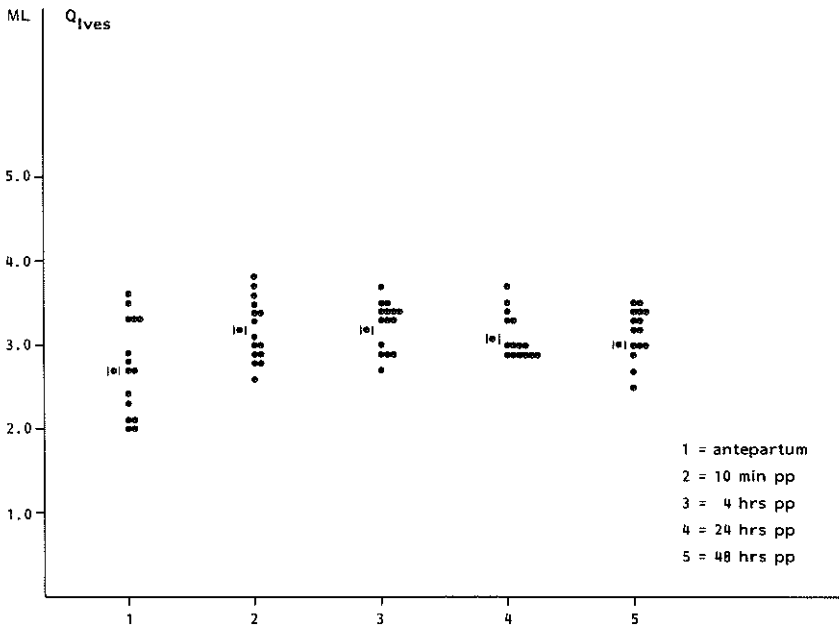
Fig. 5.16 Normal values (|.| = mean) for left ventricular volume (ES) in the antenatal-neonatal study (Q_{lves})
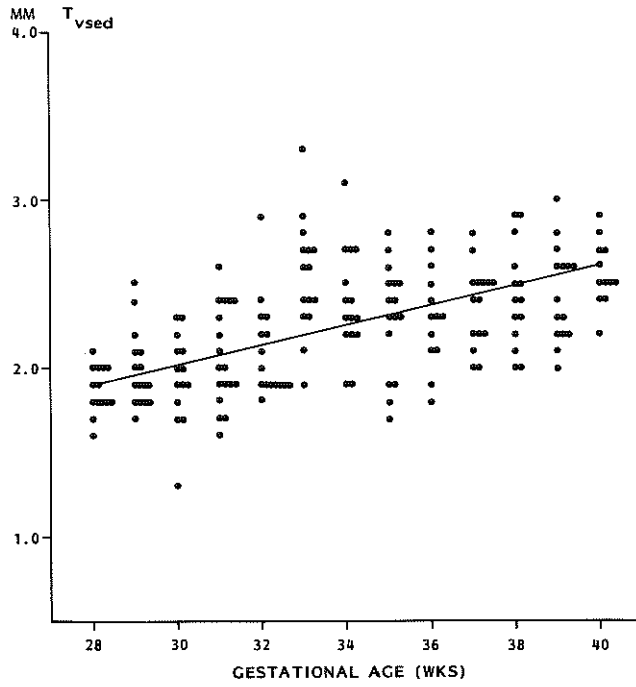
Fig. 5.17 Normal values and the linear regression line for the intra-
ventricular septal thickness (ED) in the antenatal study
(T_{vsed})

134

Fig. 5.18 Normal values and the linear regression line for the intra-
ventricular septal thickness (ES) in the antenatal study
(T_{vses})
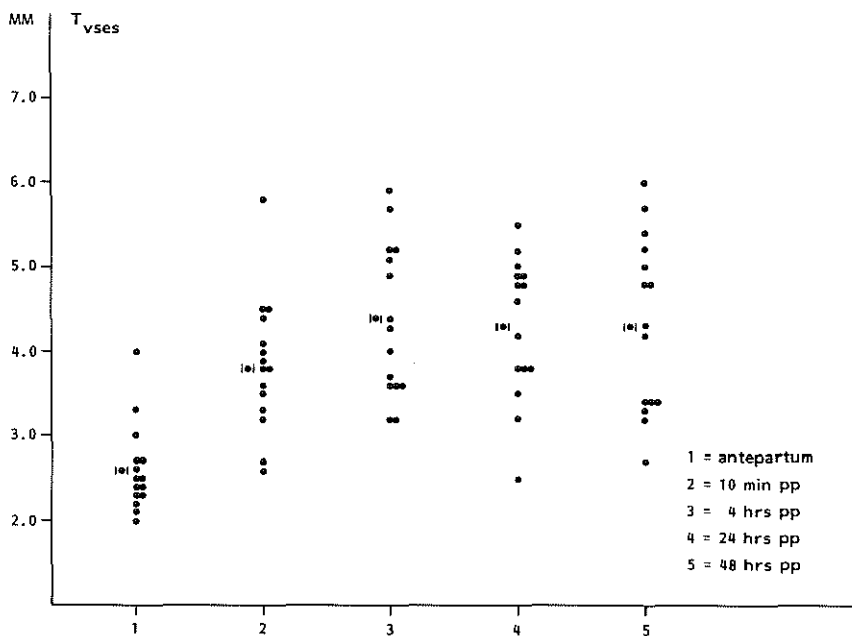
Fig. 5.19 Normal values (ⱼ.ⱼ = mean) for the intraventricular septal
thickness (ES) in the antenatal-neonatal study (T$_{vses}$)
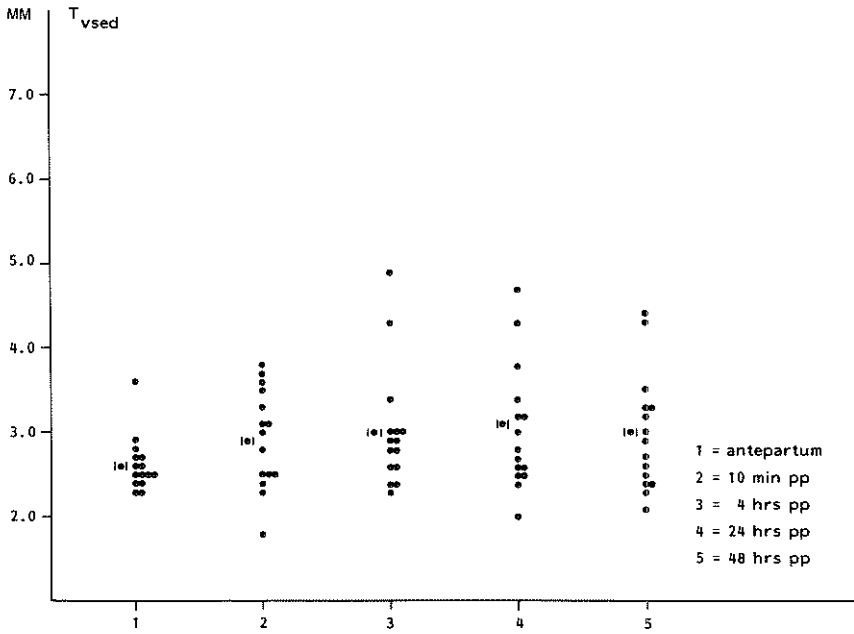
Fig. 5.20 Normal values ($|.|$ = mean) for the intraventricular septal thickness (ED) in the antenatal-neonatal study (T_{vsed})

137

MSEC   BEAT TO BEAT INTERVAL
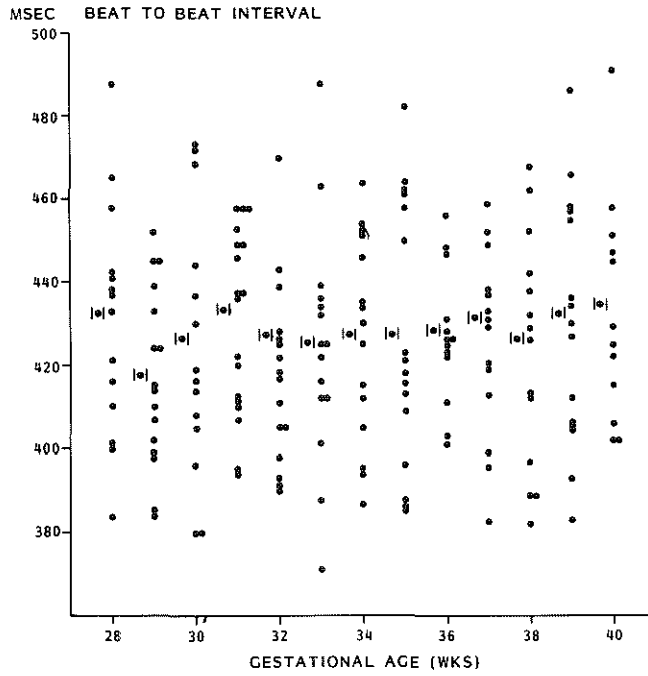
Fig. 6.1 Normal beat-to-beat interval values ($_{\vert\bullet\vert}$ = mean) in antenatal
        study
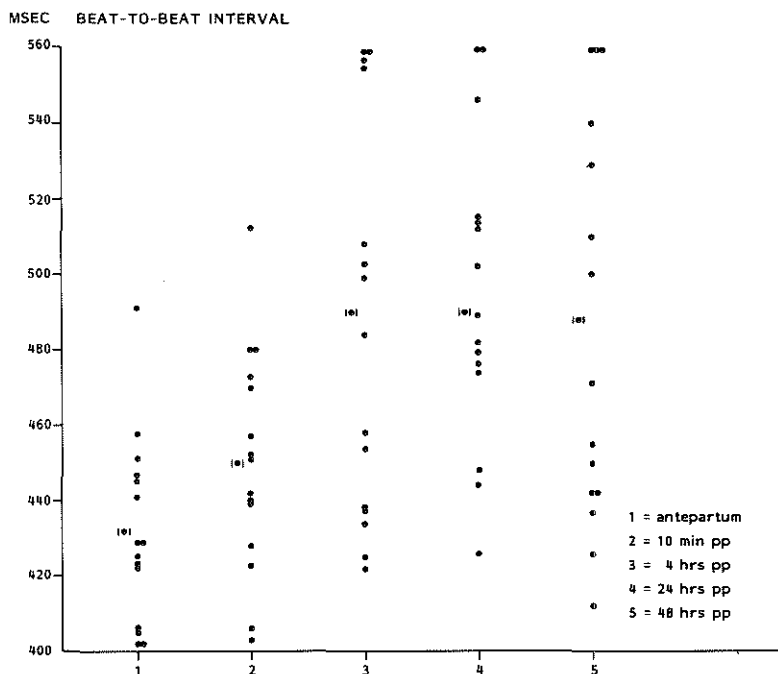
Fig. 6.2 Normal beat-to-beat interval values (¡.¡ = mean) in antenatal-
neonatal study
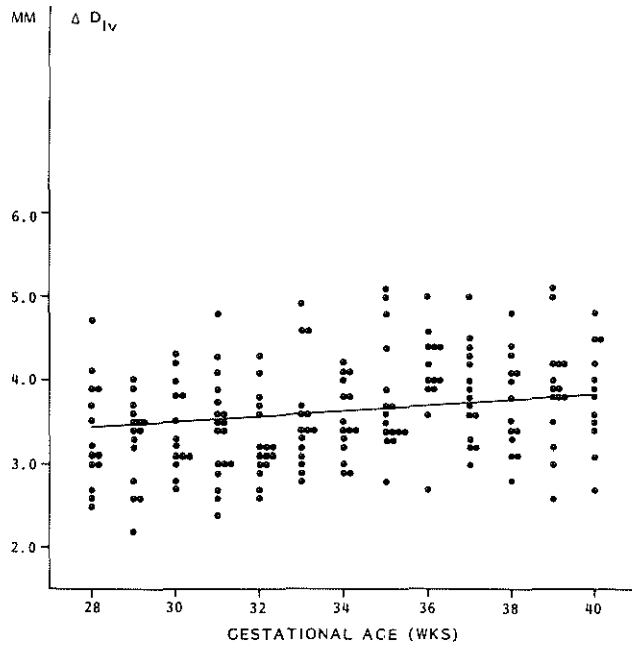
Fig. 6.3 Normal values and linear regression line for the shortening of the transverse diameter of the left ventricle (ΔD_{lv}) in the antenatal study
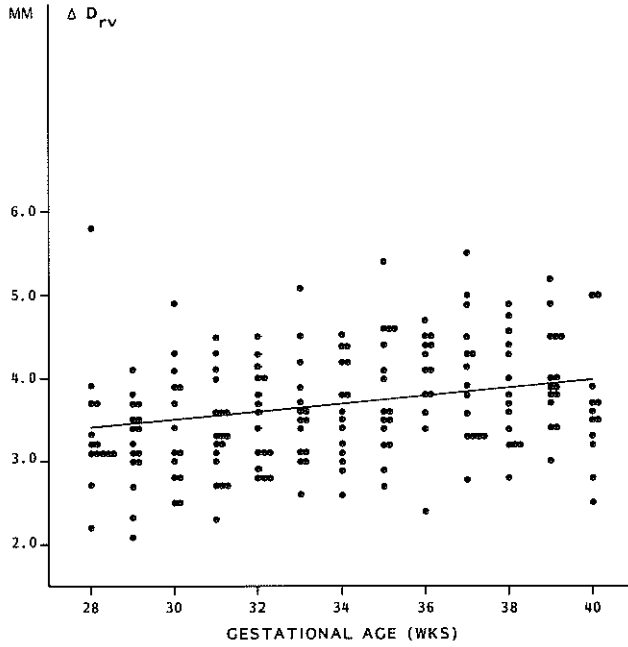
Fig. 6.4 Normal values and regression line for the shortening of the transverse diameter of the right ventricle (ΔD_{rv}) in the antenatal study
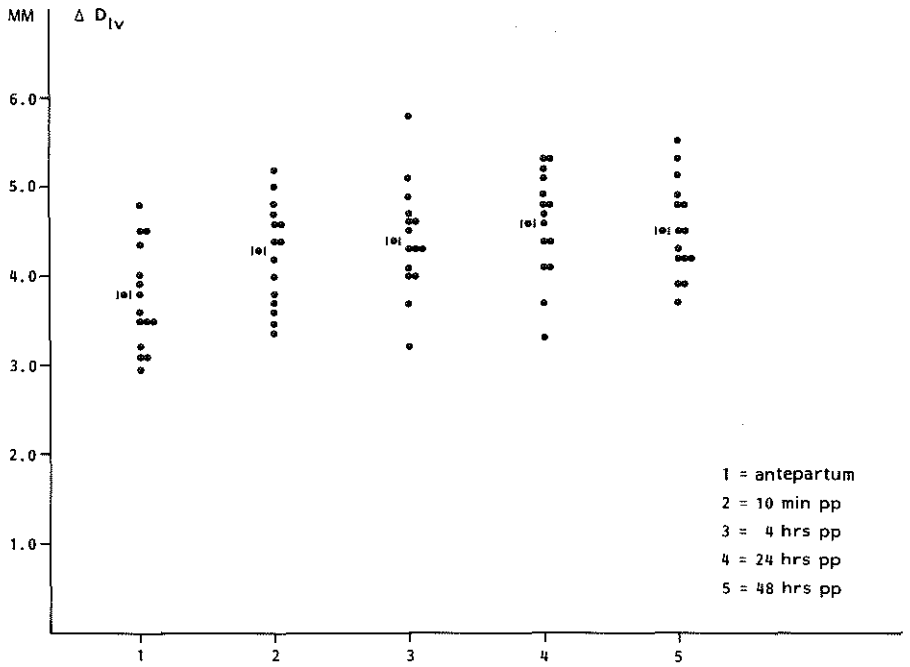
Fig. 6.5 Normal values (⊦.⊦ = mean) for the shortening of the transverse
diameter of the left ventricle (ΔD_{lv}) in the antenatal-neonatal
study

142
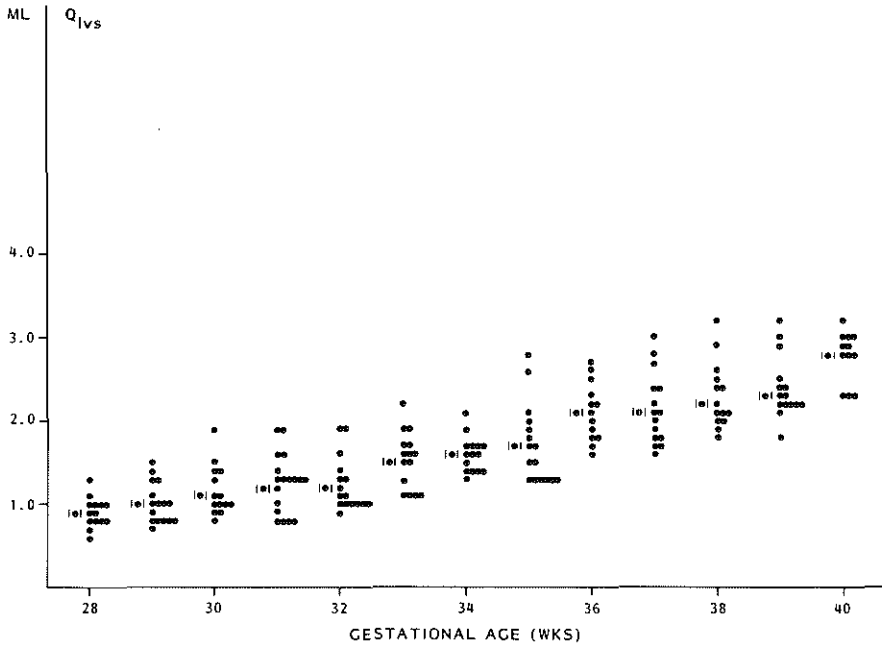
Fig. 6.6 Normal values (⊢•⊣ = mean) for the left ventricular stroke
volume (Q_{lvs}) in the antenatal study

143
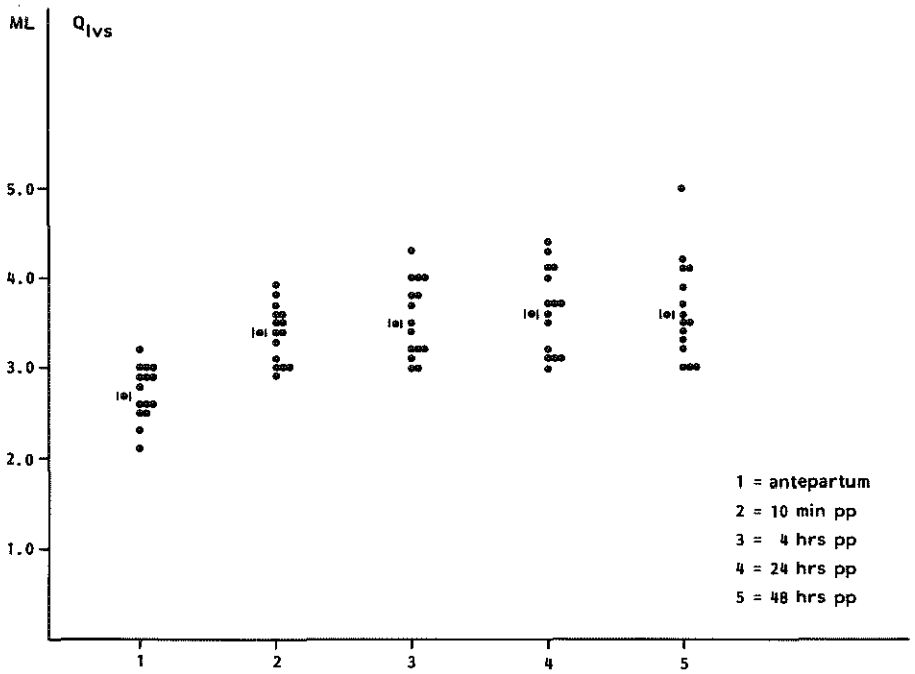
Fig. 6.7 Normal values (ı.ı = mean) for the left ventricular stroke
volume (Q_{lvs}) in the antenatal-neonatal study

144
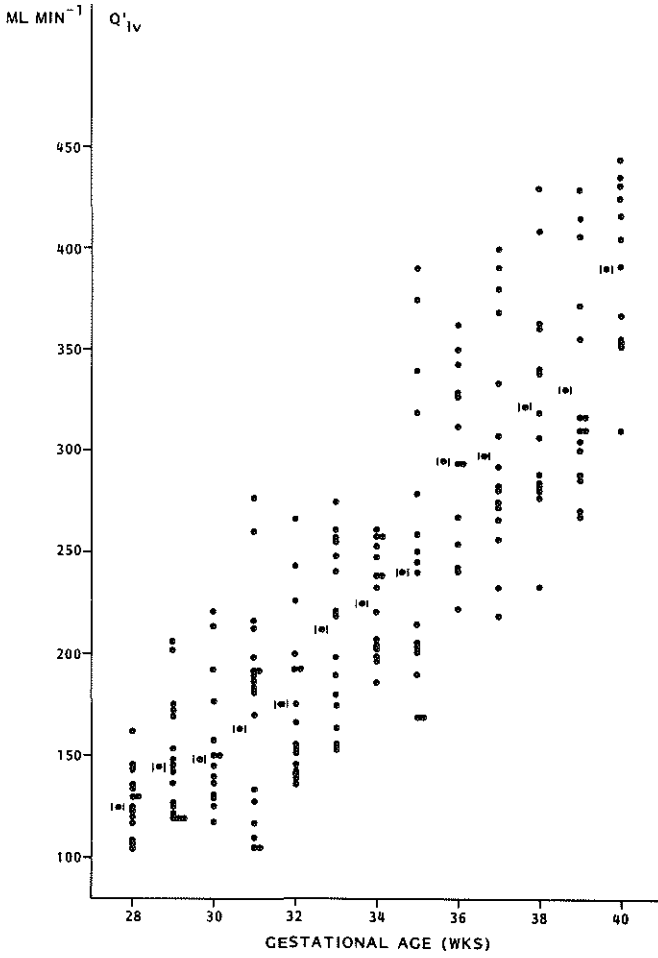
Fig. 6.8 Normal values ($\mapsto$ = mean) for the left ventricular output (Q'_{lv}) in the antenatal study
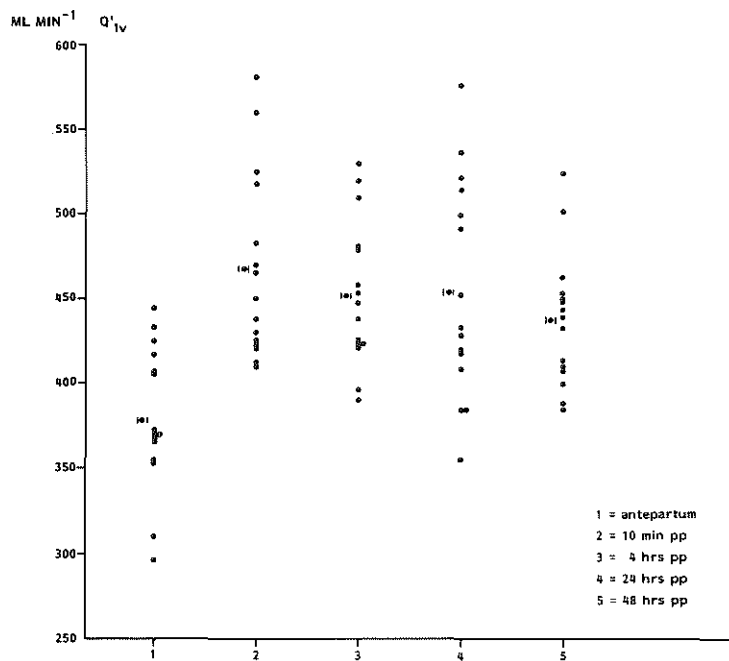
Fig. 6.9 Normal values (|.| = mean) for the left ventricular output
(Q'_{lv}) in the antenatal-neonatal study
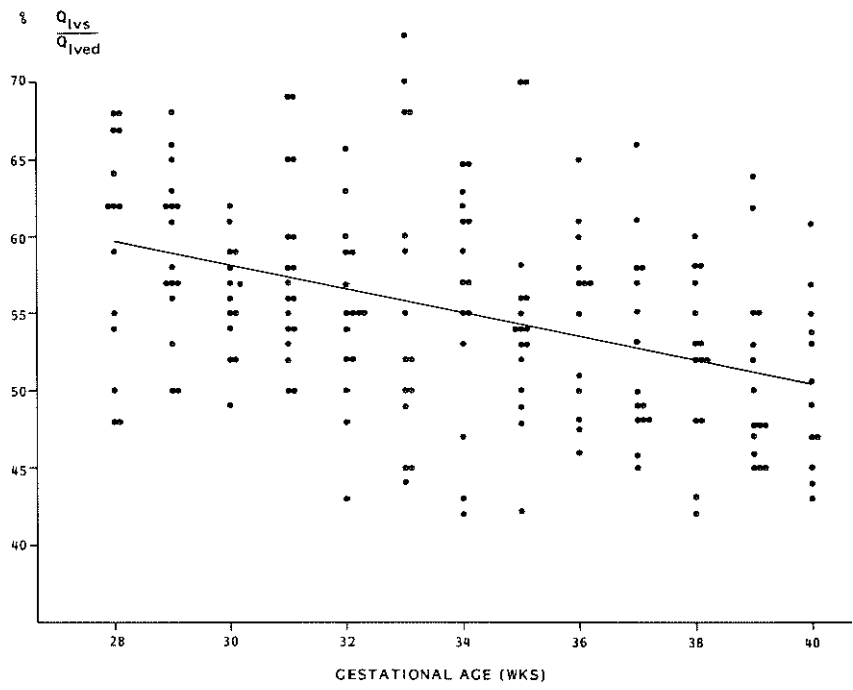
Fig. 6.10 Normal values and linear regression line for the left
ventricular ejection fraction $(\frac{Q_{lvs}}{Q_{lved}})$ in the antenatal study
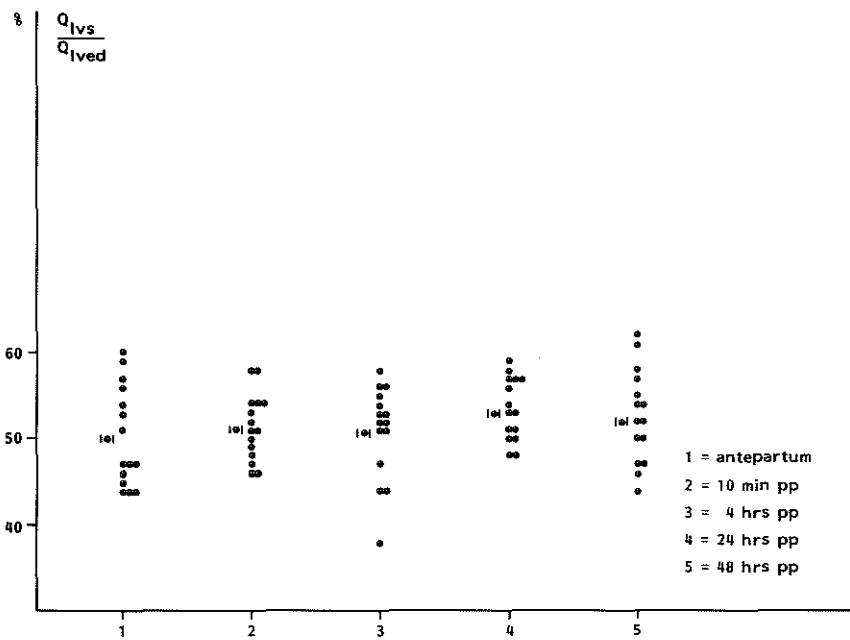
Fig. 6.11 Normal values (|.| = mean) for the left ventricular ejection
fraction ($\frac{Q_{lvs}}{Q_{lved}}$) in the antenatal-neonatal study

148
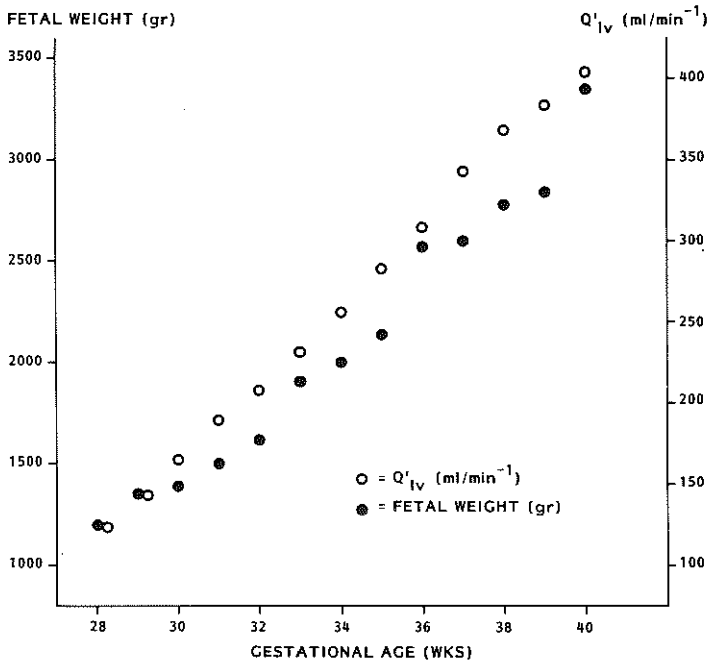
Fig. 6.12 Relationship between birth weight (50th percentile values for
male infants of primigravida according to Tables of Klooster-
man, 1970) and left ventricular output (Q'_{lv})(mean values)
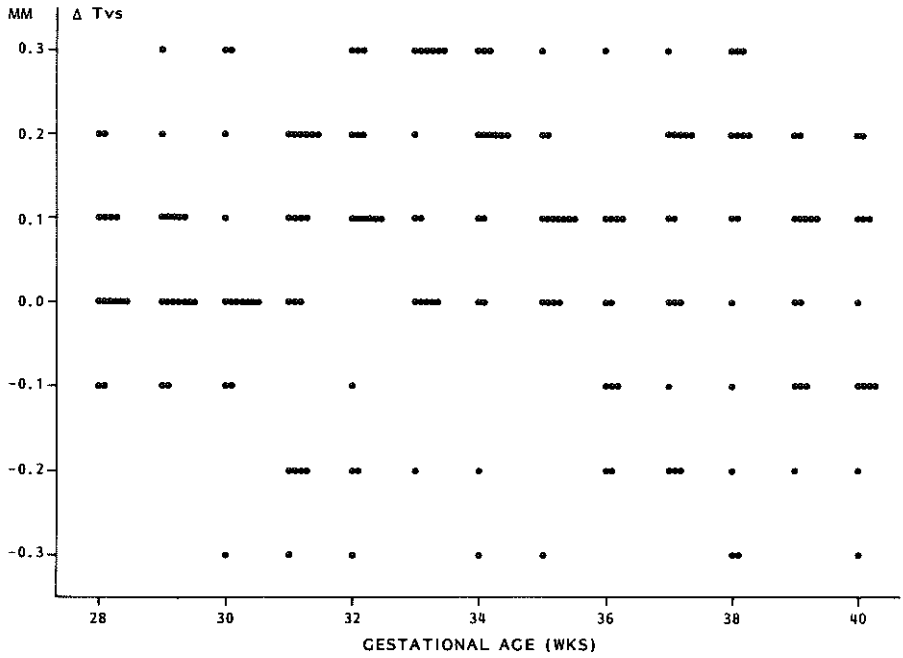in our own study

Fig. 6.13 Normal values for the change in intraventricular septal
thickness (ΔTvs) during systole in the antenatal study

150

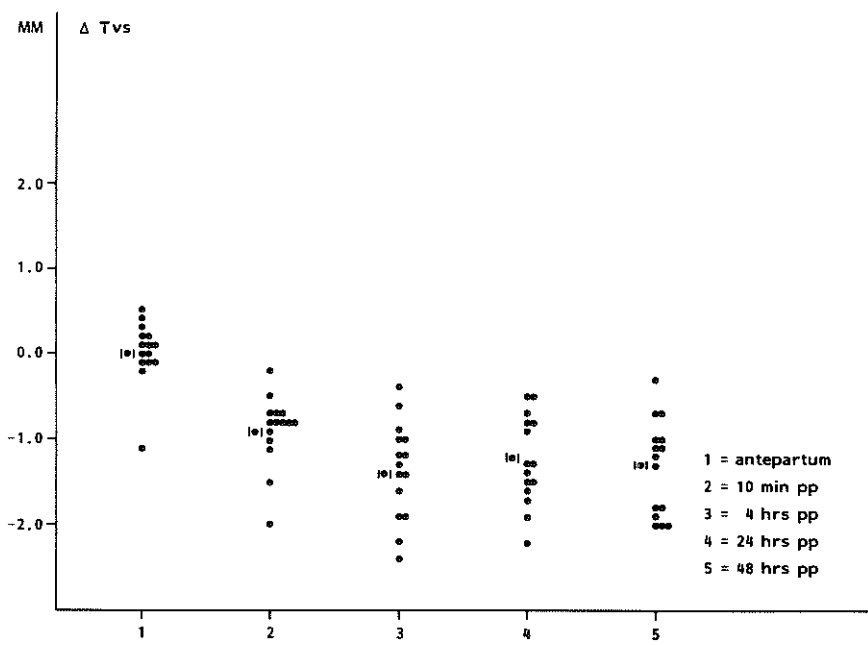Fig. 6.14 Normal values (ı.ı = mean) for the change in intraventricular
        septal thickness (ΔTvs) during systole in the antenatal-
        neonatal study
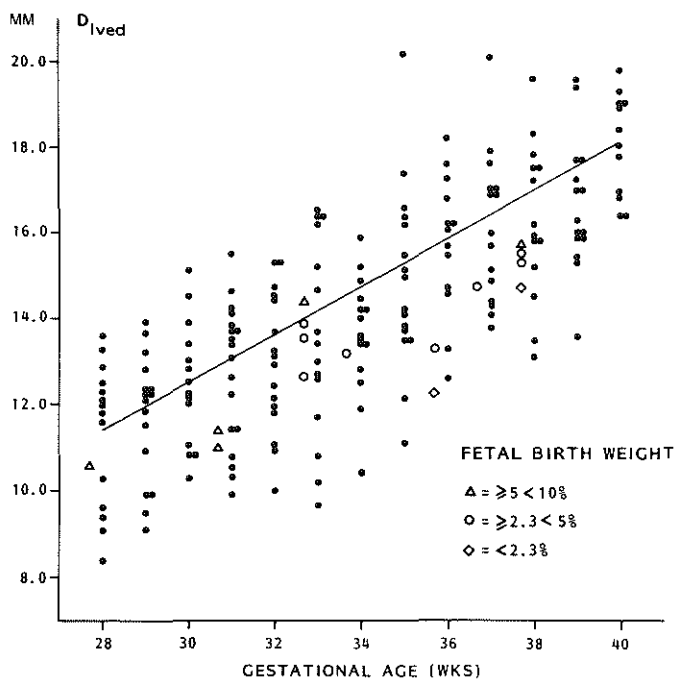
Fig. 7.1 Data on left ventricular diameter (ED) from 15 small-for-dates
(Δ,O,$\Diamond$) plotted in the normal curve for that particular para-
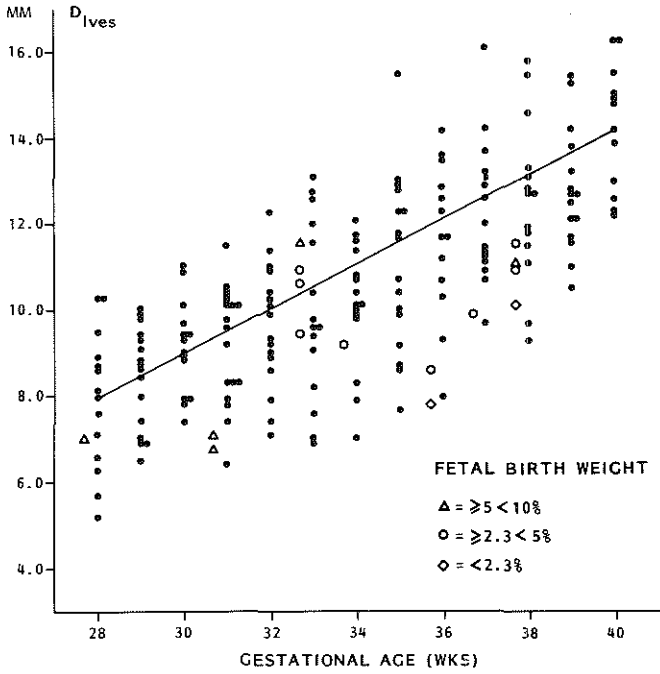meter (D_{lved})(Ch. 5)

Fig. 7.2 Data on left ventricular diameter (ES) from 15 small-for-dates
($\triangle$,0,$\diamondsuit$) plotted in the normal curve for that particular para-
meter (D_{lves})(Ch. 5)

Fig. 7.3 Data on right ventricular diameter (ED) from 15 small-for-dates
        (Δ,O,◊) plotted in the normal curve for that particular para-
        meter (D_{rved})(Ch. 5)

Fig. 7.4 Data on right ventricular diameter (ES) from 15 small-for-dates
(Δ,O,◊) plotted in the normal curve for that particular para-
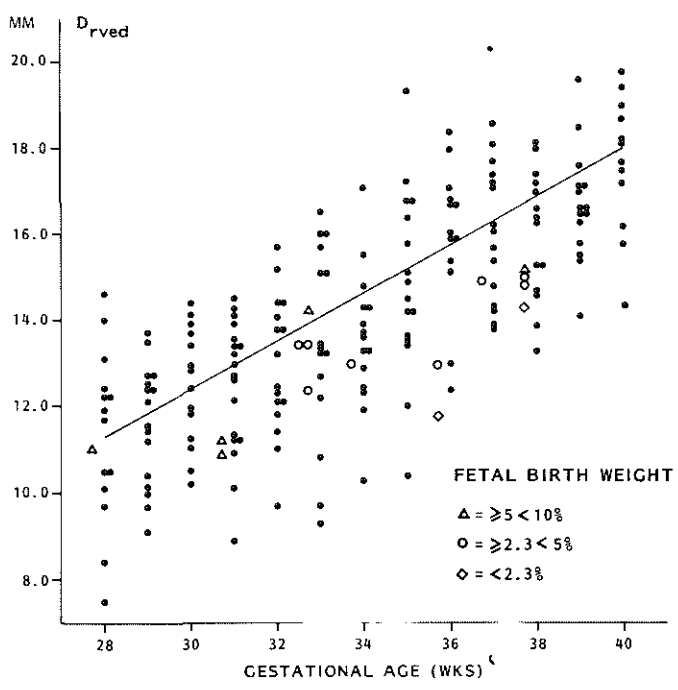meter (D_{rves})(Ch. 5)

Fig. 7.5 Data on right-to-left ventricular ratio (ED) from 15 small-for-
dates (Δ,O,$\Diamond$) plotted in the normal curve for that particular
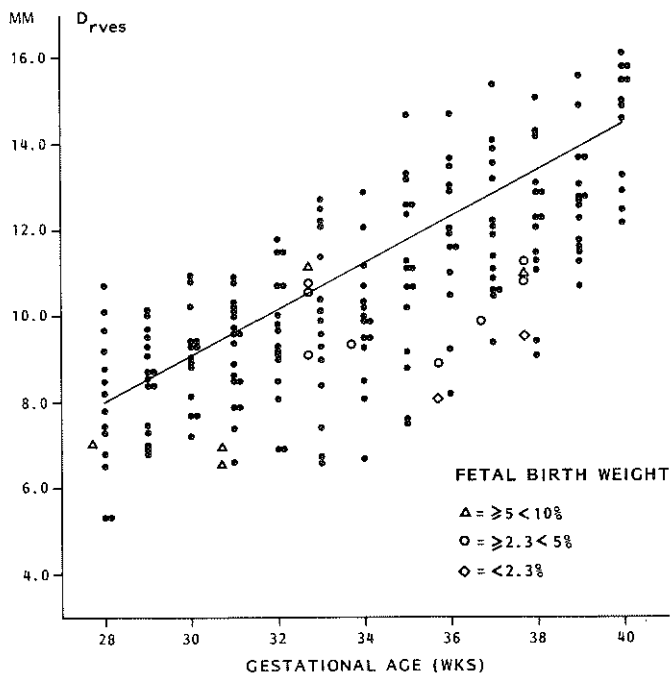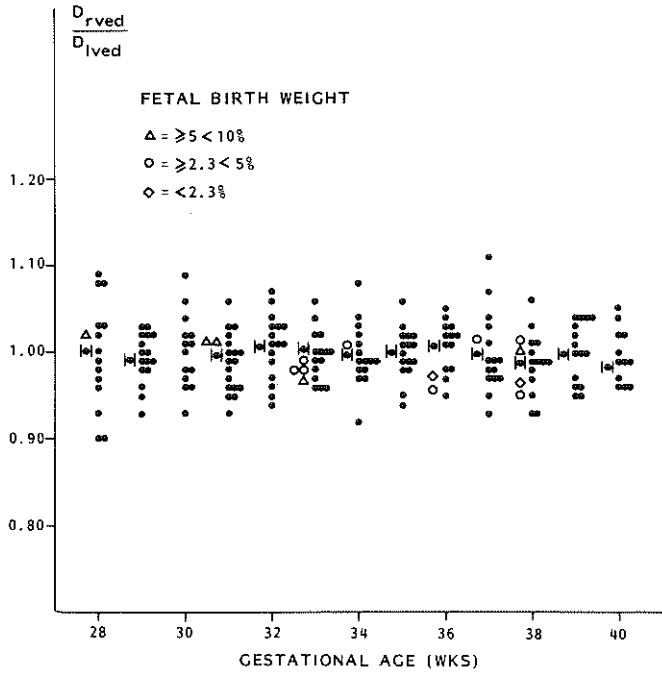parameter ($\frac{D_{rved}}{D_{lved}}$)(Ch. 5)

Fig. 7.6 Data on right-to-left ventricular ratio (ES) from 15 small-for-dates (Δ,0,$\Diamond$) plotted in the normal curve for that particular parameter ($\frac{D_{rves}}{D_{lves}}$)(Ch. 5)

Fig. 7.7 Data on left ventricular volume (ED) from 15 small-for-dates
        (Δ,ο,◊) plotted in the normal curve for that particular para-
        meter (Q_{lved})(Ch. 5)

Fig. 7.8 Data on left ventricular volume (ES) data from 15 small-for-
dates (Δ,O,$\Diamond$) plotted in the normal curve for· that particular
parameter (Q_{1ves})(Ch. 5)
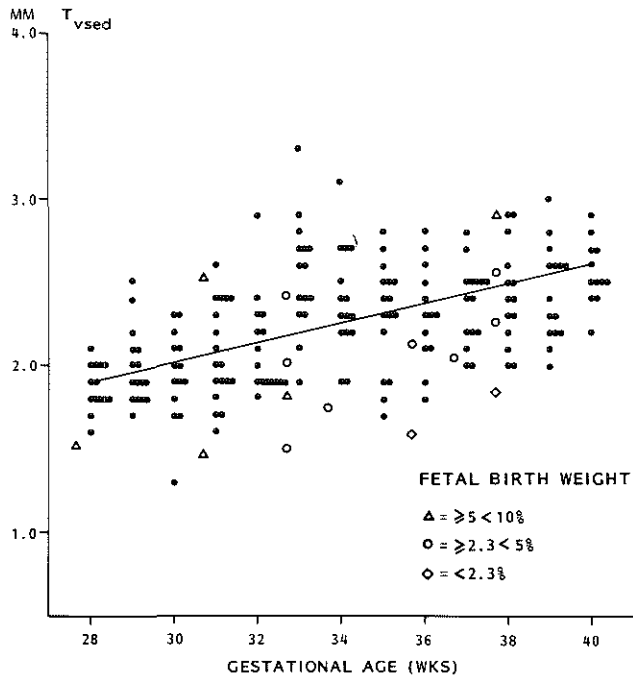
Fig. 7.9 Data on intraventricular septal thickness (ED) from 15 small-
for-dates (Δ,O,◊) plotted in the normal curve for that
particular parameter (T_{vsed})(Ch. 5)
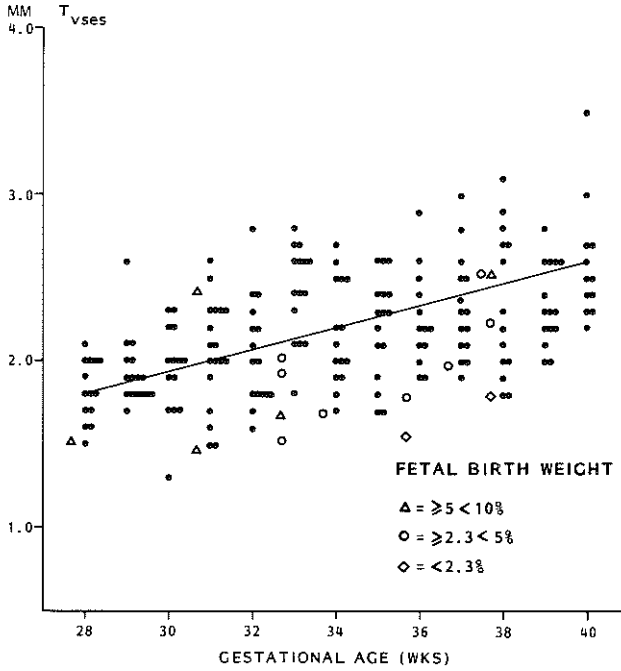
Fig. 7.10 Data on intraventricular septal thickness (ES) from 15 small-
for-dates (Δ,O,$\Diamond$) plotted in the normal curve for that
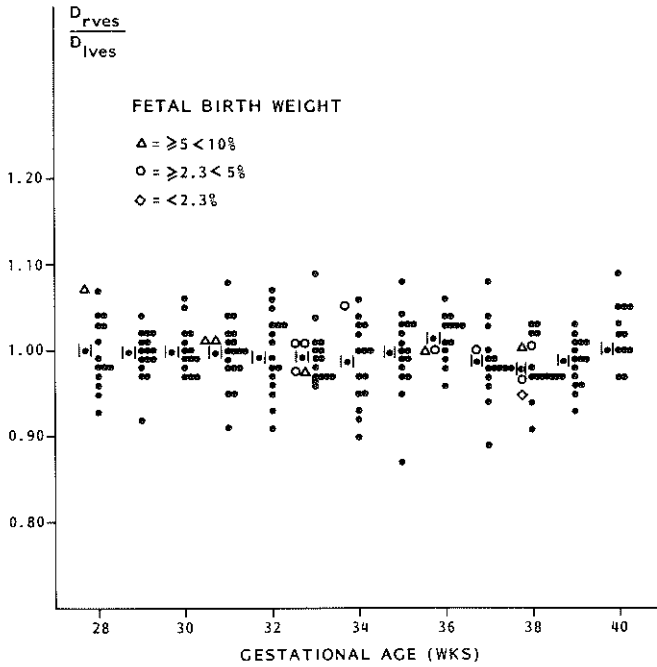particular parameter (T_{vses})(Ch. 5)
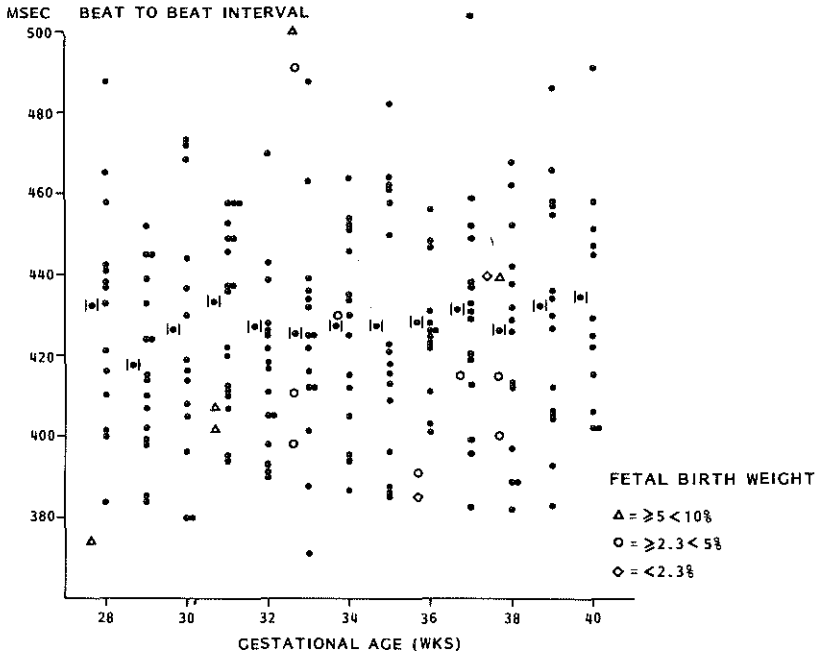
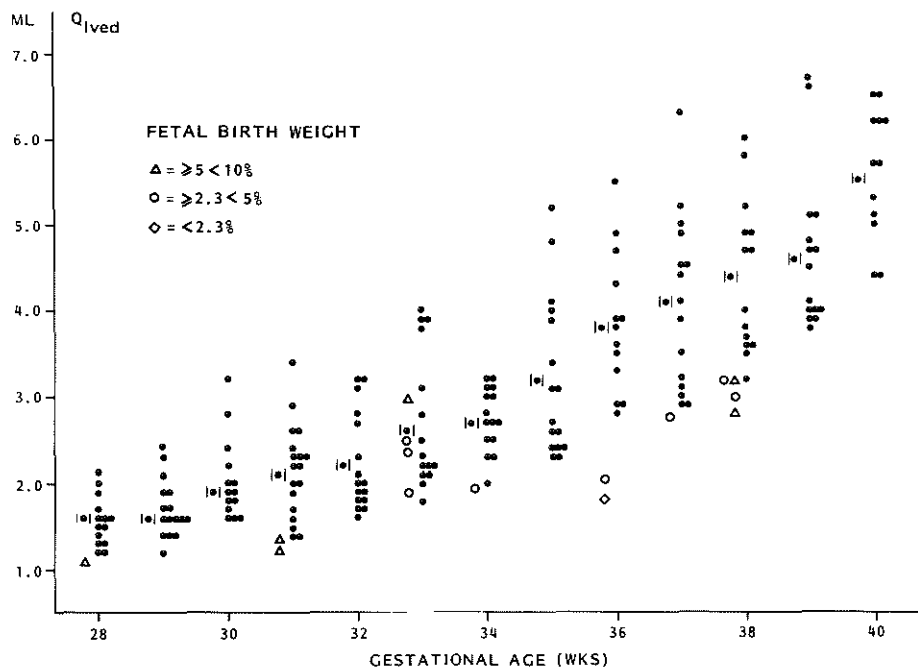Fig. 7.11 Data on beat-to-beat interval from 15 small-for-dates (Δ,O,◊) plotted in the normal curve for that particular parameter (Ch. 5)

162
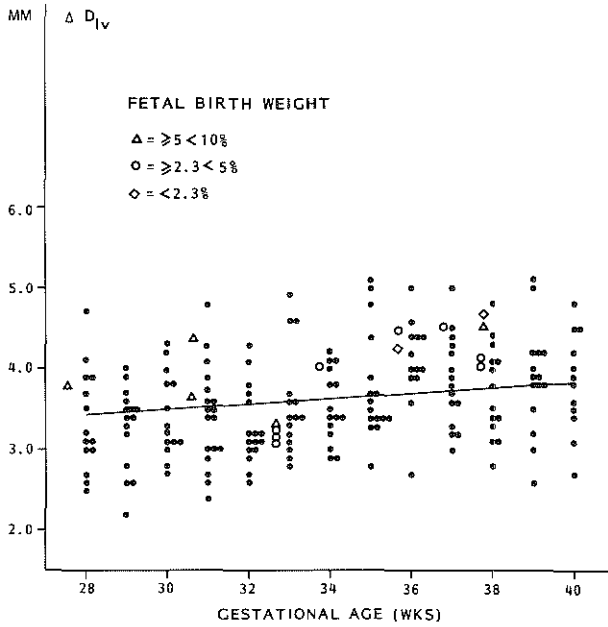
Fig. 7.12 Data on left ventricular shortening (ΔD_{1v}) from 15 small-for-dates (Δ,O,$\Diamond$) plotted in the normal curve for that particular parameter (Ch. 5)
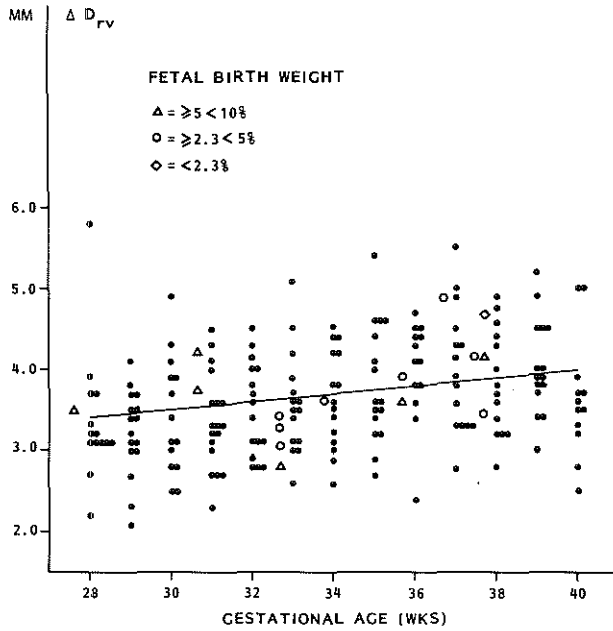
Fig. 7.13 Data on right ventricular shortening (ΔD_{rv}) from 15 small-for-dates ($\Delta, 0, \diamond$) plotted in the normal curve for that particular parameter (Ch. 5)

Fig. 7.14 Data on left ventricular stroke volume (Q_{lvs}) from 15 small-
for-dates (Δ,O,$\Diamond$) plotted in the normal curve for that
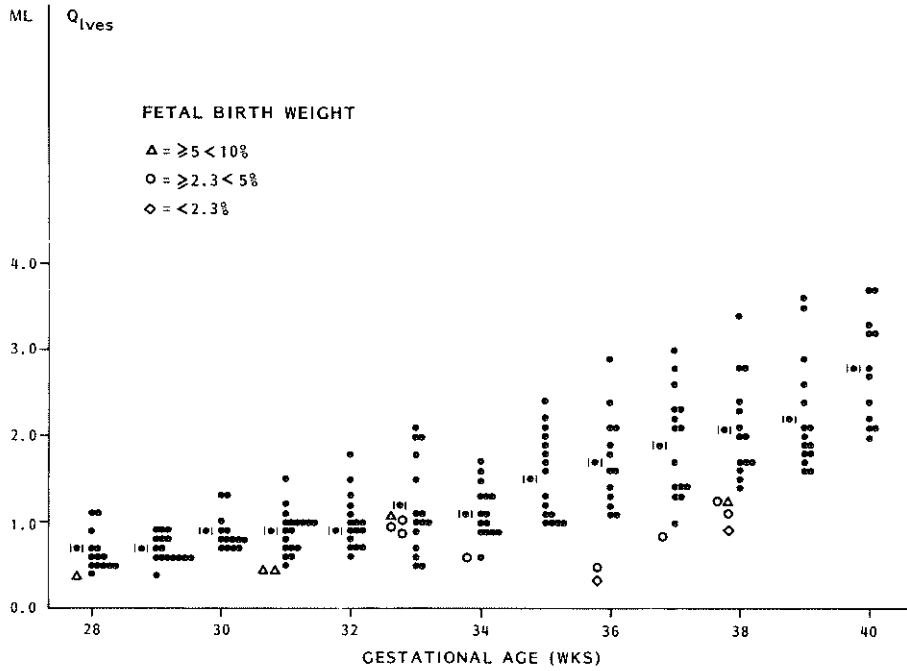particular parameter (Ch. 5)

Fig. 7.15 Data on left ventricular output (Q'_{lv}) from 15 small-for-dates $(\Delta, 0, \Diamond)$ plotted in the normal curve for that particular para-meter (Ch. 5)

166
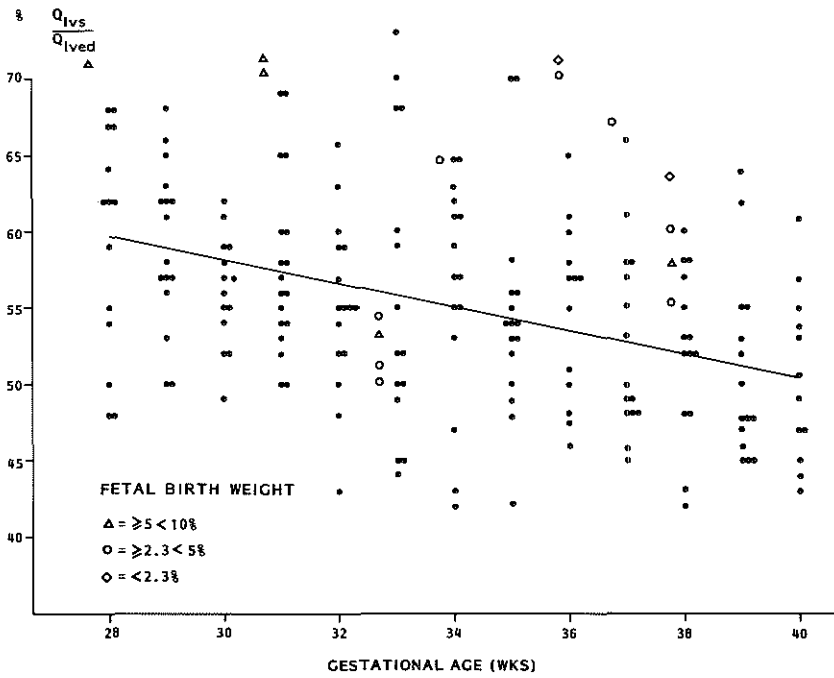
Fig. 7.16 Data on left ventricular ejection fraction ($\frac{Q_{lvs}}{Q_{lved}}$) from 15 small-for-dates (Δ,O,$\Diamond$) plotted in the normal curve for that particular parameter (Ch. 5)

REFERENCES

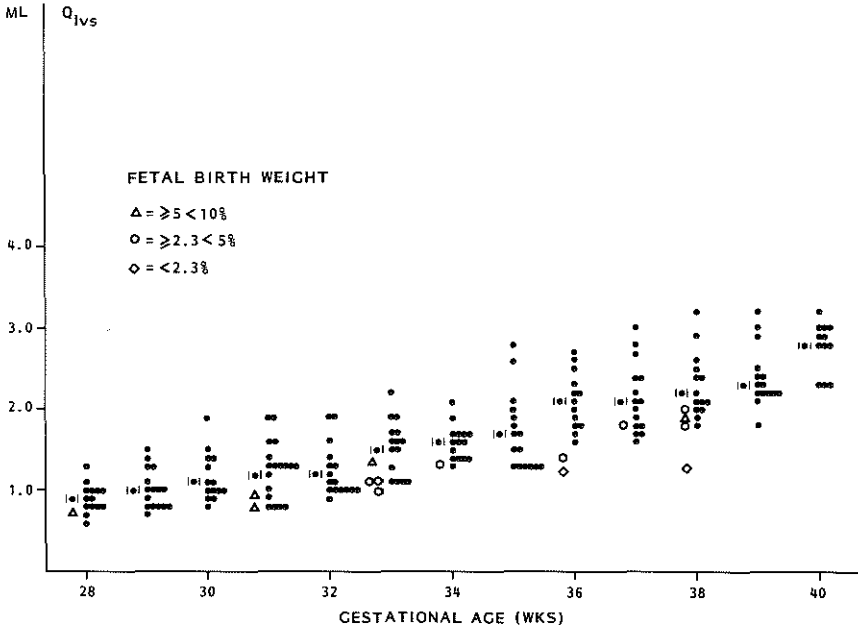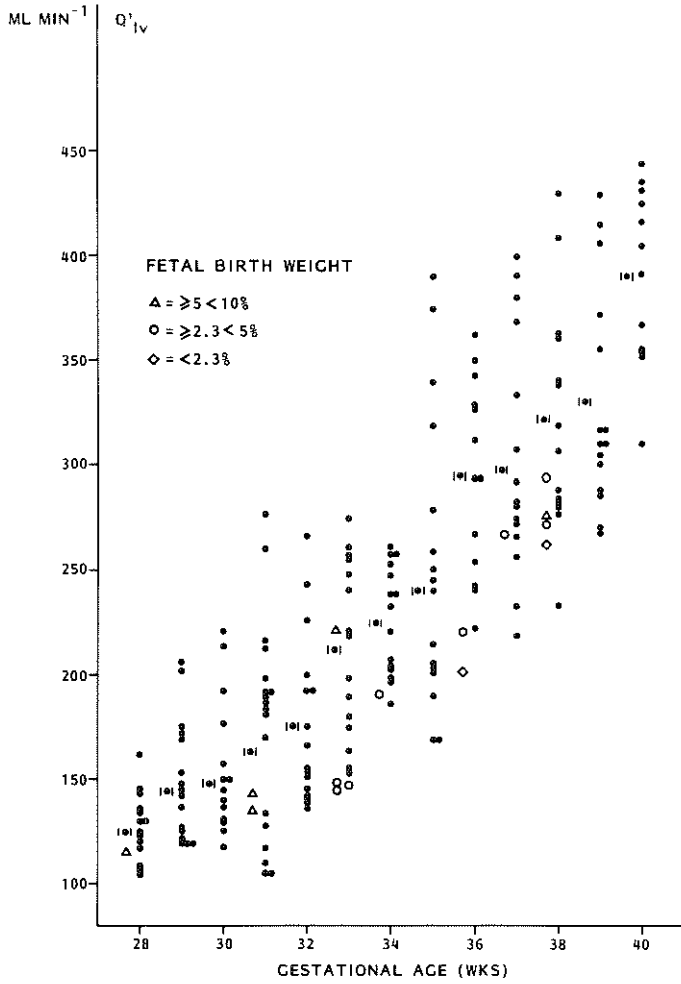Allan, L.D., Joseph, M.C., Boyd, E.G.C.A., Campbell, S.,
    Tynan, M.J.: M-mode echocardiography in the developing
    human fetus. Br.Heart J. 47: 573, 1982.

Allan, L.D., Tynan, M.J., Campbell, S., Wilkinson, J.L.,
    Anderson, R.H.: Echocardiographic and anatomical correlates
    in the fetus. Br.Heart J. 44: 441, 1980.

Anderson, D.F., Bissonette, J.M., Faber, J.J., Thornburg,
    K.L.: Central shunt flows and pressures in the mature
    fetal lamb. Am.J.Physiol. 241: 60, 1981.

Arcilla, R.A., Oh, W., Wallgren, G., Hanson, G., Gessner,
    I.H., Lind, J.: Quantitative studies of the human neonatal
    circulation. II. Haemodynamic findings in early and late
    clamping of the umbilical cord. Acta Pediat.Scand. (Suppl.)
    179: 23, 1967.

Assali, N.S., Kirschbaum, T.M., Dilts, P.V. Jr.: Effects of
    hyperbaric oxygen on uteroplacental and fetal circulation.
    Circ.Res. 22: 573, 1968.

Assali, N.S., Morris, J.A., Beck, R.: Cardiovascular haemo-
    dynamics in the fetal lamb before and after lung expansion.
    Am.J.Physiol. 208: 122, 1965.

Baars, A.M., Merkus, J.M.W.M.: Fetal echocardiography: a new
    approach to the study of the dynamics of the fetal heart
    and its component parts. Eur.J.Obstet.Gynaecol.Reprod.
    Biol. 7: 91, 1977.

Barrett, M.J., Jacobs, L., Power, J., Woods, A., Bloom, S.,
    Meister, S.G.: Underestimation of cavity diameter by two-
    dimensional echocardiography: Inherent errors in the far
    field. Ultrasound in Medicine and Biology 8: 10, 1982.

Barclay, A.E., Franklink, K.J., Prichard, M.M.L.: The foetal
    circulation. Oxford: Blackwell Scientific Publications,
    1944.

Barcroft, J.: Researches on prenatal life. Oxford: Blackwell
    Scientific Publications, 1946.

Bloemsma, C.A.: Echoscopische meting van de foetale schedel-
    en rompgrootte. Thesis, Erasmus University Rotterdam, 1978.
Boerth, R.C.: Postnatal development of myocardial contractile
    function in the cat. Circulation 46: II-36, 1972.
Bommer, W., Weinert, L., Neumann, A., Neef, J., Mason, D.T.,
    DeMaria, A.: Determination of right atrial and right
    ventricular size by two-dimensional echocardiography.
    Circulation 60: 91, 1979.
Brinkman, C.R. III, Johnson, G.H., Assali, N.S.: Hemodynamic
    effects of bradycardia in the fetal lamb. Am.J.Physiol.
    223: 1465, 1972.
Burnard, E.D.: Influence of delivery on the circulation. In:
    The heart and circulation in the newborn infant. Cassels,
    D.E., ed.; Grune and Stratton, New York, 1966.
Campbell, A.G.M., Dawes, G.S., Fishman, A.P. et al: The
    release of a bradykinin-like pulmonary vasodilator sub-
    stance in foetal and new-born lambs. J.Physiol. (London)
    195: 83, 1968.
Campbell, S., Thoms, A.: Ultrasonic measurement of fetal
    abdominal circumference ratio in the assessment of growth
    retardation. Br.J.Obstet.Gynaecol. 84: 165, 1977.
Campbell, S., Wilkin, D.: Ultrasonic measurement of fetal
    abdominal circumference in estimation of fetal weight.
    Br.J.Obstet.Gynaecol. 82: 689, 1975.
Cate, F.J. ten, Kloster, F.E., Van Dorp, W.G., Meester, G.T.,
    Roelandt, J.: Dimensions and volumes of left atrium and
    ventricle determined by single beam echocardiography.
    Br.Heart J. 36: 737, 1974.
Cohn, H.E., Sacks, E.J., Heymann, M.A., Rudolph, A.M.:
    Cardiovascular responses to hypoxemia and acidemia in
    fetal lambs. Am.J.Obstet.Gynecol. 120: 817, 1974.
Cordero, L. Jr.: Heart rate changes during the first hour of
    life. Biol.Neonate 20: 270, 1972.
Cross, K.W., Dawes, G.S., Mott, J.C.: Anoxia, oxygen
    consumption and cardiac output in new-born lambs and adult
    sheep. J.Physiol. 146: 316, 1959.

Davila, J.C., Sanmarco, M.E.: An analysis of the fit of mathematical models applicable to the measurement of left ventricular volume. Amer.J.Cardio. 18: 31, 1966.

Dawes, G.S.: Foetal and neonatal physiology. Chicago, IL: Yearbook Medical Publishers, 1968.

Dawes, G.S.: Foetal blood gas autonomy. Foetal Autonomy, Ciba Foundation Symposium, ed. G.E.W. Wolstenholme, M. O'Conner, p. 162, London: Churchill, 1969.

Dawes, G.S., Mott, J.C., Widdicombe, J.G.: The foetal circulation in the lamb. J.Physiol. 126: 563, 1954.

Dawes, G.S., Mott, J.C., Widdicombe, J.G.: Patency of the ductus arteriosus in newborn lambs and its physiological consequences. J.Physiol. 128: 361, 1955.

Dawes, G.S., Mott, J.C., Widdicombe, J.G., Wyatt, D.G.: Changes in the lungs of the newborn lamb. J.Physiol. 121: 141, 1953.

Dodge, H.T., Sandler, H., Baller, D.W., Lord, J.D.: The use of biplane angiography for the measurement of left ventricular volume in man. Am.Heart J. 60: 762, 1960.

Downing, S.E., Talner, N.S., Gardner, T.H.: Ventricular function in the newborn lamb. Am.J.Physiol. 208: 931, 1965.

Edler, I., Hertz, C.H.: The use of ultrasonic reflectoscope for continuous recording of movements of heart walls. Kung Fysiograf Sallsk Lund Fordhandl 24: 40, 1954.

Egeblad, H., Bang, J., Northeved, A.: Ultrasonic identification and examination of fetal heart structures. J.Clin.Ultrasound 3: 95, 1975.

Eik-Nes, S.H., Marsál, K., Brubakk, A.O., Kristoffersen, K.: Ultrasonic measurement of human fetal blood flow. In: Ultrasonic assessment of human fetal weight, growth and blood flow. Thesis by S.H. Eik-Nes, Malmö, 1980.

Eik-Nes, S.H., Brubakk, A.O., Ulstein, H.K.: Measurement of human fetal blood flow. Br.Med.J. 280: 183, 1980.

Emery, J.L., MacDonald, M.S.: The weight of ventricles in the later weeks of intra-uterine life. Br.Heart J. 22: 563, 1960.

Emery, J.L., Mithal, A.: Weights of cardiac ventricles at
    and after birth. Br.Heart J. 23: 313, 1961.

Epstein, M.L., Goldberg, S.J., Allen, H.D., Konecke, L.L.,
    Wood, J.: Great vessel, cardiac chamber and wall growth
    patterns in normal children. Circulation 51: 1124, 1975.

Faber, J.J., Green, J.J.: Foetal placental blood flow in the
    lamb. J.Physiol. 223: 375, 1972.

Faber, J.J., Green, J.J., Thornburg, K.L.: Embryonic stroke
    volume and cardiac output in the chick. Develop.Biol. 41:
    14, 1974.

Feigenbaum, H.: Echocardiography. Philadelphia, Lea and
    Febliger, Ch. 3, 1972.

Frank, O.: Zur Dynamik des Herzmuskels. Z.Biol. 32: 370, 1895.

Friedman, W.F.: The intrinsic physiologic properties of the
    developing heart. In: Neonatal Heart Disease, edited by
    W.F. Friedman, M. Lesch and E.H. Sonnenblick, Grune and
    Stratton, New York, 1972.

Fulton, R.M., Hutchinson, E.C., Jones, A.M.: Ventricular
    weight in cardiac hypertrophy. Br.Heart J. 14: 413, 1952.

Galenus: On the usefulness of the parts of the body. Cornell
    University Press Ithaca, New York, 1968.

Garrett, W.J., Robinson, D.E.: Fetal heart size measured in
    vivo by ultrasound. Pediatrics 46: 25, 1970.

Gill, R.W., Kossoff, G.: Pulsed Doppler combined with B-mode
    imaging for blood flow measurement. Contribution to
    Gynecology and Obstetrics 6: 139, 1979.

Gruenwald, P.: Chronic fetal distress and placental
    insufficiency. Biol.Neonat. 5: 215, 1963.

Gruenwald, P.: Growth of the human fetus. I. Normal growth
    and its variations. Am.J.Obstet.Gynec. 94: 1112, 1966.

Hansmann, M., Voigt, U., Baeker, H.: Die Wertigkeit intra-
    uterin mit Ultraschall messbarer Parameter für die
    Gewichtsklassenschätzung des Feten. Arch.Gynäk. 214: 314,
    1973b.

Hansmann, M., Voigt, U., Lang, H.: Ultraschallmessdaten als
    Parameter zur Erkennung einer intrauterinen Wachstum-
    retardierung. Arch.Gynäk. 214: 194, 1973a.

Harinck, E.: Wederzijdse beïnvloeding van de beide hart-
    helften en veranderingen hiervan na de geboorte. Akad.
    Proefschrift Leiden, 1974.

Harvey, W.: Exercitatio anatomica de motu cordis et sanguinis
    in animalibus. Franoforti, Sumptibus, Guilelmi Fitzeri,
    1628.

Herrmann, G.R., Wilson, F.N.: Ventricular hypertrophy. A
    comparison of electrocardiographic and post mortem
    observations. Heart 9: 91, 1922.

Hermann, H.J., Bartle, S.H.: Acute mitral regurgitation in
    man. Hemodynamic evidence and observations indicating an
    early role for the pericardium. Circulation 36: 839, 1968.

Heymann, M.A., Berman, W. Jr., Rudolph, A.M., Whitman, V.:
    Dilatation of the ductus arteriosus by prostaglandin E,
    in aortic arch abnormalities. Circulation 59 (1): 169,
    1979.

Heymann, M.A., Rudolph, A.M.: Effect of exteriorization of
    the sheep fetus on its cardiovascular function. Circ.Res.
    21: 741, 1967.

Hill, D.E., Myers, R.E., Holt, A.B., Scott, R.E., Cheek, D.B.:
    Fetal growth retardation produced by experimental placental
    insufficiency in the rhesus monkey. Biol.Neonate 19: 68,
    1971.

Hislop, A., Reid, L.: Weight of the left and right ventricle
    of the heart during fetal life. J.Clin.Pathol. 25: 534,
    1972.

Hobbins, J.C., Kleinman, C., Creighton, D.: Fetal echocardio-
    graphy: Indirect evaluation of in utero fetal flow
    patterns. In: Proceedings of Society for Gynecologic
    Investigation. 25th Annual Meeting, Atlanta, Georgia,
    p. 48, 1978.

Hort, W.: Morphologische Untersuchungen am Herzen vor,
    während und nach der postnatalen Kreislaufumschaltung.
    Virchows Arch.Path.Anat. 326: 458, 1955.

Hort, W.: The normal heart of the fetus and its metamorphosis
    in the transition period. In: The Heart and Circulation in
    the Newborn and Infant, edited by D.E. Cassels; Grune and
    Stratton, New York, 1966.

Huggett, A.St.G.: Foetal blood gas tensions and gas trans-
    fusion through the placenta of the goat. J.Physiol. 62:
    373, 1927.

Ianniruberto, A., Iaccarino, M., De Luca, I., Gianfrate, P.:
    Analisi ecografie delle strutture cardiache fetali. Nota
    tecnica. In: Atti Congresso Nazionale S.T.S.U.M. Edited
    by A. Ianniruberto, Terlizi, Italy, p. 285, 1977.

Jong, P.A. de, Stolte, L.A.M., Kleinhout, J., Monkhorst, M.,
    Prins, H., Voorhorst, F.J., Janssens, J., Veth, A.F.L.:
    Heart rate pattern of the newborn infant. Abstracts 17th
    Federatieve Vergadering, p. 218, 1974.

Kececioglu-Draelos, Z., Goldberg, S.J., Sahn, D.J.: How
    accurate is the ultrasonic estimation of ventricular
    septal defect size? Pediatric Cardiology 3: 189, 1982.

Keen, E.N.: The postnatal development of human cardiac
    ventricles. J.Anat. 89: 484, 1955.

Kirkpatrick, S.E., Covell, J.W., Friedman, W.F.: A new
    technique for the continuous assessment of fetal and
    neonatal cardiac performance. Am.J.Obstet.Gynecol. 116:
    963, 1973.

Kirkpatrick, S.E., Naliboff, J., Pitlick, P.T., Friedman,
    W.F.: The influence of post stimulation potentation and
    heart rate on the fetal lamb heart. Am.J.Physiol. 229:
    318, 1975.

Kirkpatrick, S.E., Pitlick, P.T., Naliboff, J., Friedman,
    W.F.: Frank-Sterling relationship as an important
    determinant of fetal cardiac output. Am.J.Physiol 231 (2):
    495, 1976.

Kleinman, C.S., Hobbins, J.C., Jaffe, C.C., Lynch, D.C.,
    Talner, N.S.: Echocardiographic studies of the human fetus.
    In: Proceedings Symposium on Development Biology of the
    Society for Pediatric Research. New York, 1978.

Kloosterman, G.J.: On intrauterine growth. Int.J.Gynaecol.
    Obstet. 8: 895, 1970.

Lauer, R.M., Evans, J.A., Aoki, M., Kittle, C.F.: Factors
    controlling pulmonary vascular resistance in fetal lambs.
    J.Pediat. 67: 568, 1965.

Lee, F.Y.L., Batson, H.W.K., Alleman, N. et al: Fetal cardiac
    structure: identification and recognition. Am.J.Obstet.
    Gynecol. 129: 503, 1977.

Lewis, T.: Observation on ventricular hypertrophy with
    especial reference to preponderance of one or other
    chamber. Heart, 5: 367, 1914.

Lind, J., Stern, L., Wegelius, C.: Human foetal and neonatal
    circulation. Edited by J.A. Anderson. Charles C. Thomas
    Publisher, Springfield, Illinois, U.S.A., 1964.

Mahon, W.A., Goodwin, J.W., Paul, W.M.: Measurement of
    individual ventricular outputs in the fetal lamb by an
    indicator dilution technique. Circulation Res. 19: 191,
    1966.

Müller, W.: Die Massenverhältnisse des menschlichen Herzens.
    Leopold Voss, Hamburg und Leipzig, 1883.

Murata, Y., Takemura, H., Kurachi, K.: Observation of fetal
    cardiac motion by M-mode ultrasonic cardiography. Am.J.
    Obstet.Gynecol. 111: 287, 1971.

Naeye, R.L.: Abnormalities in infants of mothers with toxemia
    of pregnancy. Am.J.Obstet.Gynecol. 95: 276, 1966.

Pohlman, A.G.: The fetal circulation through the heart. Bull.
    Johns Hopkins Hosp. 18: 409, 1907.

Pombo, J.F., Troy, B.L., Russell, R.O. Jr.: Left ventricular
    volumes and ejection fraction by echocardiography.
    Circulation 43: 480, 1971.

Popp, R.L., Harrison, D.C.: Ultrasound cardiac echography for
    determining stroke volume and valvular regurgitation.
    Circulation 41: 493, 1970.

Recavarren, S., Arias-Stella, J.: Growth and development of
    the ventricular myocardium from birth to adult life.
    Br.Heart J. 26: 187, 1964.

Reynolds, S.R.M.: Fetal and neonatal pulmonary vasculature
    in Guinea-pig in relation to hemodynamic changes at birth.
    Amer.J.Anat. 98: 97, 1956.

Robinson, D.E., Garrett, W.J., Kossoff, G.: Fetal anatomy
    dysplayed by ultrasound. Invest.Radiol. 3: 442, 1968.

Roelandt, J.: Practical echocardiology, Ultrasound in
    biomedicine series. Volume one. D. White, General Editor.
    Research Studies Press, 1977.

Romero, T., Covell, J., Friedman, W.F.: A comparison of
    pressure-volume relations of the fetal, newborn and adult
    heart. Am.J.Physiol. 222: 1285, 1972.

Rudolph, A.M.: Fetal and neonatal pulmonary circulation.
    Ann.Rev.Physiol. 41: 383, 1979.

Rudolph, A.M., Heymann, M.A.: The circulation of the fetus
    in utero. Methods for studying distribution of blood flow,
    cardiac output and organ flow. Circ.Res. 21: 163, 1967.

Rudolph, A.M., Heymann, M.A.: Circulatory changes during
    growth in the fetal lamb. Circ.Res. 26: 289, 1970.

Rudolph, A.M., Fixler, D.E., Stage, L. et al: Evaluation of
    a Doppler catheter probe to measure cardiac output.
    J.Surg.Res. 15: 243, 1974.

Rudolph, A.M., Heymann, M.A.: Fetal and neonatal circulation
    and respiration. Ann.Rev.Physiol. 36: 187, 1974.

Rudolph, A.M., Heymann, M.A.: Cardiovascular function in the
    mammalian foetus. S.Afr.Med.J. 47: 1859, 1974.

Rudolph, A.M., Heymann, M.A.: Control of the ductus arteriosus.
    Physiol.Rev. 55 (1): 62, 1975.

Rudolph, A.M., Heymann, M.A., Lewis, A.B.: Physiology and
    pharmacology of the pulmonary circulation in the fetus
    and newborn. In: Lung biology in health and disease. The
    development of the lung, ed. W.A. Hodson, New York, Marcel
    Dekker, 1977.

Rudolph, A.M., Heymann, M.A., Teramo, K.A.W., Barrett, C.T.,
    Räihä, N.C.R.: Studies on the circulation of the previable
    human fetus. Pediat.Res. 5: 452, 1971.

Sabatier, R.B.: Mémoire sur les organes de la circulation du
    sang du foetus. Mém.Acad.Roy.Sc., Paris, 198: 778, 1778.

Sahn, D.J., DeMaria, A., Kisslo, J., Weyman, A.:
    Recommendations regarding quantitation in M-mode echo-
    cardiography: Results of a survey of echocardiographic
    measurements. Circulation 58: 1072, 1978.

Sahn, D.J., Lange, L.W., Allen, H.D., Goldberg, S.J.,
    Anderson, C., Giles, H., Haber, K.: Quantitative real-time
    cross-sectional echocardiography in the developing normal
    human fetus and newborn. Circulation 62, 3: 588, 1980.

Shinebourne, E.A.: Growth and development of the cardio-
    vascular system. In: Scientific Foundations of Pediatrics,
    ed. J.A. Davies and J. Dobbing, London, William Heineman,
    Medical Books Ltd., 13b, 198, 1974.

Spigelius, A.: De formatu foetu. Patavy: Jo Bap. de Martinis
    et Liviu Pasquatu, 1626.

Stahlman, M., Gray, J., Young, W.C., Shepard, F.M.: Cardio-
    vascular response of the neonatal lamb to hypoxia and
    hypercapnia. Am.J.Physiol. 213 (4): 899, 1967.

Starling, E.H.: The Linacre Lecture on the law of the heart.
    London. Longmans Green and Co., 1918.

Suzuki, K., Minei, L.J., Schnitzer, L.E.: Ultrasonographic
    measurement of fetal heart volume for estimation of
    birthweight. Obstet.Gynecol. 43: 867, 1974.

Versprille, A., Harinck, E., Nie, C.J. van, Jansen, J.R.C.,
    Neef, K.J. de: Functional interaction of both ventricles
    and the changes during the neonatal period in relation to
    the changes of geometry. Circulation in the newborn.
    Edited by L.D. Longo, New York, Garland Publishing Inc.,
    1977.

Vesalius, A.: The Epitome of Andreas Vesalius. Translated
    by L.R. Lind. The M.I.T. Press, Cambridge, Massachusetts
    and London, 1969.

Visser, G.H.A., Dawes, G.S., Redman, C.W.G.: Numerical
    analysis of the normal human antenatal fetal heart rate.
    Br.J.Obstet.Gynaecol. 88 (8): 792, 1981.

Vosters, R., Wladimiroff, J.W., Vletter, W.: Assessment of
    fetal and neonatal cardiac geometrics by means of real-time
    ultrasound. In: Echocardiology. Edited by C.T. Lancee.
    The Hague, Martinus Nijhoff, p. 355, 1979.

Wells, P.N.T.: Biomedical ultrasonics. Academic Press, London,
    New York, San Francisco, 1977.

Wigglesworth, J.S.: Experimental growth retardation in the
    foetal rat. J.Path.Bact. 88: 1, 1964.

Williams, H.B., Powers, J.D., Hamlin, R.L.: Ventricular wall
    thickness in the fetal dog. Am.J.Vet.Res. 40 (5): 696,
    1978.

Winick, M.: Cellular changes during placental and fetal growth.
    Am.J.Obstet.Gynecol. 109: 166, 1971.

Winsberg, F.: Echocardiography of the fetal and newborn heart.
    Invest.Radiol. 7: 152, 1972.

Wladimiroff, J.W., Bloemsma, C.A., Wallenburg, H.C.S.:
    Ultrasonic assessment of fetal head and body sizes in
    relation to normal and retarded fetal growth. Am.J.Obstet.
    Gynecol. 131: 857, 1978.

Wladimiroff, J.W., McGhie, J.S.: Ultrasonic assessment of
    cardiovascular geometry and function in the human fetus.
    Br.J.Obstet.Gynaecol. 88: 870, 1981a.

Wladimiroff, J.W., McGhie, J.S.: M-mode ultrasonic assessment
    of fetal cardiovascular dynamics. Br.J.Obstet.Gynaecol.
    88: 1241, 1981b.
Wladimiroff, J.W., Vosters, R.P.L., Vletter, W.: Ultrasonic
    measurement of fetal and neonatal ventricular dimensions.
    Contrib.Gynec.Obstet. 6: 109, 1979.
Wladimiroff, J.W., Vosters, R., Vletter, W.: Real-time
    assessment of fetal and neonatal cardiac dynamics. In:
    Real-time Ultrasound in Obstetrics. Edited by M.J. Bennett
    and S. Campbell, Blackwell Scientific Publications,
    Oxford, p. 79, 1980.
Yuan, S.S.H., Heymann, M.A., Rudolph, A.M.: Relationship
    between ventricular weight, pressure and myocardial blood
    flow in the newborn piglet. Circulation 34 (III): 243,
    1966.
Zak, R.: Cell proliferation during cardiac growth. Am.J.
    Cardiol. 31: 211, 1973.

CURRICULUM VITAE

Name: Robertus Petrus Leonardus Vosters
Date of Birth : 12 April 1946
Place of Birth: Munstergeleen

Education: 1966   : Diploma Gymnasium β from the St.
                          Michiellyceum in Geleen
         6 July 1973: Medical Degree from the Rijks-
                          universiteit in Utrecht
         1 July 1981: Registration as Gynaecologist

Resident Posts   : 1 December 1972 - 1 January 1974:
                          Dept. Internal Medicine, Bethel
                          Ziekenhuis, Delft (J.F. Geurtsen †,
                          Dr. W. Hart and Dr. J. de Regt)
                        : Dept. Surgery, Bethel Ziekenhuis,
                          Delft (Dr. C.A. Broodman, Dr. Ph.
                          Gallas and Dr. M.A. Verschuyl)

                        : 1 January 1974 - 1 August 1975:
                          Dept. Obstetrics and Gynaecology,
                          St. Clara Ziekenhuis, Rotterdam
                          (Dr. J.M. Versteeg and F. Bootsman)

                        : 1 August 1975 - 1 July 1976:
                          Dept. Obstetrics and Gynaecology,
                          Ikazia Ziekenhuis, Rotterdam
                          (Dr. H.F. Heins, A.W. van Cappellen
                           and M.J.P.F. Straub)

Specialist training   : 1 July 1976 - 1 October 1977:
                         Rijkskweekschool for Midwifery,
                         Rotterdam (Director: Dr. R.H. Gevers)

                       : 1 October 1977 - 1 February 1981:
                         Dept. Obstetrics and Gynaecology,
                         Academisch Ziekenhuis Dijkzigt,
                         Rotterdam (Head: Prof.Dr. A.C.
                         Drogendijk)

                       : 1 February 1981 - 1 July 1981:
                         Dept. Obstetrics and Gynaecology,
                         Zuiderziekenhuis, Rotterdam (Head:
                         Dr. F.B. Lammes)

Current Position   : Member of the Dept. Obstetrics and
                         Gynaecology, Academisch Ziekenhuis
                         Dijkzigt, Rotterdam, with a particular
                         interest in Clinical Genetics